Author:
Manning, Alex

Title:
Modelling the physical and biogeochemical causes of OAE2

Modelling the physical and biogeochemical causes of OAE2

By

Alexander Edward Manning

School of Geographical Sciences
University of Bristol

A dissertation submitted to the University of Bristol in accordance with the requirements of the degree of Doctor of Philosophy in the Faculty of Science.

September 2021

Word count:34,327

Abstract

Oceanic anoxic events (OAEs) are periods in Earth's history during which a large portion of the ocean became dysoxic. As large perturbations of the earth's carbon cycle, the mechanics of what caused OAEs are particularly interesting, especially given contemporary concerns about decreasing oxygen levels in a warming ocean. OAE2, one of the more globally widespread OAEs, occurred at 103 Ma and marks the boundary between the Cenomanian and the Turonian stage.

OAE2 has been extensively studied, both using data and modelling. However, most modelling relies on box models or low-resolution Earth-System models, with few studies using full GCMs due to the prohibitive modelling spin-up times. This thesis explores the physical and biogeochemical causes of OAE2 using the computationally efficient HadCM3L GCM. It covers three aspects:

(1) A model comparison of the Cenomanian and Maastrichtian paleogeographies shows that a restricted circulation is necessary but insufficient for OAE2 to develop. This restricted paleogeography is particularly important in the proto-North Atlantic, the area in which anoxia first develops.

(2) An ensemble of model runs for the Cenomanian with varying orbital parameters shows that orbital variation can alter the spread and magnitude of ocean anoxia without obliterating it. Orbital variation is unlikely the driving cause behind OAE2 but could have caused anoxic variations within the OAE, resulting in changes in distribution or sediment layering.

(3) Comparing HadCM3L with previous OAE2 modelling highlights the importance of a detailed representation of the ocean ecosystem. HadCM3L, which includes an NPZD ocean ecosystem, does not achieve global anoxia when the nutrient inventory is doubled in the ocean, a difference caused by the top-down control of phytoplankton and detritus.

Overall, the results show the importance of a more comprehensive representation of the physics and biology of the ocean. Future modelling OAEs work needs to make more use of these more comprehensive models to progress our understanding of OAEs.

Acknowledgements

I would like to thank my excellent supervisors, Paul Valdes and Fanny Monteiro for all the support and expertise the have provided throughout my PhD. I am enormously grateful for all the help they have provided throughout my PhD and thankful for their positive and useful discussion in the face of all problems I encountered.

I would also like to thank everyone in BRIDGE, the School of Geographical Sciences and the University of Bristol for the friendly and open environment in which studying has been a pleasure. Many thanks to all who I shared an office with throughout my PhD, for providing tea, cake, and support.

Massive thanks to all my friends, both inside and outside Geography, for all the camps, trips, BBQs on the downs over the course of my PhD. Huge thanks to my Parents, Sister and Family for being brilliant!

Particular extra thanks go to Tamsin, without whom it simply would not have been possible for me to complete this thesis.

Author's declaration

I declare that the work in this dissertation was carried out in accordance with the requirements of the University's Regulations and Code of Practice for Research Degree Programmes and that it has not been submitted for any other academic award. Except where indicated by specific reference in the text, the work is the candidate's own work. Work done in collaboration with, or with the assistance of, others, is indicated as such. Any views expressed in the dissertation are those of the author.

SIGNED: ..... DATE: .....

Contents

List of Figures

List of Tables

List of Acronyms

BRIDGE Bristol Research Initiative for the Dynamic Global Environment

OAE1a oceanic anoxic event 1a

OAE3 oceanic anoxic event 3

OAE2 oceanic anoxic event 2

OAE oceanic anoxic event

WIS western interior seaway

NPZD nutrient-phytoplankton-zooplankton-detritus

CIE carbon isotope excursion

LIP large igneous province

DSDP deep sea drilling project

ITCZ inter-tropical convergence zone

GCM general circulation model

EMIC earth system model of intermediate complexity

HadOCC Hadley Centre Ocean Carbon Cycle

HadCM3 the Hadley Centre coupled model version 3

HadCM3BL HadCM3B with a lower resolution ocean

FAMOUS Fast Met Office UK Universities Simulator

cGENIE the grid enabled integrated earth system model

CLIP Caribbean large igneous province

H_2S hydrogen sulphide

CO_2 carbon dioxide

pCO_2 partial pressure of carbon dioxide

TCO_2 total dissolved inorganic carbon

DIC dissolved inorganic carbon

$\delta^{13}C$ the δ^{13}C isotopic signature

$\delta^{15}N$ the δ^{15}N isotopic signature

$^{87}Sr/^{86}Sr$ ^{87}Sr/^{86}Sr

Chapter 1

Introduction

1.1 Oceanic anoxic events

Oceanic anoxic events (OAEs) were major climatic events, during which large parts of the global ocean experienced low oxygen levels and anoxic conditions (Arthur and Sageman 1994; Schlanger and Jenkyns 1976). Identified from widespread carbon and organic-rich sediments which indicate deposition of marine sediments in anoxic conditions (Schlanger and Jenkyns 1976), these events occurred mainly during the Cretaceous and Jurassic periods (Jenkyns 2010). The mechanics of what caused these huge perturbations in the Earth's carbon cycle to occur and the manner in which they developed are particularly interesting and provide important information to aid our understanding of contemporary concerns about decreasing oxygen levels in a warming world.

OAEs were times of large change in the biogeochemical cycles of the Earth's oceans, and have been widely studied as important examples of how

and why the Earth's climate reacts to huge forcing (Jenkyns 2010; Joo et al. 2020; Monteiro et al. 2012). Their large positive carbon isotope excursions (CIEs) (Jenkyns 2010; Jenkyns and Weedon 2003) are indicative of these large changes in the global carbon cycle. Other studies have reported on the occurrence of major changes in marine primary production (Jarvis et al. 2011; Monteiro et al. 2012; Wagner et al. 2004), major changes and extinction events in marine ecosystems (Falzoni and Petrizzo 2020; Forkner et al. 2021), sea-level rise (Jenkyns 1980), and changes in ocean currents and mixing (Wilson and Norris 2001) to have occurred during OAEs.

Within the current evidence base, there is knowledge of many contrasting OAEs within geological time: a few events have been identified in the Paleozoic, with the earliest being in the early Mississippian (Cheng et al. 2020). OAEs become more frequent and widespread in the Mesozoic (Jenkyns 2010) and occur less frequently into the Cenozoic, with the most recent identified in the middle Miocene (Singh et al. 2022). Whilst they all have been identified by the presence of organic rich sediments, these events are extremely varied and most are understood not to have spread to a global extent (Singh et al. 2022). The Mesozoic anoxic events are the largest and most globally widespread, particularly the Early Toarcian (T-OAE), Early Aptian (OAE1a) and Cenomanian/Turonian (OAE2), and have consequently been most well studied (Singh et al. 2022). Of these, OAE2 is the most well defined and widespread, and constituted the largest change in the ocean carbon cycle (Jenkyns 2010; Singh et al. 2022).

Despite the intensive study and improving understanding of OAEs, their exact causes and development continue to be discussed and debated. In-

deed, it is plausible that a combination of differing mechanisms were the leading cause of distinct OAEs and the increase in deposition of organic matter seen in the sediments. Firstly, it has been widely suggested that OAEs were driven by increased productivity in the ocean surface (Kuypers et al. 2002; Scaife et al. 2017), in turn increasing the supply of organic matter to the deep ocean and consuming oxygen upon its remineralization (Jenkyns 2010). Also widely referred to is that OAEs were driven by a decrease in oxygen supply to the deep ocean, preventing oxidation of organic matter from the surface and allowing it to build up in the sediments (Arthur and Sageman 1994; Corbett and Watkins 2013; Scopelliti et al. 2004). Many recent studies have focused upon increased primary production as the main driver of the development of OAEs (Du Vivier et al. 2014; Scaife et al. 2017), with some consensus that volcanism from large igneous provinces (LIPs) caused increased weathering and subsequent nutrient flux to the oceans (Joo et al. 2020).

1.2 Oceanic anoxic event 2

Oceanic anoxic event 2 (OAE2), also known as the Bonarelli event, is one of the more recent globally notable OAEs (Monteiro et al. 2012). Occurring at (93.90 ± 0.15) Ma (Meyers et al. 2012), OAE2 forms the boundary between the Cenomanian and Turonian stages of the Cretaceous.

Identified as a thin layer of black shale (for example, outcropping in the Italian Apennines, as seen in Figure 1.1) present in ocean basin sediments (Schlanger and Jenkyns 1976), OAE2 was an important global-scale event

in which all ocean basins saw widespread anoxia (Ostrander et al. 2017). The OAE2 event has been identified as having many of the common features of OAEs discussed in section 1.1, such as being a major extinction event for phytoplankton (Kuhnt et al. 2017), a time of rising sea levels (Bjerrum et al. 2006), and a time of large changes in the global carbon cycle (Jenkyns 2010; Monteiro et al. 2012).

Figure 1.1: Black shale layer characteristic of the Bonarelli event, Furlo Gorge, Pesaro and Urbino, Italy.

In line with other OAEs, there has been a rise in the study of OAE2 in recent years, as seen through an increase in relevant scientific publications in this research area, particularly within the past 20 years (see Figure 1.2). This has notably seen an expansion in the study of key processes that led to

the onset of OAE2 development, which have been the subject of extensive research, and remain the subject of discussion.

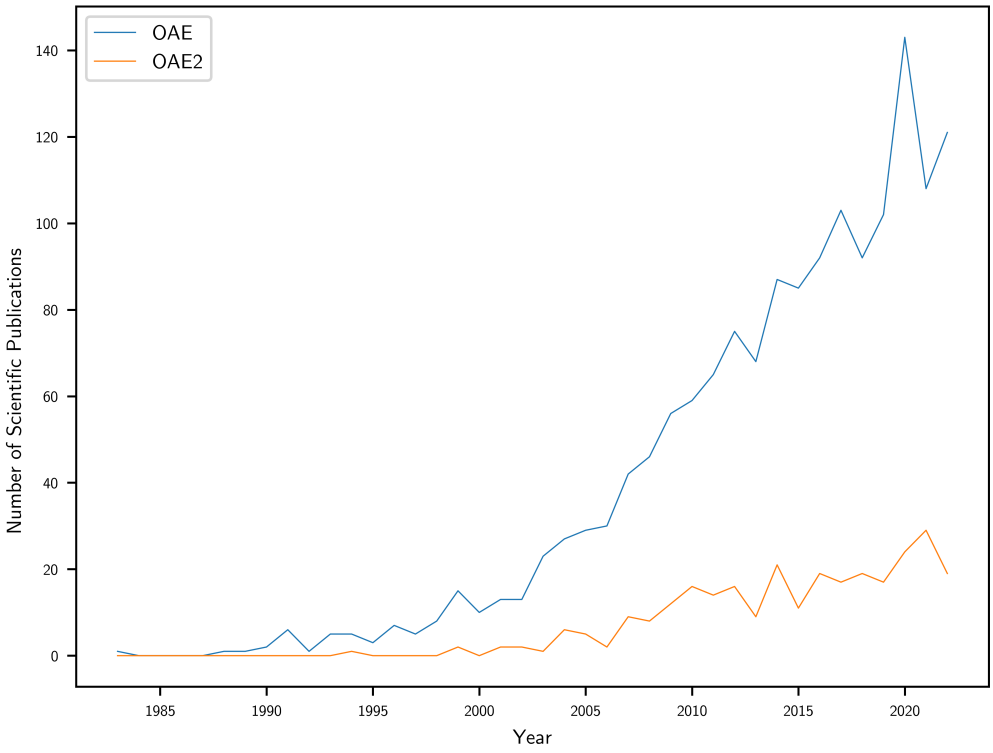

Figure 1.2: Number of scientific publications published per year since 1983, based on a Web of Science literature search up until the end of 2022. For the literature search, the following key words were used: Oceanic anoxic event 2 (search term: "oceanic anoxic event 2" OR "oceanic anoxic event II") and Oceanic anoxic event (search term: "oceanic anoxic event")

1.3 The development of OAE2

The conditions leading up to OAE2 are a complex set of interlinked physical and biogeochemical processes. It is likely that the event itself resulted from the alignment of a complex picture of multiple different conditions (Jenkyns 2010). An increase in the release of carbon dioxide (CO_2) to the

atmosphere, caused by a LIP (Du Vivier et al. 2014) or other volcanism has become the consensus as to the initial impetus for the OAE (Joo et al. 2020). These LIPs consisted of large outpourings of basaltic magma into the earth's crust, lasting for a period of around a million years (Blackburn et al. 2013; Bryan et al. 2010). These huge geologic events are thought to have supplied huge amounts of CO_2 to the atmosphere, and to have generally occurred in tandem with OAEs (Percival et al. 2015). There has been discussion in the literature as to the exact timing of LIPs with respect to OAEs (Percival et al. 2015), however recent work has been done to reinforce the idea of the a LIP as the cause of OAE2 (Kuroda et al. 2007; Scaife et al. 2017). Indeed, four LIPs have been identified as occurring around the time of OAE2: the Caribbean LIP, Madagascar LIP, Ontong Java LIP and High Arctic LIP, with the Ontong Java LIP and High Arctic LIPs having been linked to OAE2 sediments (Scaife et al. 2017).

However, various studies (Monteiro et al. 2012; Nederbragt et al. 2004) have shown that increased atmospheric CO_2 alone is unlikely to be the direct cause of anoxia in the ocean and that other factors also led to the development of the OAE. These other factors are broadly categorised according to their physical and biological effects and encompass principally: increased primary production in the ocean (stemming from an increased supply of nutrient to the ocean, and/or increased nutrient supply to the ocean euphotic zone) and/or alteration of the ocean circulation to reduce ventilation of deep ocean waters and prevent their oxygenation. There is some consensus (Jenkyns 2010; Monteiro et al. 2012) that an increase in primary productivity was necessary for the development of OAE2. Still,

debate remains as to the cause of this increased production (Joo et al. 2020), and in addition, on the importance of ocean circulation (Hay 2008) compared to circulation and stratification (Arthur and Sageman 2011).

A more detailed discussion of the processes involved in OAE2 will be given in section 1.5.

1.4 The use of observations and modelling to assess the development of OAE2

Within the literature that has explored the processes associated with OAE2 development, studies tend to employ either proxy studies of sediments or computational models, or sometimes a comparison of the two.

1.4.1 Proxy Studies of Sediments

There is a wide range of literature that has involved the analysis of sediment data from the OAE2 time period to our improve understanding of the setting in which the OAE took place and the conditions which resulted. Evidence for seafloor anoxia is generally derived from the amount of carbon buried, presence of benthic foraminifera, and lamination of sediments (Arthur and Sageman 1994; Monteiro et al. 2012; Schlanger and Jenkyns 1976).

Schlanger and Jenkyns (1976) were the first to identify geographically widespread black shales in deep sea drilling project (DSDP) and outcrop data as events during which widespread changes in the global carbon cycle

occurred. Drawing on the stratigraphic evidence, Schlanger and Jenkyns (1976) identified the reduction in ocean oxygen and the widespread setting of both OAE2 and oceanic anoxic event 1a (OAE1a). To do this they drew on a large number of DSDP sites across the Atlantic, Indian and Pacific oceans together with rock outcrops, and identified that the characteristic band of organic rich sediment had been caused by the same event, and was found worldwide (Schlanger and Jenkyns 1976). They suggested that the cause of these events was a combination of a warm climate leading to a poorly ventilated ocean, and sea level rise increasing primary production in expanded shallow seas (Schlanger and Jenkyns 1976). Since this paper, further studies have continued to discuss the true extent and cause of these events.

Early studies identified the positive CIE associated with the burial of carbon-rich sediments at a global scale (Arthur et al. 1988; Hasegawa 1997; Jenkyns 1980). The contemporary idea of the CIE associated with an OAE is that of a negative excursion. This results from the input of CO_2 to the atmosphere, for example as a result of volcanism, followed by a large positive excursion resulting from organic matter burial (Jenkyns 2010; Robinson et al. 2017; Scholle and Arthur 1980). However, OAE2 does not follow this model, with most studies considering the excursion to be only positive (Robinson et al. 2017). One of the exceptions is Kuroda et al. (2007) who identified small negative changes with the OAE using sediments from the Gorgo Cerbara outcrop, which is suggested to be a result of a LIP. This being said, no consensus exists for the source of this isotopically light carbon (Jenkyns 2010).

Evidence of euxinia, the presence of free hydrogen sulphide (H_2S) in the water column, is an important indicator of anoxic conditions, particularly as proxy data for this has been able to give information about the state of the photic zone, rather than the benthos. Biomarkers indicating the presence of green sulphur bacteria provide evidence for a euxinic photic zone; these bacteria require H_2S in addition to light for growth (Monteiro et al. 2012; Pancost et al. 2004; Sinninghe Damsté 1998). For example, Pancost et al. (2004) used this method to show euxinia existed in the euphotic zone across the south of the proto-North Atlantic during OAE2. Studies such as this are invaluable in aiding our understanding by helping to show how far the OAE2 oxygen minimum zone spread in ocean surface waters.

A number of studies have correlated changes in sediments with orbital cycling to suggest that this cycling had both an impact on the timing of the start of OAE2 or variations within it (Ma et al. 2017; Mitchell et al. 2008; Poulton et al. 2015; Sageman et al. 2006). The long-term OAE2 event has been found to have taken place within periods of low eccentricity (Charbonnier et al. 2018; Kuhnt et al. 2017), with shorter-term fluctuations suggested to have been caused by the obliquity cycle. Behrooz et al. (2018), earlier in the Cretaceous than OAE2, derived ocean redox conditions from a DSDP core in the North of the South Atlantic, and showed that changes in productivity were caused by precession modulated by eccentricity. Moreover, Behrooz et al. (2018) suggest that the mechanism by which the changes occurred was the hydrological cycle driving nutrient supply to the ocean and stratification.

1.4.2 Modelling methods

Modelling of OAE2 presents a complex challenge. In order to properly represent the appropriate time period, models must be designed or modified to take into account known differences in boundary conditions when compared to a simulation of the modern climate; and make the assumption that other considerations were unchanged. These changes generally require long model spin-up times, on the order of thousands of years of model time, to allow equilibrium to be reached. An ideal model would also include all of the mechanisms that have been discussed above, so should include representations of climate, biogeochemical cycles, and weathering and nutrient runoff.

Box models

The simplest representations of the OAE2 system consist of box models (Fennel and Neumann 2001). Box models give a very simple, big-picture overview of the global ocean as a whole, in terms of a few state variables. However, they do not capture the complex interactions between physical and biogeochemical processes that are an important part of the ocean system (Claussen et al. 2002; Houghton et al. 1997). For instance, changes in ocean circulation will often be prescribed rather than being predicted. This does not prevent them from being powerful tools in aiding our understanding of past climates.

Simple, one-box models have been used in many studies in this field, such as Joo et al. (2020), Kump and Arthur (1999), and Payne and Kump (2007).

These models represent a single carbon reservoir for the whole ocean, where experiments alter the fluxes into and out of the box. While representing only the carbon system in a very simple way, these models allow easy and simple experiments on the carbon cycle to be undertaken. For instance, Kump and Arthur (1999) and (Owens et al. 2018) use such models to explore how ocean carbon burial affected the δ^{13}C isotopic signature (δ^{13}C) and atmospheric partial pressure of carbon dioxide (pCO_2). This shows two good examples of how a well designed box model enables perturbations to one part of the ocean-earth system to be better understood.

More complex, but still one-dimensional box models add both more boxes and more variables to represent these processes better. For instance, Lenton and Watson (2000) developed a multi-box model for the nitrogen, phosphate, carbon and oxygen cycles. This allowed Handoh and Lenton (2003) to show that oscillations in productivity and weathering could have been the cause of the pattern of OAEs across the Cretaceous. This is another example of the power of these simple models. It is unlikely that studies such as this, which simulated across an extremely long time period (50 Ma), would have been possible in more complex models, due to the extreme run time requirements that would be needed.

Still more complex box models add more boxes and begin to move into a more three-dimensional representation, with Flögel et al. (2011)'s twenty-seven boxes being perhaps an extreme example. Representing ocean basins in separate boxes allowed a full analysis of how a LIP may have caused OAE2, and allowed the implications of Redfield-ratio change caused by the addition of phosphate to the oceans to be studied. These increasingly more

complex models often incorporate the outputs of short general circulation model (GCM) simulations to provide otherwise unknown parameters, such as the circulation between ocean boxes (Flögel et al. 2011).

As a class of models, box models are an incredibly useful tool, combining speed with large flexibility. However, by necessity, they contain only a small subset of processes that take place in the real climate system; generally those processes which are thought to be important in relation to the issue being studied.

More Complex Models

Earth system models of intermediate complexity (EMIC) (Claussen et al. 2002) provide a more complex representation of the Earth system as a whole. Rather than including representations of only processes thought to be key to the study in question, they generally include the majority of processes found in more complex models, but often in a parameterized form to reduce complexity and increase speed (Claussen et al. 2002).

the grid enabled integrated earth system model (cGENIE) (Ridgwell and Hargreaves 2007) is an example of an EMIC which has been used extensively for the study of OAE2 (Hülse et al. 2016; Monteiro et al. 2012; Naafs et al. 2019). cGENIE makes use of common trade-offs seen in EMIC, simplifying and parameterizing circulation equations, having a simpler ecosystem than full GCMs, and generally being run at a low resolution. cGENIE does, however, have a more numerous and complex representation of ocean biogeochemical processes, such as remineralisation, compared to most, more complex models: an important consideration for OAE modelling. The in-

clusion of ocean tracers, such as H_2S, allows for easy comparison with paleoclimate data points and analysis of how these processes affect OAE2's development.

Full GCMs, generally consisting of a number of sub-models of individual parts of the Earth system coupled together, offer increasingly detailed representations of the climate system (Raju and Kumar 2020). While the complexity and number of processes modelled vary, they can generally be expected to include a fully dynamic ocean with some form of a biogeochemical model, a fully dynamic atmosphere, and a land surface model representing vegetation. As these models have improved over time, increasing resolutions and decreasing parameterization has meant they represent the world in ever-increasing detail. However, the slower run times of this type of model cause problems for modelling of OAEs and paleoclimate more generally. This is becoming a greater problem with newer models. For instance, the last Hadley Centre model, HadGEM3-GC2 (specifically the Earth system version, UKESM1 (Sellar et al. 2019)) simulates 1.87 model years per real day (Williams et al. 2015) using 1000 or more cores (for comparison, the current University of Bristol HPC computer has 14000 cores). Hence the very latest GCMs cannot be spun-up for problems such as OAEs since a single 2000 year integration (the very minimum require for spin-up) would take 3 years of continuous access to 1000 cores (or likely 6 to consider typical queue times). Also key to consider here is that this time frame is similar to that taken for typical model upgrades and therefore, within this time period, the original model choice would likely no longer be the latest version.

The Hadley Centre coupled model version 3 (HadCM3) fills a useful niche between EMIC and modern GCMs, and has been used extensively for studies of both the modern earth-ocean system and paleoclimates (Valdes et al. 2017). While running almost four orders of magnitude faster (at approximately 100 model years per wall-clock day using just 28 cores) than GCMs such as HadGEM3, HadCM3 still retains the fully coupled dynamic ocean and atmosphere characteristic of a GCM. Combining this with an ocean biogeochemical system of medium detail, it is an ideal tool for studying paleoclimate events such as OAE2, where the interaction of both biogeochemistry and the physical climate is important for a full understanding. One example of HadCM3's use in paleoclimate modelling, is Armstrong et al. (2016), who used the model to understand how atmospheric circulation and precipitation changes affected deposition of Kimmeridge Clays. This study used HadCM3L simulations to show how the position of the inter-tropical convergence zone (ITCZ) during that time period would have created tropical conditions leading to increases in organic carbon burial.

More details of HadCM3 will be given in section 2.1.

1.5 Processes affecting the development of OAE2

In the following sections of this literature review, the key mechanisms identified for their impact on OAE2 development will be summarised according to the key literature. This will be synthesised according to two key groups

of processes: biological and physical. These sets of processes are heavily linked, and the way in which ocean circulation affects biogeochemistry is examined as part of the physical section.

1.5.1 Biological ocean processes and their effects for OAE2 development

Marine productivity and export is a key driver of ocean oxygen levels, and therefore understanding ocean biological processes is key for advancing our knowledge of OAEs. In this section the way in which marine productivity is thought to mediate OAE2 development is discussed.

A range of studies consider an increase in marine productivity to have been a driving factor in the development of OAE2, for instance Jenkyns (2010), Monteiro et al. (2012), and Schlanger and Jenkyns (1976). In this scenario, an increase in marine productivity is caused by one or more of a number of mechanisms, including the addition of nutrients to the oceans or an increased supply of nutrient to the euphotic zone. This increase in productivity in the surface ocean provides large amounts of additional organic matter to the ocean below the photic zone. This organic matter falling from the surface ocean is remineralised back to ocean nutrients and carbon dioxide: a process which consumes in the first instance, oxygen (Kwon et al. 2009). Since an increase in export production has been shown to increase the speed of this microbial loop (Azam et al. 1983), it therefore follows that increasing organic mater exported from the photic zone can be expected to reduce oxygen concentration deeper in the water column. In

the context of OAE2, this mechanism is supported by studies that suggest that ocean nutrient content can be seen to increase during the OAE (Mort et al. 2007; Nederbragt et al. 2004).

Marine productivity in the modern ocean is limited by the availability of nitrate across the majority of the surface, with phosphate having a more minor limiting effect and iron becoming important in some regions of upwelling (Moore et al. 2013). However, at geological timescales the availability of phosphate is thought to be more important to that of nitrate (Tyrrell 1999), and the development of ocean anoxia is also thought to have increased the supply of the other key limiting nutrient, nitrate, to the ocean. While remineralisation of organic matter consumes oxygen in oxic conditions, when oxygen is unavailable a number of other chemical species act as electron acceptors to allow remineralisation to continue. One such reaction uses nitrate to remineralise organic matter, and is thought to increase when ocean anoxia increases (Junium and Arthur 2007) since in the reducing environment created by anoxia other chemical species must be used for remineralisation. This removal of nitrate from the ocean would favour nitrogen fixation and overall increase the supply of nitrate to the ocean (Higgins et al. 2012; Monteiro et al. 2011). This is supported by an excursion in the δ^{15}N isotopic signature (δ^{15}N) values which occurred during OAE2, suggesting much more nitrogen fixation was occurring than in the modern ocean (Junium and Arthur 2007).

Although iron supply to the ocean is thought to have been increased during OAE2 (Arthur et al. 1987; Snow et al. 2005) by increased activity of hydrothermal vents (associated with LIPs and large scale benthic vul-

canisim), it is not thought to have been the most important cause of OAE2 due to the timing of these events (Ando et al. 2009; Turgeon and Creaser 2008). Indeed, although Ando et al. (2009) agree that trace metal abundance increased around the start of OAE2, by comparing an excursion in $^{87}Sr/^{86}Sr$ with the onset of the $\delta^{13}C$ excursion, they show that the increase in oceanic trace metals predated OAE2 by 0.60 Ma.

Sedimentary accumulation rates of phosphate before OAE2 suggest that the ocean content of this key nutrient increased at this time (Mort et al. 2007); an effect caused by enhanced weathering increasing fluvial inputs of phosphate to the oceans (Jenkyns 2010; Schlanger and Jenkyns 1976). Additionally, there is evidence to suggest that sediments becoming anoxic, caused by water column anoxia above, cause phosphate to be recycled from sediments, further sustaining the OAE (Alcott et al. 2019, 2022; Tsandev and Slomp 2009). Using a model of the modern marine phosphate cycle, Tsandev and Slomp (2009) show that this mobilisation of phosphate from the sediments is an important factor in the spread of anoxia in the deep sea and that without it the spread of anoxia is either reduced, or requires an increase in the external supply of phosphate by 80 %. In this study, an OAE was able to be sustained by internal recycling of phosphate causing a positive feedback loop, rather than external forcing. Moreover, Kraal et al. (2010) and Beil et al. (2020) show this effect to be present in the sediment record where in some areas black shales depleted of phosphate relative to oxic sediments were identified, showing the removal and recycling of phosphate from these sediments. Studies have suggested that this effect acted as a positive feedback loop on the OAE, since decreasing ocean oxygen

levels allow further recycling of phosphate, and is necessary to sustain the OAE for a prolonged period (Beil et al. 2020; Tsandev and Slomp 2009; Wallmann 2003; Wallmann 2010). However some studies of modern shallow anoxic environments have shown enhanced burial of phosphate in these areas (Arning et al. 2009; Cosmidis et al. 2013), which suggests that these effects may have been limited to the deep ocean only (Beil et al. 2020).

1.5.2 Physical ocean processes and their effects on OAE2 development

The physical ocean, the circulation of ocean waters and their ventilation to the surface is extremely important in mediating an OAE (Du Vivier et al. 2014). Indeed, while the outlined effects of primary productivity on the ocean nutrient supply are widely regarded as the most important factors in OAE development (Jenkyns 2010), it is likely that changes to ocean circulation itself had a marked impact (Martin et al. 2012). Particularly important to the ocean ecosystem is the supply of nutrients to the ocean surface, and it has been suggested that during OAE2 increased upwelling supplied this (Leckie et al. 2002; Poulsen et al. 2001). In the following section, the literature on the state of the ocean circulation is discussed and the role of the ocean circulation on OAE2 development is explained.

The Cenomanian Ocean Circulation

The Cenomanian ocean circulation has often been characterised as sluggish, with older studies suggesting this slow circulation as a cause of the develop-

ment of OAE2 (Arthur and Sageman 1994; Bralower and Thierstein 1984), since a slower supply of warmer water to the deep ocean additionally implies a smaller supply of oxygen (Bralower and Thierstein 1984; Pedersen and Calvert 1990; Schlanger and Jenkyns 1976). This reduced supply of oxygen to deep ocean basins was thought to have reduced remineralisation rates in these areas and enhanced burial (Kuypers et al. 2002). The reason for this sluggishness is attributed to the reduced temperature gradient both between the equator and the poles, and between the ocean surface and bottom waters (Hay 1988). This slow circulation has been used in these studies to explain the build up of anoxia in the deep ocean simply by reducing ventilation with the surface (Bralower and Thierstein 1984).

However, although there is considerable uncertainty and little consensus in the circulation of the Cenomanian paleocean (Ladant et al. 2020; Zheng et al. 2016), more recent studies have suggested that the ocean circulation may have been stronger than previously thought (Donnadieu et al. 2016; Ladant et al. 2020; Martin et al. 2012). In this hypothesis, most recent studies (Donnadieu et al. 2016; Jenkyns 2010; Kuypers et al. 2002; Monteiro et al. 2012) subscribe to the view that enhanced primary productivity was more important, where the more active ocean circulation allows an enhanced supply of nutrient to the ocean surface, allowing increased productivity. In this way, ocean circulation remains an important factor in controlling the development of OAE2 (Zheng et al. 2016) Indeed, some studies, such as Topper et al. (2011), who used a regional model of the proto-North Atlantic, still suggest that circulation may have been the trigger of the OAE, by enhancing coastal upwelling and supply of nutrient-rich water from

the Pacific to the proto-North Atlantic. These studies explain enhanced production at the south of the proto-North Atlantic basin (Kuypers et al. 2002) to be a result of enhanced upwelling in this region combined with inflow of nutrients from the surface Pacific (Topper et al. 2011; Totman Parrish and Curtis 1982).

In this stronger circulation concept, deep water is generally thought to have been formed in both the north and south of the Pacific Ocean (Donnadieu et al. 2016; Otto-Bliesner et al. 2002; Poulsen et al. 2001), as a result of winter cooling; with sinking of waters in more equatorial seas now considered less important. While in most recent studies this deep water formation is agreed to drive a meridional overturning circulation in the large Cenomanian Pacific Ocean (Trabucho Alexandre et al. 2010), the flows of water between the ocean basins remain much discussed, both in modelling studies (Topper et al. 2011; Trabucho Alexandre et al. 2010) and in studies using proxy data (Martin et al. 2012; Robinson et al. 2010). Although previously a westward flowing global low latitude current was thought to have existed (Poulsen et al. 1998), proto-North Atlantic Ocean has been found to have a restricted, more estuarine circulation in many modelling studies (Topper et al. 2011; Trabucho Alexandre et al. 2010).

The circulation in the proto-North Atlantic basin continues to be much discussed since it is highly susceptible to highly uncertain paleogeographic differences. In addition, proxy data suggest that the development of the OAE began here, for example Monteiro et al. (2012) and Trabucho Alexandre et al. (2010) show that this area reaches anoxic conditions during the pre-OAE2 and that anoxia was reached in the whole global ocean later.

Neodymium isotopes, which are preserved in fossil fish teeth, have been used as a proxy to gain understanding of water mass distribution during OAE2. Studies have identified a number of different water masses using this method: North Atlantic (MacLeod et al. 2008), Southern Ocean (Robinson et al. 2010) and Tethyan (Soudry et al. 2006). These water masses have been used to support, variously, a supply of deep water from the Pacific to the proto-North Atlantic (Donnadieu et al. 2016), formation of deep water within the proto-North Atlantic itself (Martin et al. 2012), and a supply from the Tethys (Puceat et al. 2005; Zheng et al. 2016). The difference of opinion in interpretation of both proxy data, along with differences in modelled circulations, means the controls on the proto-North Atlantic circulation remain uncertain.

Orbital Cycling

Orbital, or Milankovitch, cycling is a well-known phenomenon causing variations in the amount of incoming solar radiation supplied to the Earth (Berger 1978). This cycling causes changes in both the earth's atmospheric and ocean systems, and therefore has the potential to cause changes in the ocean's oxygen concentration, for example to strengthen or weaken OAE2 (Meyers et al. 2012; Mitchell et al. 2008). This section explains how orbital mechanics cause solar insolation changes, and discusses previous studies on what effect this may have had on OAE2.

The mechanics of the Earth's orbit around the sun, acting through the four individual components of eccentricity, orbital precession, obliquity and axial precession, cause variations in solar insolation received by the Earth.

The cycles act predominately to vary the spatial and temporal distribution of solar radiation reaching the Earth in a given year, rather than the total amount; indeed eccentricity is the only component that changes the annual radiation at all (Berger 1978). The climatic response to these cycles have been identified for many years (Raymo and Huybers 2008) as causing regular changes in the Earth's climate, and have been the subject of many studies (e.g. Laskar et al. (1993), Hays et al. (1976) and others). They are the fundamental cause of Quaternary climate variations.

Solar insolation change from orbital cycling is a result of the combination of four orbital parameters, which combine to create a seasonal pattern. Firstly, eccentricity is the variation in the shape of the Earth orbit, as shown in Figure 1.3. Varying between a near-circular orbit and a more elliptic one, this component has cycles of approximately 100 ka and 400 ka. Since eccentricity changes the distance of the Earth to the Sun, it is the only component to change annual incoming solar radiation across the orbital cycle, with the other components acting to redistribute insolation across a year and latitudinally (Berger 1978).

Secondly, obliquity is the tilt of the Earth's orbit, in relation to the orbital plane (Figure 1.4). It's values vary between 21.80° and 24.40° (Maslin 2020), with a modern value of 23.40°. Obliquity varies on a cycle of ≈41 ka.

Thirdly, apsidal precession is the movement of the major axis of the Earth's orbital ellipsoid around the Sun (Figure 1.5). This changes the time in a year the Earth is closest to the sun and has less impact when eccentricity is low. Apsidal precession has a cycle period of ≈112 ka.

Finally, axial precession is a function of the movement of the direction

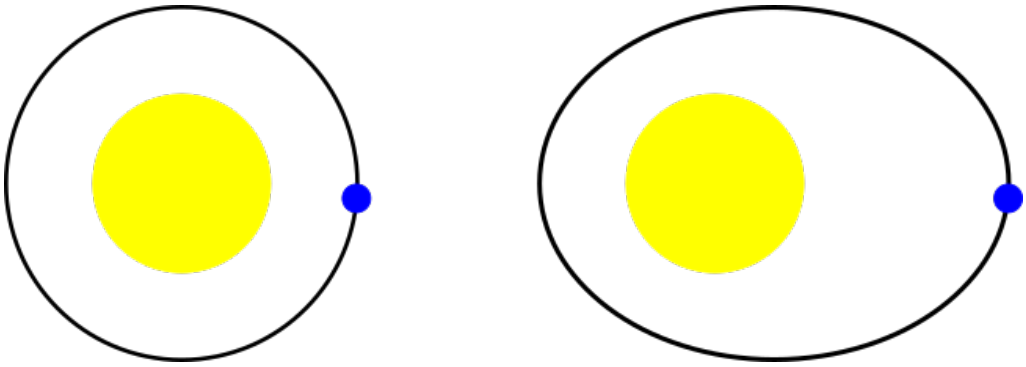

Figure 1.3: Diagram of Earth's (blue) orbit around the sun (yellow) with a circular orbit (left) and high eccentricity (right).

Figure 1.4: Diagram showing the Earth (blue) with a low obliquity (left) and a high obliquity (right). The red line shows the Earth's axis of rotation.

of Earth's rotation axis (Figure 1.6). This component changes the season during which the Earth is close to the sun, and varies at a period of ≈26 ka. When combined with apsidal precession, it results in the ellipse changing on an average ≈22 ka but this slightly varies in time.

In the modern period these orbital cycles are well known, and the orbital configuration and therefore solar insolation pattern for a given year may be calculated accurately. However, in the deep past, inherent randomness in

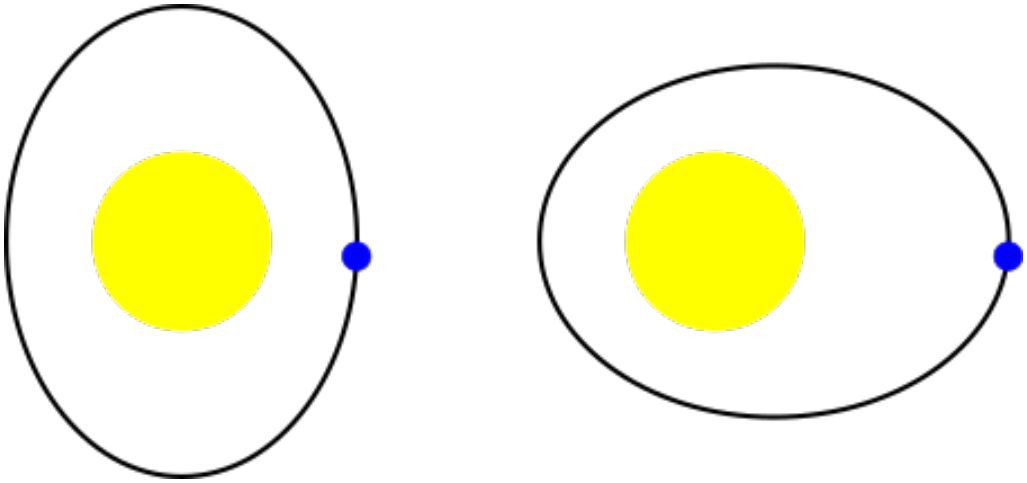

Figure 1.5: Diagram showing apsidal precession of the Earth's (blue) orbit around the sun (yellow). Both sides of the diagram show the same time of year, but at that time of year the Earth in the right-hand diagram is further from the sun.

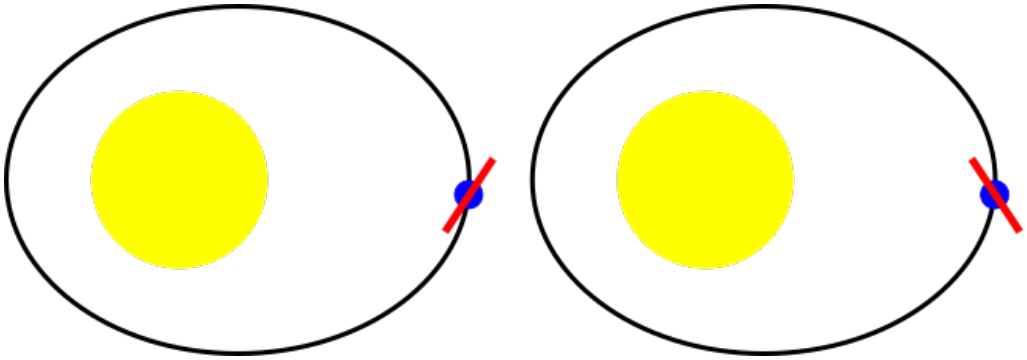

Figure 1.6: Diagram showing the effect of axial precession of the earth (blue) around the sun (yellow). Both sides of the diagram show the same time of year. The left diagram shows a northern hemisphere winter with the axis of the Earth's rotation (red) pointing away from the sun, with the right diagram showing the opposite.

the orbital system creates problems in this calculation. While there are continuing improvements in this area of research, at the current time this calculation cannot give accurate results beyond 58 Ma (Laskar et al. 2004; Ma et al. 2017; Zeebe and Lourens 2019). This leaves the time period in which OAE2 occurred uncertain, meaning it is not possible to simply calculate solar insolation for a given year although the basic pattern of change continues through time with some small changes in periodicity.

Many studies have discussed how orbital variability may have affected the onset or development of OAE2, as sedimentary stratification thought to have been caused by changes in solar insolation can be widely seen in OAE2 (Meyers et al. 2012; Mitchell et al. 2008). These studies have generally used cyclostratigraphic techniques to identity orbital cycling in sediments, and have shown that orbital conditions at the start of OAE2 made the development of an OAE during this period more likely (Batenburg et al. 2016; Meyers et al. 2012). Mitchell et al. (2008), cyclostratigraphically analysing the oscillation between organic-rich cherts and limestones, even go as far as to suggest that OAEs themselves may be periodic events driven by orbital cycling, linking OAEs to long stable periods of low solar insolation caused by eccentricity variations.

Orbital variability is often thought of as modulating OAE2 sediment deposition through changes in continental weathering and sediment input to the ocean through rivers (Batenburg et al. 2016; Charbonnier et al. 2018) since the sedimentary layers themselves are associated with other signs of more rapid weathering (Dummann et al. 2021). In this model, outflow from rivers is increased and the input of nutrients to the ocean stimulates primary

production (Beckmann et al. 2005) and consequently anoxia (Beckmann et al. 2005; Behrooz et al. 2018; Flögel et al. 2008). The rapid weathering necessary for this model is thought to be a result of movement of the ITCZ, caused by eccentricity (Sarr et al. 2022).

The spatial temperature changes caused by orbital forcing also have a large scope for causing changes in the circulation of the oceans, and thereby ocean oxygen levels. One mechanism by which orbital forcing could affect the ocean circulation is by the modification of the strength and location of the formation of deep water (Meyers et al. 2012), caused by obliquity due to it's larger impact on the high latitudes where deep water formation takes place. This hypothesis is supported by a modelling study in Sarr et al. (2022) whose application of the IPSL-CM5A2 Earth System Model showed that deep water formation changes, caused by variation in the precipitation - evaporation moisture balance, had an impact on the spatial spread of oxygen. While orbitally induced warming could have increased ocean surface stratification and reduced ventilation of the deep oceans (Helmond et al. 2015), most studies agree this effect is unlikely to have occurred alone, and that the biological effects discussed in this literature review, would have occurred in tandem with circulation changes (Jenkyns 2010; Joo et al. 2020; Monteiro et al. 2012).

1.6 Summary

This literature review has introduced key concepts on which the rest of this thesis is built upon. Ocean anoxic events have been introduced (section

1.1), with a particular focus on OAE2 (section 1.2), the largest and most widespread of the Cretaceous OAEs. A number of key ocean processes, attributed for their impact on the onset and development of OAE2 have been introduced. These are broadly split into physical processes which control the Cenomanian ocean circulation (section 1.5.2) and changes in ocean biogeochemistry which affect euphotic zone export (section 1.5.1). However it is important to remember that all these processes are interlinked, particularly that the ocean circulation is able to control biological production by mediating the supply of nutrients to the surface ocean.

OAE2 modelling (section 1.4.2) and proxy studies (section 1.4.1) are widely used methods in the study of OAE2, with modelling studies predicting the Cenomanian climate from a mechanistic understanding of processes in the modern day, and proxy studies using sediments to gain an understanding of what the climate was like from the evidence laid down at the time. However, the review also showed that there have been very few GCM based studies of OAE2 which included a direct representation of biogeochemical processes.

Whilst our understanding of OAE2 is expanding, there remains a lack of certainty regarding which mechanisms and processes were essential for the development of an OAE, which contributes to it's development and continuation, and which were inconsequential or only relevant for a particular OAE.

This thesis aims to contribute to some of the key questions which continue to be discussed in OAE2 literature. Of notable interest is the particular set of conditions in the Cenomanian which made it more likely that

an OAE would develop, how the ocean circulation and biogeochemistry interacted to cause ocean anoxia, and to what extent models used for the study of OAE2 are able to capture the complex ecosystem dynamics which occurred during OAE2.

The purpose of this thesis is to respond to these identified research gaps, to present a series of high spatial resolution full-GCM modelling experiments, to enable us to consider the development of OAE2, with a particular focus on the key biological and physical processes. A modelling approach is used for this study, to allow us to fully quantify the strength of the various processes and mechanisms of change.

1.7 Thesis aims, research questions and objectives

With consideration to the current evidence and literature identified here in regard to the physical and biogeochemical causes of OAE2, this section will highlight the key aims, research questions and objectives of this thesis.

1.7.1 Thesis aims and structure

Overall, this thesis aims to investigate the interaction between the physical climate system and biogeochemistry, to build on our current understanding of the key causes and effects of OAE2. To achieve this aim, we use a relatively high resolution, high complexity model: HadCM3L, to be outlined in section 2.1. This allows us to focus on how the ocean biogeochemical

system of OAE2 is affected by the physical climate, and how improvements or changes in modelling aid our understanding of OAE2.

This thesis is presented through three standalone chapters, written to answer three key, research questions which are outlined in the following sections: 1.7.2 - 1.7.4. Each chapter contains its own brief literature review of the topic, as well as model description and methodology. The final chapter concludes the thesis, discussing the main results from each chapter, and suggesting further work.

1.7.2 Research Question 1: What is the role of paleogeography in mediating the development of OAE2?

Ocean paleogeography: the position and size of the continents and depth of the oceans, has been widely noted as key to ocean circulation control, which points to its potential scope to affect the development of OAE2 by changing ocean ventilation patterns. Whilst earlier applications in this field have been made to improve our understanding of the role of paleogeography in OAE2 development, these previous studies have typically used box models or models of relatively low resolution. These models suffer either from a lack of representation of ocean circulation or a circulation with simplified and parameterised ocean motion equations when compared to a full general circulation model (GCM).

Therefore, the first research chapter (chapter 3) of this thesis: "Paleogeographical Preconditioning of the Late Cretaceous Oceanic Anoxic Event

(OAE2)", examines the affect of global paleogeography on the development of OAE2. A comparison is made between the Cenomanian pre-OAE2 general circulation model (GCM) simulations, where model oxygen levels are depleted in the proto-North Atlantic, with simulations of the Maastrichtian, where they are not. The differences between these simulations, and their causes, are discussed in depth in order to enhance our understanding of how ocean paleogeography may have affected OAE development.

1.7.3 Research Question 2: How do contrasting orbital scenarios affect OAE2?

Numerous studies have used the stratigraphic analysis of sediments to examine orbital cycling during OAE2, with a particular focus on how this may have affected the development and strength of the OAE. Orbital cycling has been shown to be present during OAE2, however the mechanisms by which it occurred, and the extent to which it was an important driver in controlling the onset and decline of the OAE itself remains discussed. In addition, very few modelling studies have examined how orbital cycling may have caused changes in ocean anoxia, and in particular OAE2 has not been extensively studied in this way.

To expand on this, the second research chapter (chapter 4) of this thesis: "The Effect of Orbital Cycling on the Development of OAE2" explores how orbital cycling is able to affect ocean benthic oxygen levels. A series of GCM simulations with differing orbital parameters were produced, and the change in ocean oxygen concentration for each scenario was examined. Two

simulations, which represent two extreme but real orbital scenarios, were analysed in detail to explore the mechanisms by which orbital change is able to alter deep ocean oxygen levels. Using these simulations, this chapter presents important results, demonstrating the role of ocean circulation as a mechanism linking orbital change to ocean oxygen.

1.7.4 Research Question 3: How do differences in the representation of biogeochemical processes of OAE2 affect our understanding of it?

It is widely understood that our knowledge of ocean primary production and export is vital in building our understanding of how OAE2 developed; additional export and therefore remineralisation being an important mechanism for lowering ocean oxygen levels. However it cannot be ignored that, within the existing modelling literature, models used to examine ocean anoxia, parameterise ocean biogeochemistry in very different ways, with more and less complex representations used depending of the model in question. It is important for us to understand what causes the models to respond in different ways since this will enable us to better understand how well the models represent the OAE and what this means for our understanding of the development of the OAE.

To examine how these differences in models affect ocean oxygen concentration, the third research chapter of this thesis (chapter 5): "The role of physical and biological complexity in modelling OAE2" compares the response of ocean oxygen levels in the model used throughout this the-

sis: HadCM3L, and a contrasting model, which has also been widely used for OAE2 simulations: cGENIE. HadCM3L and cGENIE treat the parameterisation of biological processes in different ways. HadCM3L contains a simple nutrient-phytoplankton-zooplankton-detritus (NPZD) ecosystem, while cGENIE has a much simpler representation of biological processes and exports from the euphotic zone at a fixed ratio controlled by nutrient availability, light and temperature. Through these comparisons, this study discusses the key differences between the two models which raises a number of key questions that should be considered when modelling ocean anoxia.

Chapter 2

Methods

Whilst the respective three research chapters of this thesis serve to be standalone, with model selection and configurations detailed within each study, this methods chapter aims to provide an overview of the modelling methods selected for this thesis. This includes key model selection and configuration that is relevant for all three of the research chapters, and provides additional detail for reference.

2.1 HadCM3L

The HadCM3L was selected for all three chapters of this study, since it is able to simulate the OAE2 time period at relatively high resolution with detailed representation of the physical climate and ocean biogeochemistry. It is one of only a handful of models that represent the physical climate system using equations fully traceable to CMIP5 and CMIP6 models, that includes a representation of ocean carbon cycle, and can be run for the long

timescales needed for paleo integrations. The development and characteristics of HadCM3L are outlined in this section.

The HadCM3 group of climate models were originally developed by the Hadley Centre, part of the UK Met Office. Presented in Gordon et al. (2000), HadCM3 was one of the first GCMs to be able to run without climatic drift (Gordon et al. 2000; Valdes et al. 2017). It has been used in a large number of studies since its development (Pope et al. 2000; Spencer et al. 2007; Stott and Kettleborough 2002; Valdes et al. 2017), and consequently its weaknesses have been studied extensively and are very well known. Despite having been superseded for modern simulations by various iterations of the HadGEM families of models of which UKESM1 (Sellar et al. 2019) is the most recent iteration, HadCM3 remains an important tool for paleoclimate modelling due to its useful combination of speed and detail (Valdes et al. 2017).

Despite the cessation of the development and use of HadCM3 by the Met Office, it continues to be used and developed in the Bristol Research Initiative for the Dynamic Global Environment (BRIDGE) research group at the University of Bristol and in other research groups. Valdes et al. (2017) examines in detail the differences between various configurations of HadCM3 which remain in use. Valdes et al. (2017) also show that the skill at simulating present day climate is comparable to the more modern, CMIP5, models. All of the model simulations in this project made use of the HadCM3B with a lower resolution ocean (HadCM3BL) configuration, using the lower-resolution ocean but the same resolution as the atmosphere resolution of HadCM3.

2.1.1 General Model Characteristics

HadCM3BL as used in this study has a fully dynamic atmosphere and ocean with a resolution of $3.75° \times 2.50°$, giving 96×73 grid cells across the world atmosphere and ocean (Cox et al. 2000; Valdes et al. 2017). Vertically, HadCM3BL has 19 levels in the atmosphere and 20 in the ocean, with thinner levels near the ocean surface to better represent the euphotic zone (Valdes et al. 2017).

Ocean biogeochemistry and carbon modelling in HadCM3 requires the addition of an optional ocean ecosystem model, the Hadley Centre Ocean Carbon Cycle (HadOCC). Originally presented in Palmer and Totterdell (2001), HadOCC adds a NPZD ecosystem to the model, the main state variables being nutrient, phytoplankton, zooplankton and detritus; represented in terms of nitrogen units, and alkalinity and total dissolved inorganic carbon (TCO_2) (Palmer and Totterdell 2001). All of these variables are moved around the model grid as ocean tracers, with biological processes occurring each time step.

HadOCC makes the assumption of a nitrogen-limited ocean and calculates the carbon content of phytoplankton, nutrient and detritus at a fixed ratio (Palmer and Totterdell 2001). A summary of the biological processes represented in the model is as follows, with the equations and greater detail of these processes available in the appendix of Palmer and Totterdell (2001):

Primary production occurs in the surface ocean and is limited by nutrient, light and temperature. Mortality of both phytoplankton and zoo-

plankton contributes to detritus, along with excretion from zooplankton. Zooplankton consume both phytoplankton and detritus by a Holling type three relationship, in proportion to the availability of each. Detritus sinks at a fixed rate; the only HadOCC variable to do so. It is remineralised back to nutrient at two fixed rates: faster in the surface ocean (above 164.80 m) and slower below this level.

HadOCC as described by Palmer and Totterdell (2001) does not include a representation of dissolved oxygen; however, the work of Williams et al. (2014) to add oxygen to Fast Met Office UK Universities Simulator (FAMOUS) has been previously adapted to run as part of HadCM3BL. This module adds oxygen as a tracer in the ocean, with representation of the flux of oxygen across the surface ocean, and the production or consumption of oxygen being in proportion to the flows of dissolved inorganic carbon (DIC) in HadOCC. Oxygen is produced in the ocean in proportion to the amount of production which takes place, and is removed in proportion to remineralisation, and other processes which produce DIC directly (zooplankton and phytoplankton excretion, mortality and respiration) (Williams et al. 2014). This representation of oxygen in the ocean provides an extremely useful tool for understanding the spatial distribution of oxygen in the ocean. It should be noted however that this module does not change the amount of remineralisation that occurs in the model ocean; while oxygen is prevented from becoming negative, a lack of oxygen does not prevent remineralisation from occurring.

It should also be added that the ocean model of FAMOUS is identical to the ocean component of HadCM3L (same resolution, and same physical pa-

rameterisations) so that the fundamental behaviours are similar. However, we decided to use HadCM3L for this project because the lower resolution of the FAMOUS atmosphere (7.5 x 5 degrees x 11 levels) does influence the skill of the model. Valdes et al. (2017) show that the FAMOUS model has lower skill (in simulating present day climate) than any model that is part of CMIP5. Since one of our overall aims was to model OAEs using a state-of-the-art model, we felt that it was better to use HadCM3L rather than FAMOUS.

The model configuration described above was identical for all HadCM3BL simulations used in this project. This basic model configuration was run with a different paleogeography to modern simulations representing the different time periods studied, replacing the modern land-sea mask, bathymetry and topography with that of the time period. These paleogeographies are developed according to the methods of Markwick and Valdes (2004). The Cenomanian paleography used in all three chapters for simulations of OAE2 was developed as part of this project from data provided by CGG Robertson. This involved placing the bathymetry onto the HadCM3BL model grid, with appropriate smoothing to prevent large discontinuities in the ocean floor. The Maastrichtian paleogeography used in Chapter 3 was previously developed at BRIDGE, also from CGG Robertson data. These Maastrichtian boundary conditions have been used in previous studies with CGG Robertson.

Other changes, and the rationale behind them, from the basic model configuration described here are detailed as appropriate in each chapter of this thesis.

2.2 cGENIE

The main purpose of this thesis is to examine the representation of OAE events within a relatively high resolution model. However, solely in Chapter 5, the cGENIE (Ridgwell et al. 2007) model is used for comparison with HadCM3L and we therefore briefly describe it here.

cGENIE has seen extensive use in studies of OAE2 (Hülse et al. 2016; Monteiro et al. 2012; Naafs et al. 2019), and other OAEs (Adloff 2021; Adloff et al. 2021). As a fast EMIC able to model ocean biogeochemical cycling, it is well suited to this task as it is able to simulate extremely rapidly the long time periods required, and can provide simulation of both the physical ocean and ocean ecosystem. However, in order to achieve far greater speeds than GCMs it contains a simplified model of the ocean circulation and atmosphere detailed below, and is usually used at a much lower resolution that HadCM3L and other GCMs.

It was chosen for comparison in this thesis since it is a model which has been frequently used to study OAE2, which therefore makes it a useful comparison for the new GCM simulations presented in chapter 5.

2.2.1 General Model Characteristics

cGENIE is a flexible EMIC, which includes a 3D ocean circulation with a reduced set of equations based on frictional-geostrophic physics coupled with a 2D energy-moisture-balance model of the atmosphere and a dynamic sea ice model. This physical model framework (C-GOLDSTEIN) is described in (Edwards and Marsh 2005). The use of geostrophic balance means that the

tropical ocean circulation is poorly represented. Moreover, the replacement of momentum advection with a simple frictional term leads to a distortion of tropical Kelvin waves (Edwards and Marsh 2005). Similarly, the replacement of a dynamic atmosphere with a 2-D energy-moisture balance model means that the atmospheric circulation is poorly represented (indeed cGENIE requires GCM input of wind stress). In addition, weaknesses of the moisture transport parameterisation requires an additional "tuneable" constant which is the Pacific-Atlantic moisture transport. Without including this term, the modern day Atlantic circulation would be wrong.

cGENIE is used in this thesis with a 36x36 cell grid, giving increments of 10° in longitude; in latitude, cells are ≈3.20° at the equator but 19.20 at the poles, increasing with the sine of latitude. Although it is possible to run cGENIE at higher resolutions, this is not typically useful since the reduced physics prevents a more detailed representation (Marsh et al. 2015). The use of constant changes in sine of latitude implies that the polar resolution of cGENIE is much poorer than HadCM3L (which uses constant increments in latitude). In the ocean, the model has eight levels unequally spaced to be narrower at the ocean surface.

The version of cGENIE used here is fully described in Ridgwell et al. (2007) and includes a biogeochemical model describing many ocean tracers. This allows cGENIE to model ocean production export and oxygen concentration; key processes which make it useful for modelling OAE2. Ocean production and export occurs at a fixed rate relative to the availability of ocean nutrient, and is limited by light availability and ocean temperature. For more details of the scheme, see chapter 5.

Chapter 3

Paleogeographical Preconditioning of the Late Cretaceous Oceanic Anoxic Event (OAE2)

3.1 Preface

This chapter has been submitted as a paper to Paleoceanography where it is awaiting our response to review comments. For the completion of this work, Johnny Williams, ran the Maastrichtian simulations, updated HadCM3L to work with the oxygen update originally developed for FAMOUS, and contributed to experiment design. Alexandra Ashley and Jim Harris (CGG Roberson) provided the paleogeographies used in the simulations. In addition, Paul Valdes provided technical assistance with the model simulations,

and along with Fanny Monteiro, provided assistance, feedback and advice for all aspects of the study. The final manuscript was written by Alexander Manning with contributions from all co-authors and has been adjusted for inclusion in this thesis in line with the content of the other chapters.

This chapter includes a brief description of the model configuration; a fuller explanation of the HadCM3 model can be found in chapter 2. Likewise, a fuller explanation of processes affecting OAEs is found in chapter 1, while here the explanation is limited to that required for understanding in the context of paleogeography.

3.2 Abstract

Widespread OAEs are a striking feature of the Mesozoic carbon cycle, with the Cenomanian OAE2 ($\sim$ 93.5 Ma) being a well-studied example of these events. The precise triggers of these events are still debated but ocean circulation, which controls most sources and sinks of oxygen at depth, is likely to play an important role in the formation of OAEs. We present results from a 3D global, coupled ocean-atmosphere-carbon climate model, which represents the physics and biogeochemistry of the Earth system at relatively high spatial resolution. We focus on the effect of paleogeography on the development of OAE2, by comparing the Cenomanian with the Maastrichtian (66 Ma), a time period when ocean oxygen levels were much higher. The model demonstrates that the paleogeography plays a critical role in controlling the ocean circulation and oxygen supply to the deep ocean, with the proto-North Atlantic basin at the Cenomanian particularly susceptible to

low oxygen concentrations in the deep ocean. Specifically, gateway differences in the tropics and sub-tropics lead to a reduced input of high-latitude, oxygenated waters into the proto-North Atlantic basin when compared to the Maastrichtian. This restricted basin also results in an accumulation of nutrients, which, along with stronger upwelling, amplifies primary production and oxygen consumption in the equatorial Atlantic. We conclude that the paleogeography of the Cenomanian "preconditioned" the North-proto Atlantic to have lower oxygen, thus implying that the required trigger for a full OAE may have been smaller than during other time periods.

3.3 Introduction

OAEs are critical paleoclimatic events, during which large parts of the ocean experience intense deoxygenation. They principally occurred in the Cretaceous and Jurassic periods of the Mesozoic era (Schlanger and Jenkyns 1976). These events are characterised by positive carbon excursions indicative of strong carbon cycle perturbations. They are also associated with a widespread sediment deposition of black shales, which are organic carbon-rich sediments indicative of deposition in anaerobic conditions (Schlanger and Jenkyns 1976). These events are also associated with periods of increased volcanism (Adams et al. 2010), warming (Friedrich et al. 2012), and often increases in nutrient supply to the oceans (Meyer and Kump 2008). One of the most recent OAE events (OAE2) occurred at the Cenomanian-Turonian boundary, where black shale deposition was present in most oceanic basins (Jarvis et al. 2011). Preceding OAE2, black shales deposition was

still present, but much less widespread, with evidence for anaerobic conditions in the equatorial Atlantic. (Jenkyns 2010) This black shale deposition contrasts with the situation later in the Cretaceous, and specifically at the Campanian-Maastrichtian boundary, where benthic waters are thought to have been relatively rich in oxygen (Friedrich et al. 2005).

OAEs have been extensively studied and modelled, and numerous theories put forward on their existence (Joo et al. 2020). A number of factors are thought to contribute towards increasing the likelihood of an OAE, including reduced ocean circulation, warming temperature, increased nutrient run-off, and release of atmospheric carbon dioxide (Arthur and Sageman 2011). These factors are thought to interact and combine to reduce the oxygen concentration in the deep ocean. However their relative importance is poorly understood and richly debated, and likely to differ between separate Oceanic Anoxic Events. There is some consensus to suggest that the quantity and spatial distribution of nutrients delivered to the ocean is a dominant control on the development of OAEs (Jenkyns 2010; Joo et al. 2020; Monteiro et al. 2012). This increase in nutrient supply is generally thought to derive from increased weathering, resulting from increased volcanism, accompanied by sediment sources (Jenkyns 2010; Mort et al. 2007).

Modelling studies have been used to assess the interactions between climate, biogeochemistry and ocean anoxia during OAEs, with different degrees of representation of the coupling between nutrient supply, ocean production, warming and ocean currents. The majority of published biogeochemical modelling studies have relied on box models (e.g. Flögel et al. (2011), Joo et al. (2020), Kump and Arthur (1999), and Tsandev and

Slomp (2009)). Changes in the C:N ratio is generally pinpointed (Flögel et al. 2011; Tsandev and Slomp 2009) as the main trigger of production and therefore extra burial of organic matter.

However, box models have no (or relatively simple in the case of Flögel et al. (2011)) spatial structure, preventing a full assessment of the spatial variability of ocean redox-stage observed during OAEs. For this we need a spatially resolved model. Monteiro et al. (2012) studied the spatial variability of anoxia by using a physical-biogeochemical Earth system model at relatively low spatial resolution. This study compared the impact on ocean deoxygenation due to higher temperatures (as a result of CO_2 changes) and higher marine productivity (driven by higher nutrient supply). They concluded that temperature increase alone was insufficient and that increased nutrients were the dominant control on the spread of anoxia and euxinia observed during OAE2. They also noted the role of paleogeography in controlling the spatial distribution of anoxia (by deepening the Caribbean gateway), although the low model resolution and the use of frictional-geostrophic equations might impact the representation of ocean circulation.

Another study applied the same model to examine how euxinic events over the Phanerozoic varied with different paleogeographies (Meyer and Kump 2008). This study argued that the observed spread of euxinia can only be caused by changes in nutrient supply and that changes in ocean stagnation could not account for the changes during euxinic events. However, their study was focused on these events and did not consider the impact of paleogeography on "pre-conditioning" low oxygen concentrations

in the deep ocean.

Paleogeography can have an important role in the distribution and level of oxygen present in the ocean, by influencing ocean circulation and hence oxygen supply to the deep ocean. In general paleogeographic changes do not happen rapidly and hence cannot cause an OAE itself. However, because ocean currents have a strong influence on oxygen supply, changes in paleogeography could play a role in pre-conditioning certain time periods to be particularly favourable for OAE events.

The only exception to the speed of change is paleogeographic changes associated with sea-level rise, which can happen on timescales equivalent to an event. Bjerrum et al. (2006) used a box model to show that changes in sea level could have a significant impact on carbon burial and ocean oxygen levels due to the resulting changes in the area of shelf seas. Arthur and Sageman (2011) argue that sea-level rise may have controlled the development of organic-rich sediments during OAE2. They suggested that sea-level change influenced the depth of the sills, and subsequently influenced ocean circulation and oxygen minimum zones. They did not perform any modelling as part of this study and thus it remains a conceptual model only.

Although there have been few studies using full 3-D biogeochemical GCMs, a number of studies have used atmosphere-ocean GCMs without biogeochemistry to demonstrate the important role of paleogeography on ocean currents, using relatively high spatial resolution. They show that the connection between the North and South Atlantic is particularly important in determining ocean currents during OAE2 (Poulsen et al. 2001). Similarly,

Donnadieu et al. (2016) and Ladant et al. (2020) argue that ocean currents are dramatically affected by differences in continental configuration seen in the time periods of their study (94 and 71Ma). Specifically, they show that changes in sill depths can have major impacts on ocean circulation and they then argue that this controls deep ocean oxygen levels. Trabucho Alexandre et al. (2010) also used a physics only GCM to argue that paleogeographic conditions during the mid-Cretaceous created a nutrient trap in the North Atlantic, with strong upwelling along the southern margin enhancing black shale formation.

While these models represent ocean circulation within the relatively high spatial resolution, they do not include any ocean biogeochemistry so we can only speculate on the role of ocean currents onto the ocean redox-state. Here, we investigate the role of paleogeography on ocean circulation and ocean oxygen distribution by comparing the Cenomanian period, which experienced OAE2 and presented low oxygen levels in the Equatorial Atlantic before the onset, with the Maastrichtian period, which had well-oxygenated water globally. To investigate this, we use a fully coupled 3-D atmosphere-ocean biogeochemical Earth System model. To our knowledge, this is the first fully-coupled full complexity Earth system model with a comprehensive representation of the physical climate system and a representation of biogeochemistry to investigate the role of continental configuration in preconditioning anoxia of the Cretaceous ocean.

3.4 Methods

3.4.1 Model Description

We use the climate model HadCM3L coupled to a new oxygen cycling scheme (Williams et al. 2014) and a NPZD biogeochemical cycling scheme (Palmer and Totterdell 2001). HadCM3L uses the atmosphere component of HadCM3 (Pope et al. 2000) at a resolution of 3.75^o x 2.5^o x 19 unequally spaced levels in the vertical (more levels near the surface and near the tropopause). It is coupled to a full primitive equation ocean model also at 3.75^o x 2.5^o and 20 unequally spaced levels in the vertical, with more levels near the surface (c.f. HadCM3 uses 1.25^o x 1.25^o degree resolution but this would make it to computationally expensive for the lengths of run required). The model is also coupled to a terrestrial carbon cycle model, called TRIFFID, which simulates the growth and decay of vegetation and the creation and storage of soil carbon. However, it does not represent the longer-term storage of peats and permafrost. The precise version of this model is referred to as HadCM3LB-M2.1Da and is fully described in Valdes et al. (2017). HadCM3L's performance is comparable to other CMIP5 models, global air and surface temperature, and ocean temperature and salinity (Valdes et al. 2017).

The model is coupled to a simple ocean carbon cycle model, HadOCC (Palmer and Totterdell 2001). The HadOCC model is a biogeochemical module that features an explicit representation of the marine ecosystem, which is assumed to be limited by nitrogen availability. The biogeochemical compartments include dissolved nutrient, total CO_2, total alkalinity,

phytoplankton, zooplankton and detritus. In the current version of the model, the atmospheric CO_2 concentration is unaltered by feedbacks with the ocean (i.e. the ocean carbon cycle "sees" the atmospheric concentrations but any outgassing or absorption of carbon into the ocean does not change the atmospheric CO_2). Hence atmospheric CO_2 is a specified constant in all simulations. An early version of this model was used in some of the pioneering studies of the feedbacks between the carbon cycle and future climate change (Cox et al. 2000).

The model also represents oxygen utilisation, based on Williams et al. (2014), who introduced an oxygen cycle into the Fast Met Office UK Universities Simulator (FAMOUS). We adapted the code for HadCM3L but all of the processes and mechanisms are unchanged from Williams et al. (2014). See Figures 3.14 and 3.15 in the supplementary material for a validation of this configuration's representation of modern ocean oxygen. The oxygen model follows that of the second phase of the Ocean Carbon-Cycle Model Intercomparison Project, OCMIP. It represents the air-sea exchange of oxygen (and CO_2) and the rate of biological production of oxygen is simply proportional to the rate of consumption of dissolved inorganic carbon. The model does not represent euxinia and in this paper we used a global nutrient inventory equivalent to the modern ocean (so as to leave the validation and tuning of the NPZD model as described in Palmer and Totterdell (2001)). It is therefore important to understand that the simulations shown in this paper do not represent the development of a 'full' OAE, but instead indicate precursor low oxygen conditions seen just before an OAE occurs.

Overall, HadCM3L has a less complex representation of biogeochemical

cycling when compared with other models used to study OAEs (such as GENIE and some more complex box models), but this is balanced by an improved representation of the physics and atmospheric and ocean circulation. It is also appreciably higher spatial resolution than some previous modelling studies of OAEs, yet is sufficiently efficient computationally to perform the long runs required (Valdes et al. 2017). This makes HadCM3L an excellent tool for understanding interactions between biochemical cycles and ocean and atmospheric circulation.

3.4.2 Model Configuration

A number of model runs were undertaken, simulating different scenarios at the onset of OAE2 in the Cenomanian, and were compared with equivalent runs simulating the Maastrichtian. We chose the Maastrichtian as the most recent end-member of Cretaceous paleogeographies. In practice, we will show that the key characteristic is the paleogeographic structure around the tropical proto-Atlantic.

The Cenomanian and Maastrichtian simulations use high-resolution paleogeography constructed and provided by CGG Roberston using the methods described in Markwick and Valdes (2004). These high-resolution paleogeographies were converted onto the resolution of the climate model using simple area and volume conserving regridding techniques.

The "baseline" simulations run used three times pre-industrial CO_2 concentrations (840 ppmv). We also ran with higher and lower levels but the conclusions were qualitatively similar and hence in this paper we focus en-

tirely on the 3xCO_2 simulations. This allows us to directly compare the effects of paleogeographic change only. While carbon dioxide levels in the Maastrichtian are thought to have been lower than in the Cenomanian, the aim of this paper is to highlight the important role of paleogeography and not perform the most realistic simulations for any time period.

The two runs have different continental configuration, topography and bathymetry. Of particular importance to ocean simulations are the continental configuration and bathymetry, which is shown in Figure 3.1. In the Cenomanian bathymetry, the proto-North Atlantic is much more enclosed and restricted, both by the presence of a sill at the western edge and the restriction of the channel between South America and Africa. The presence of these features is supported in a paleogeography of the same time period by Scotese (2014). In contrast, the Maastrichtian basin is much more open to the South and West, however with some continuing restrictions to the east of the proto North Atlantic. These paleogeoraphies have enclosed lakes not connected to the global ocean. While in a model simulation this would ordinarily cause the drift of salinity, a correction, described in Valdes et al. (2021), is applied whereby lots water is returned evenly across the ocean surface.

For both runs, the ocean carbon model was originally initialised with modern levels of ocean nutrient, oxygen and other tracers. The ocean nutrient tracer is conserved in the model and there is no loss or gain of nutrient from river runoff or sedimentation.

All simulations were run for at least 2000 years, starting from previous simulations with a physical ocean at equilibrium for those time periods of at

least 4000 years. Trends in temperature are uniformly small and trends in volume integrated ocean oxygen are less than $2\,\mu mol_{O_2}\,L^{-1}$ per millennium. All results are the average of the last 100 years of the simulation.

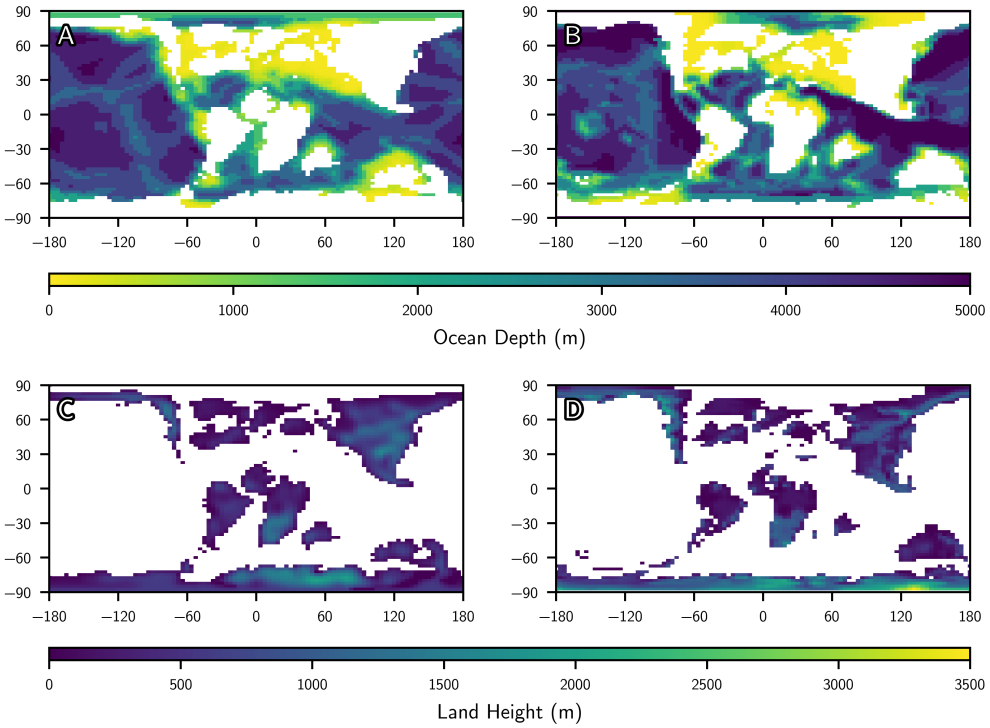

Figure 3.1: Ocean bathymetry and orography used in Cenomanian (A and C) and Maastrichtian (B and D) model runs. A and B show the model depth of the ocean floor at the resolution of the GCM, with land mask shown in white. C and D show the height of model topography above sea level, with the ocean mask shown in white.

3.5 Results

Overall, the differences in paleogeography make a relatively small impact on the global mean climate and biogeochemistry. The global mean sea surface temperatures are 24.40 °C for the Maastrichtian and 26.30 °C for the Ceno-

manian, comparable to estimates in current literature (Linnert et al. 2014; Robinson et al. 2019; Thibault et al. 2016). The slightly warmer Cenomanian is largely due to the high Northern latitudes. The Maastrichtian has a significantly larger Arctic ocean which is enclosed, and is colder with extensive sea ice. Over most of the rest of the ocean, the differences are much smaller and typically are less than 1 °C.

3.5.1 Distribution of oxygen

The differences in temperature are reflected in differences in surface ocean oxygen concentrations The global mean concentrations in the Maastrichtian is 226.80 $\mu mol_{O_2} L^{-1}$ and in the Cenomanian is 217.90 $\mu mol_{O_2} L^{-1}$. Again the largest differences are in the Arctic ocean ($\approx$40 $\mu mol_{O_2} L^{-1}$) whereas for most of the rest of the ocean the differences are less than 10 $\mu mol_{O_2} L^{-1}$.

At deeper levels, globally the Maastrichtian remains colder than the Cenomanian but the magnitude of the difference is much smaller. At 996m, the global mean difference is 0.60 °C which largely is because the area of the high Northern latitude ocean is much smaller and hence does not contribute to the global mean. At 2731m, the difference is very small (0.20 °C) and has reversed (i.e. the Maastrichtian is slightly warmer than the Cenomanian. At these depths, there is no Arctic ocean or N.Atlantic ocean and the global average is essentially the Pacific. In our model, there is a shift in the location of deep water formation around the Antarctic, from the South Pacific to South Atlantic (Figure 3.4) and it is this that drives the (small) change in global deep ocean temperatures.

The global mean differences in deep ocean oxygen concentrations partly reflect the temperature differences. At 996m, the global means are very similar ($173\,\mu mol_{O_2}\,L^{-1}$ for the Maastrichtian versus $172\,\mu mol_{O_2}\,L^{-1}$ for the Cenomanian. Similarly, at 2731m the difference is reversed with the Maastrichtian having slightly lower concentrations than the Cenomanian ($185\,\mu mol_{O_2}\,L^{-1}$ vs $198\,\mu mol_{O_2}\,L^{-1}$).

However, the global mean deep oxygen concentrations mask major regional changes between the two time periods, the foremost of which is the lower proto-North Atlantic deep ocean oxygen concentration in the Cenomanian compared to the Maastrichtian. Figure 3.2 shows the modelled annual mean seafloor oxygen concentrations for the two time periods. We also compare the results of our model simulations with the evidence of seafloor oxygenation. Although we have not optimised our simulations for the periods (particularly we have not changed CO_2 and nutrient inputs are unchanged so productivity is unchanged), it is important to show that the simulations are still broadly realistic. Comparison is undertaken with evidence of pre-OAE2 oxygenation, rather than conditions during OAE2, as this study focuses on the preconditioning of the ocean before the OAE rather than the perturbed system during the event. Evidence of pre-OAE2 oxic and anoxic conditions, compiled by Monteiro et al. (2012) are compared with modelled oxygen at the seafloor in Figure 3.2A. There is no evidence of benthic anoxia in the Maastrichtian, and therefore no data points are shown on 3.2B (Friedrich et al. 2005).

In the Cenomanian, model predictions for oxygen compare well with the available, if sparse, data points. Low oxygen levels in the models results

are centred around the proto-North Atlantic ocean with a typical concentration of $\approx 50\,\mu mol_{O_2}\,L^{-1}$, but with a small region between S.America and N. Africa where concentrations are less than $10\,\mu mol_{O_2}\,L^{-1}$. These regions encompass all of the points observed to have low oxygen levels pre-OAE2 3.2A. Modelled benthic low oxygen levels are confined to this central region, and to the Western edge of the western interior seaway (WIS). Modelled low oxygen levels are not seen to spread outside this central region, and in general seafloor oxygen levels are much higher outside of this area, with concentrations ranging between $140\,\mu mol_{O_2}\,L^{-1}$ to $230\,\mu mol_{O_2}\,L^{-1}$ in the tropics and sub-tropics. This again fits well with points known to have pre-OAE2 oxic conditions.

In the Maastrichtian, seafloor oxygen concentrations are a lot more uniform with concentrations in excess of $120\,\mu mol_{O_2}\,L^{-1}$ everywhere, and with typical values ranging from $140\,\mu mol_{O_2}\,L^{-1}$ to $230\,\mu mol_{O_2}\,L^{-1}$. Oxygen levels in the Arctic Ocean are much higher than the rest of the ocean due to its colder temperature, and more enclosed structure than in the Cenomanian. Overall the Maastrichtian ocean seafloor concentrations have fractionally higher oxygen levels than the Cenomanian but only by 0.60 %.

We now focus our analysis on the region with the lowest oxygen levels because this is the region we argue is "pre-conditioned" to go fully anoxic. Figure 3.3 shows the ocean oxygen concentrations at three different (constant depth) levels. We show the surface conditions (A and B), below the photic zone at 96m, at 996m depth (chosen to represent the deep ocean but maximising the ocean area compared to deeper levels), and at 2100m (the first depth level where the panama gateway is closed to flow.

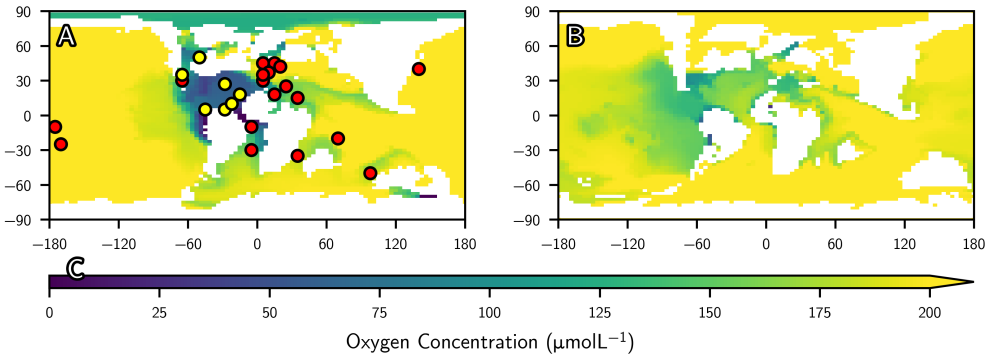

Figure 3.2: Modelled annual mean seafloor oxygen concentration ($\mu mol\, L^{-1}$), for the Cenomanian (A) and Maastrichtian (B). Concentrations are based on averages for the last 100 years of the runs. Figure 2A is overlain with conditions found in sediment samples, from Monteiro et al. (2012). Yellow points show evidence for seafloor anoxia in sediment samples, and red the presence of oxygen. Note that the depth of the seafloor is very variable so that, for instance, the anoxia in the Western Interior Seaway is at a much more shallow depth than in the tropical Atlantic.

In the surface of the Maastrichtian, no areas of particularly low oxygen concentration are seen, with a fairly uniform pattern largely linked to the ocean sea surface temperature. Even in the Tethys and proto-North Atlantic, oxygen concentration remains broadly zonally uniform across the world.

In the Cenomanian, the general distribution of surface oxygen is very similar to the Maastrichtian, with oxygen levels broadly zonally uniform. However, there is upwelling of waters with lower oxygen levels ($\approx 120\, \mu mol_{O_2}\, L^{-1}$) in the region of the North African coast. This area of low oxygen is very localised but is indicative of a larger area of low oxygen below the surface.

Below the photic zone (at 96 m), both time periods show areas of low oxygen developing near the coastal regions at low latitudes (Figure 3.3). This is more developed in the Cenomanian. In the Maastrichtian this area

of low oxygen is predominately focused outside (to the west) of the proto-north Atlantic, spreading and tailing off across the Pacific. Lower oxygen levels are also seen on the West African coast in the proto-Atlantic, however, elsewhere, oxygen levels remain relatively high at this depth. In the Cenomanian oxygen levels are lowered more markedly. A similar area of low oxygen is seen on the northwest south American coast, but in this time period this area is much more developed and spreads along the whole south shore of the central region. In the Maastrichtian, with it's wider Atlantic gateway, this area does not see low oxygen levels. An area of low oxygen is also seen in the Tethys sea at this level, which has no parallel in the Maastrichtian.

In the deep ocean (at 996 and 2100 m), low oxygen levels continue to develop in the Cenomanian, but do not in the Maastrichtian. Cenomanian oxygen levels at this depth and below are reduced across the whole proto-North Atlantic area, but not across any of the rest of the global ocean. In the Maastrichtian, the proto-North Atlantic remains connected to the Pacific until a depth of 2700m and the South Atlantic a depth of 3300m, and reduced oxygen levels are not seen at this or any deeper depths.

Circulation effects

Ocean circulation is an important driver of oxygen levels, through water mass transport via downwelling, upwelling, advection and mixing of oxygenated water. Oxygen is replenished from the atmosphere and primary production at the ocean surface, and reduced by remineralisation, so older water masses with less mixing generally exhibit lower oxygen levels.

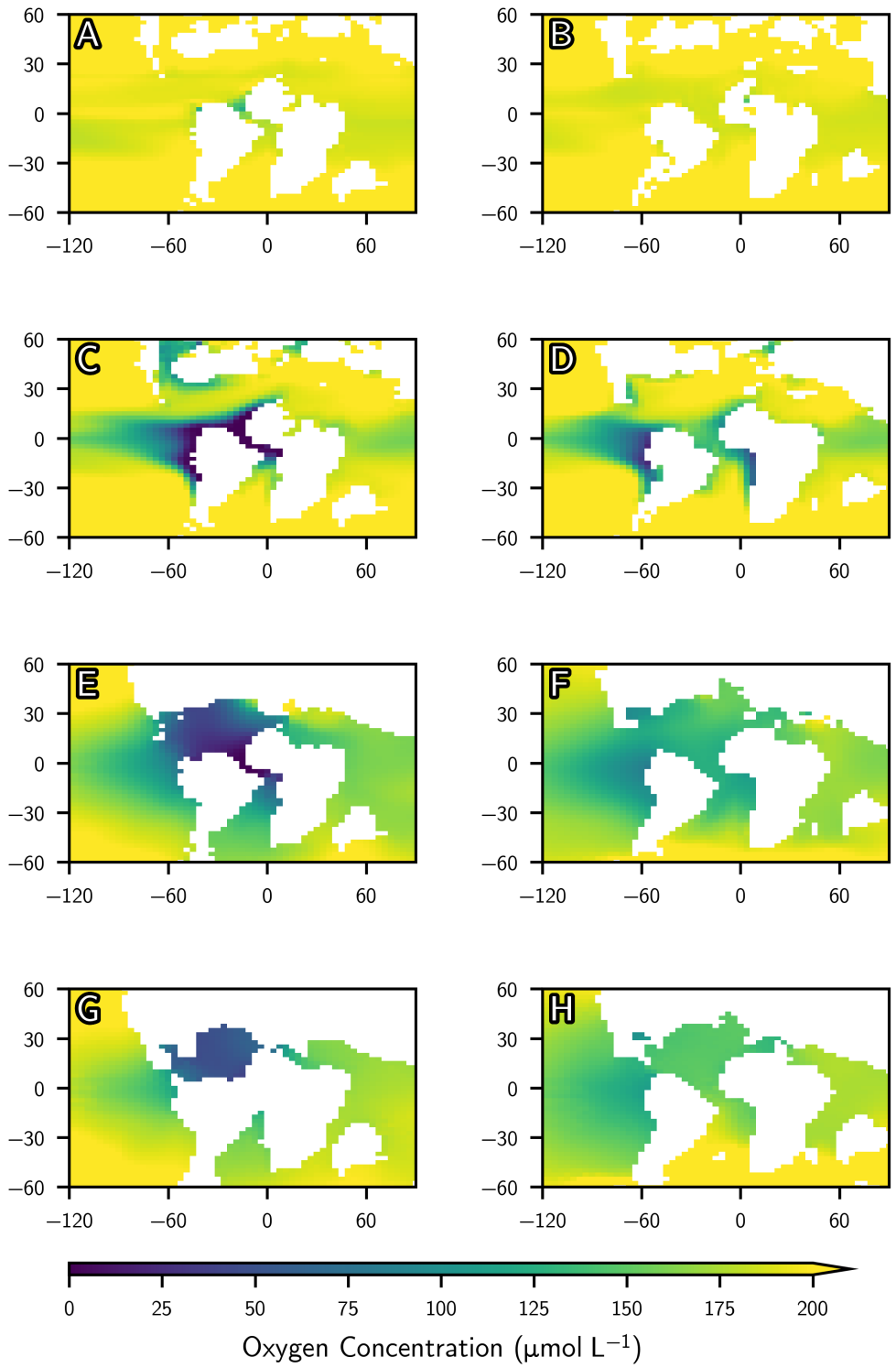

Figure 3.3: Annual mean oxygen concentration at the end of the run, for Cenomanian (left), and Maastrichtian (right). Concentration shown at the surface (A and B), below the photic zone (96 m, C and D), in the deep ocean (996 m, E and F) and at the level of closure of the Panama gateway to flow in the Cenomanian (2100m, G and H).

The ocean circulation at the surface is similar in strength and distribution between the Cenomanian and the Maastrichtian (Figure 3.6). Both paleogeographies exhibit westward flow to the Pacific, with the fastest currents onto the northern south-American coast.

Likewise, below the photic zone (Figures 3.6C and 3.6D), current magnitude and direction are broadly similar in both time periods, with flow exiting the proto-North Atlantic westward into the Pacific. At this depth, both time periods have a well developed cyclonic gyre developed in the proto-Atlantic.

However, the deep ocean circulation (Figures 3.6E and 3.6F) is markedly different between the Cenomanian and the Maastrichtian. In the Maastrichtian, younger water from the South Atlantic is able to flow northwards and supply the proto-North Atlantic (table 3.1), whereas in the Cenomanian this gateway is closed. In the Cenomanian, deep ocean currents flow from the proto-Atlantic into the Pacific, whereas they flow in the opposite direction in the Maastrichtian, as shown by the depth-integrated flow at the Panama gateway in table 3.1 and Figure 3.6E and F.

These circulation differences come from the opening and the depth of the gateways. The flow through the proto-North Atlantic in the Cenomanian (left panels, Figure 3.6) is more restricted when compared to the Maastrichtian, at all depths. In particular, less Pacific water replenishes the proto-North Atlantic in the Cenomanian than in the Maastrichtian. The lack of connection to the South Atlantic, combined with the, presence of a sill ($\approx$2000 m at its deepest point) at the Panama gateway in the Cenomanian (Figure 3.1), severely restricts circulation and causes water to remain

in this central region for much longer.

We use ocean mixed-layer depth (Figure 3.4) to indicate the locations of deep water formation. A band of deeper mixed layer depth across the north of the Maastrichtian proto-North Atlantic suggests more deep water formation occurs here (panel B compared to panel A, Figure 3.4). In the Southern hemisphere, the major areas of deep water formation move from the Pacific in the Cenomanian to the Atlantic in the Maastrichtian This is important in determining the age of water supplied by the small northward flow into the Maastrichtian proto-North Atlantic, as shown in Table 3.1.

Differences at depth but not at the surface are consistent with the fact that the wind (Figure 3.7) varies only slightly between the two time periods, the results being particularly similar across the tropics. The differences in circulation patterns between the two modelled simulations are therefore attributed to differences in bathymetry and continental configuration between the two simulations, rather than topographically controlled changes in wind circulation patterns.

These circulatory effects combine to form the pattern of water ages shown in Figure 3.5. Deep water in the Maastrichtian proto-North Atlantic is younger, supplied particularly by more deep water formation and supply from the South Atlantic, when compared with the Cenomanian.

The combined effect of nutrients

Oxygen levels depend on both ocean currents as a source of oxygen, which supply oxygen from the surface to the deep ocean, and on remineralisation of organic matter, which relies on the production levels at the surface and

	Panama	Atlantic	Tethys	WIS
Cenomanian Surface-Bottom	-0.25	0.00024	0.03	0.13
Maastrichtian Surface-Bottom	-0.31	0.077	-0.0018	0
Cenomanian 1000m-Bottom	-0.04	0	-0.16	0
Maastrichtian 1000m-Bottom	0.017	0.13	-0.09	0

Table 3.1: Depth-integrated flows though major ocean gateways into the proto-North Atlantic (Sv). Positive values refer to flow into the proto-North Atlantic.

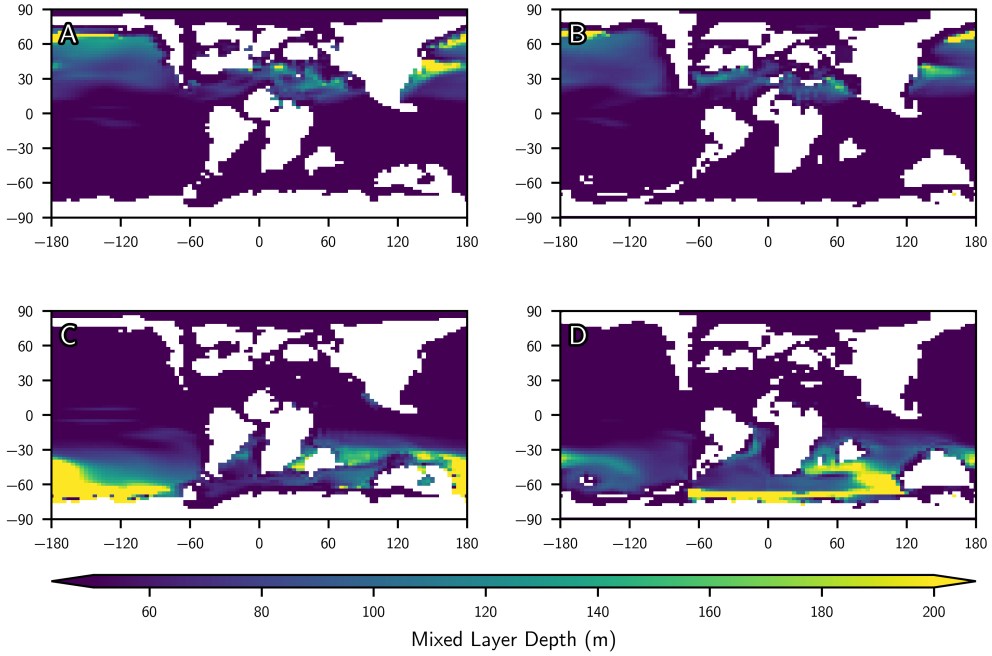

Figure 3.4: Ocean mixed layer depth, for the Cenomanian (left) and Maastrichtian (right). Shown in the Northern winter (a mean of December, January and February) (top) and Southern winter (a mean of June, July and August) (bottom).

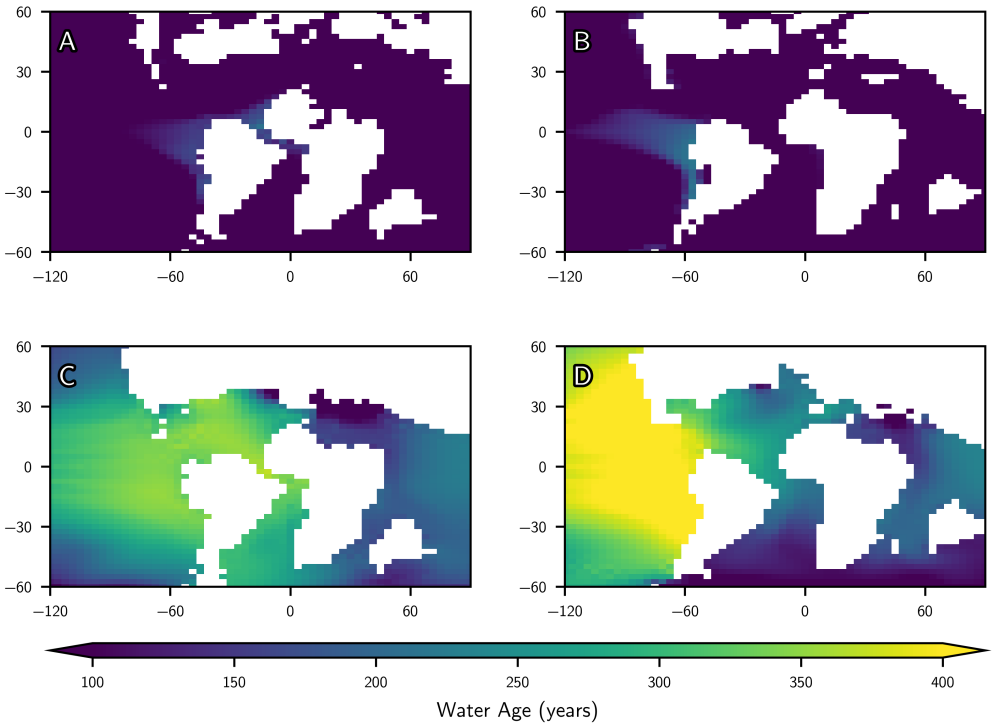

Figure 3.5: Ocean water age, for the Cenomanian (left) and Maastrichtian (right). Shown at 100m deep (top) and 1000m deep (bottom).

the settling of organic matter.

Phytoplankton concentration (3.9A and B) peaks across the equatorial Pacific in both the Cenomanian and the Maastrichtian, however, with much lower level on the east side ($\approx 1\,\mu\text{mol}\,\text{L}^{-1}$) in the Maastrichtian than in the Cenomanian (with a peak of $\approx 4\,\mu\text{mol}\,\text{L}^{-1}$). The Cenomanian also has higher phytoplankton concentrations on the northwest coast of Africa, which is of particular interest and is not seen in the Maastrichtian. Elsewhere, phytoplankton levels remain low across both time periods.

We find that the phytoplankton distribution more or less matches low oxygen level below the photic zone (Figure 3.9 versus Figure 3.3C and D). Similarly to phytoplankton concentration, low oxygen levels prevail in

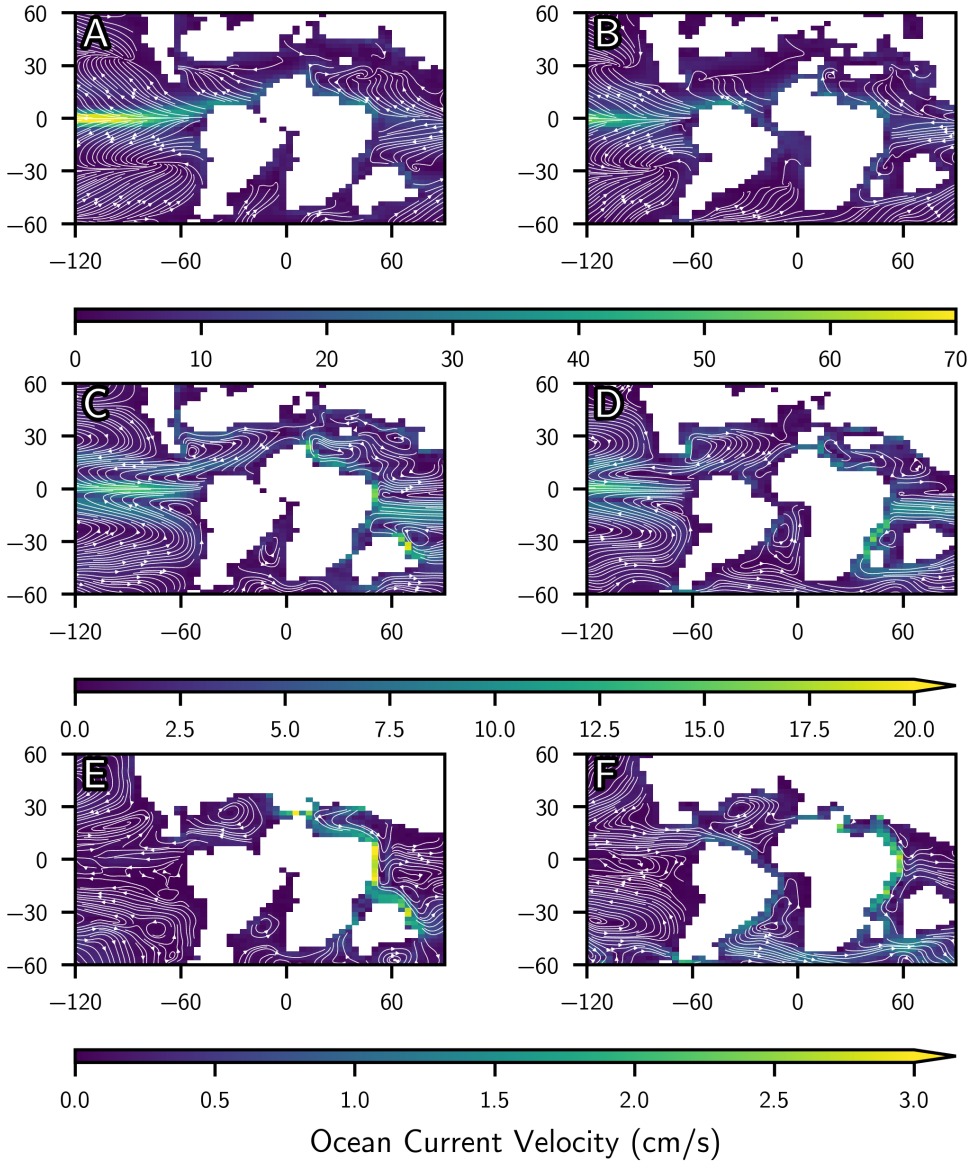

Figure 3.6: Annual mean ocean current strength at the end of the run, for Cenomanian (left), and Maastrichtian (right). Shown at the surface (top), below the photic zone (96m, middle), and deep ocean (996m, bottom). Overlaid with ocean current streamlines.

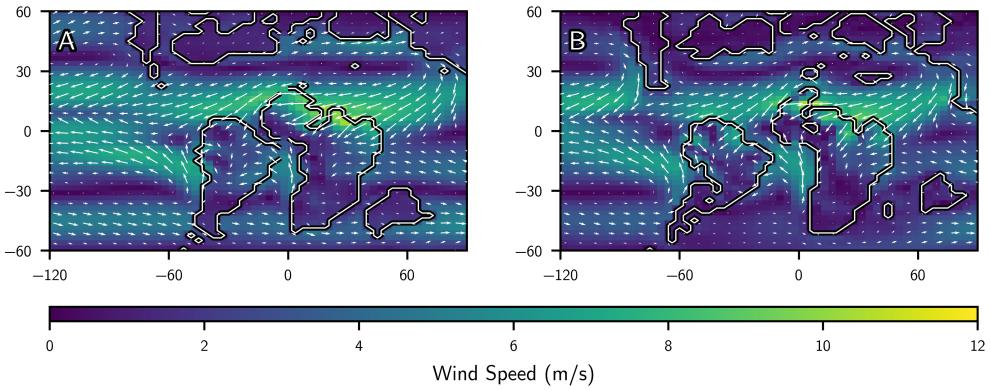

Figure 3.7: Annual mean wind magnitude and direction at 10m for Cenomanian (A), and Maastrichtian (B).

the proto-North Atlantic and do not spread as far across the Pacific. We interpret this as the result of higher phytoplankton concentration causing more export of organic matter and thus remineralisation at depth. This production effect is combined with the ocean circulation effect, where the proto-North Atlantic is not as well ventilated in the ocean interior as the Pacific Equatorial region and further from sites of deep-water formation 3.5.

Production is strongly limited by nutrients, which are mainly supplied by upwelling or deep water mixing of nutrient-rich waters back to the surface. There is then an interplay between ocean currents and production via the supply of nutrients. Here, we explore the role of changes in ocean currents between the Cenomanian and Maastrichtian on ocean nutrients, organic matter production and subsequent oxygen levels.

There are small but important differences in the upwelling patterns between the two time periods in the proto-North Atlantic, especially north of the South American and African continents (Figure 3.8). Patterns outside this area are similar, although upwelling is more intense in the Cenoma-

nian equatorial Pacific than in the Maastrichtian. This strengthening is likely due the changes in paleogeography when comparing the two simulations, with more coastal upwelling occurring in the Cenomanian compared to the Maastrichtian due to the opening of the Atlantic gateway in the Maastrichtian.

In the proto-North Atlantic, upwelling is present along the southern coast in both time periods. In the Cenomanian, this upwelling is more developed, with a mean upward vertical velocity of in the proto-North Atlantic (0-30 North, -60-30 East) $1.26 \times 10^{-6}\,\mathrm{m\,s^{-1}}$, which is 22 % higher than in the Maastrichtian. In the Cenomanian, this area of upwelling is contiguous along the whole southern coast of the proto-North Atlantic, whereas in the Maastrichtian it is clearly divided into two by the separation of South America and Africa. This divide appears to cause a reduction in coastal driven upwelling in the Maastrichtian, as a result of the removal of the coastline, with the consequent reduction in upwelling discussed above.

The stronger upwelling in the Cenomanian compared to the Maastrichtian appears to drive an increase in nutrient supply to the surface, causing higher phytoplankton biomass in the Cenomanian (Figures 3.9A and B). This higher biomass results in more organic matter exported to the subsurface (not shown), causing more remineralisation of organic matter, and subsequent nutrient release (Figures 3.9C and 3.9D) and subsurface ocean anoxia (Figure 3.3C).

The surface upwelling (at 113 m) increases by 22% in the Equatorial Atlantic from the Maastrichtian to the Cenomanian. However, oxygen levels in the ocean interior of the same region drop by 16%, which scales with

a phytoplankton concentration increase of 52%. This amplification in phytoplankton concentration relative to the upwelling increase comes from a stronger nutrient accumulation below the photic zone in the upwelling region of the equatorial Atlantic, which causes higher nutrient supply to the surface. Nutrient concentration below the photic zone in the same area increases by 150% from 5.90 µmol L^{-1} in the Maastrichtian to 14.90 µmol L^{-1} in the Cenomanian. Nutrient supply, which scales with upwelling times nutrient concentration below the photic zone, is 1.15 µmol L^{-1} more in the Cenomanian relative to the Maastrichtian.

We suggest that nutrients accumulate below the photic zone more strongly in the Cenomanian, because they are upwelled back to the surface (and recycled locally) faster than they are advected away by lateral transport. This imbalance is due to the restricted nature of the proto-North Atlantic basin.

These results indicate that the differences in oxygen distribution between the Cenomanian and the Maastrichtian result from the effect of continental configuration on ocean currents. These in turn affect the supply of oxygen-rich Pacific waters into the proto-North Atlantic and the supply of nutrient to the surface boosting production at the surface and remineralisation in the subsurface.

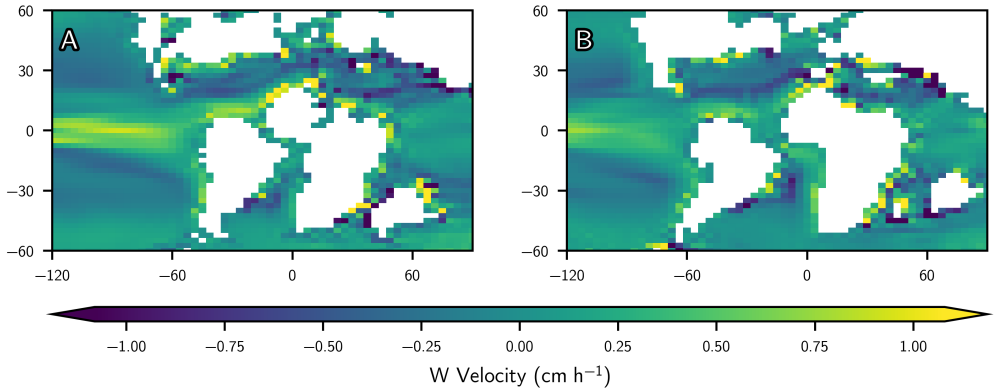

Figure 3.8: Annual mean vertical velocity below the photic zone (96m), for Cenomanian (A), and Maastrichtian (B).

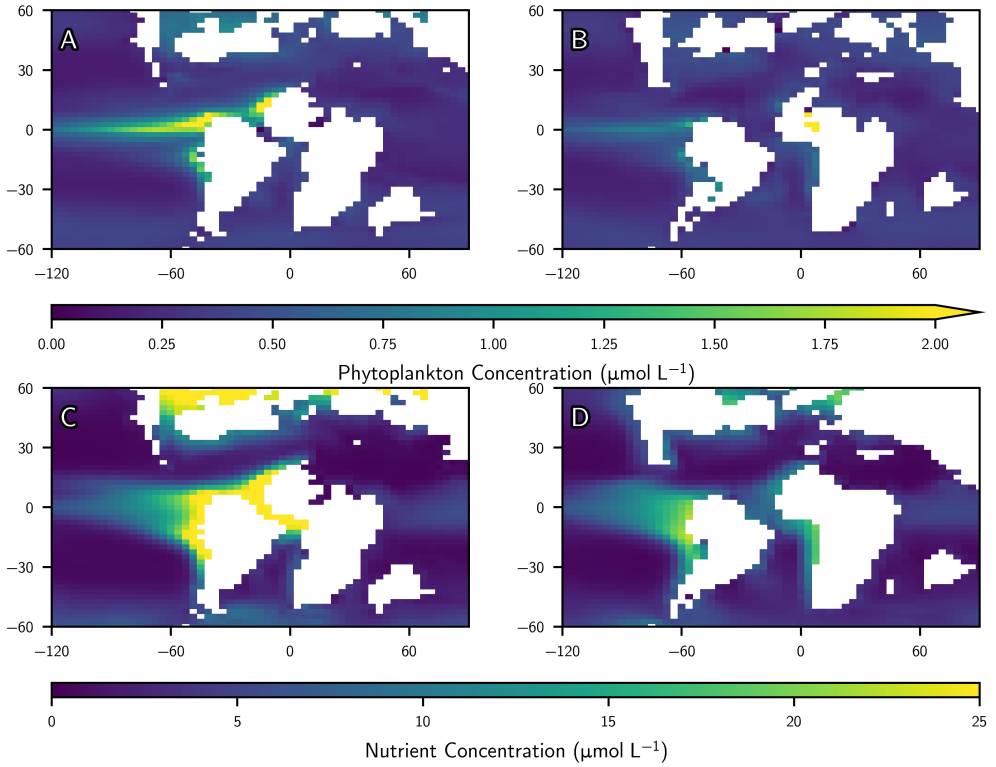

Figure 3.9: Annual mean phytoplankton concentration (top) and nutrient concentration at the base of the photic zone (96m) (bottom) for the Cenomanian (left) and Maastrichtian (right)

3.6 Discussion

Our model experiments show that the difference in paleogeography between the Cenomanian and Maastrichtian substantially impact the distribution of oxygen and the presence of anoxia in the ocean interior. The Cenomanian simulation shows the presence of ocean anoxia in the equatorial Atlantic and East Pacific below the photic zone and in the proto-North Atlantic and WIS for the deep ocean.

The more restricted nature of the ocean gateways in the Cenomanian is key for the development of seafloor/deep ocean anoxia in the proto-North Atlantic. In our simulations, the presence of the a sill at the Panama gateway and the narrowness of the South Atlantic gateway in the Cenomanian but not in the Maastrichtian cause a more restricted circulation in the proto-North Atlantic. The Cenomanian proto-North Atlantic has less water supply from both the Pacific and South Atlantic, reducing the supply of younger and oxygen-richer Pacific waters. This oxygen supply shift mirrors that seen in other models for the Cretaceous; in the lower resolution cGENIE model, ocean ventilation is similarly reduced by the sill's presence (Monteiro et al. 2012). Similarly, the circulation is consistent with the purely physical GCM simulations of Trabucho Alexandre et al. (2010) and Donnadieu et al. (2016).

The presence of these benthic features, and their absence in the Maastrichtian is affirmed in other independent geological reconstructions of the time period. Scotese (2014) show a sill to be present in the Cenomanian, and then a gradual deepening of the Panama gateway through the Creta-

ceous. This shallow Panama gateway is thought to have been caused by the Caribbean large igneous province (CLIP) (Buchs et al. 2019), which is itself put forward as one of the possible contributors to the development of OAE2 (Jenkyns 2010). While numerous studies agree that LIP vulcanisim was important in OAE development (Jenkyns 2010; Joo et al. 2020), the exact timing of the CLIP, and it's movement eastwards which would have initiated the shallowing of the Panama gateway, is less well constrained. Most of the literature (Andjić et al. 2019; Dürkefälden et al. 2019; Loewen et al. 2013) considers the CLIP to have occurred from ≈92 Ma until ≈83 Ma, however they diverge on whether the shallowing of the Panama gateway occurred toward the start of this time period (Dürkefälden et al. 2019; Loewen et al. 2013) or later on (Andjić et al. 2019).

That fact that the Atlantic gateway between South American and Africa was closed during OAE2 is more clear from the literature, and although a shallow connection existed between the two continents from the late Aptian (Erbacher 1998; Ye et al. 2017), subsistence did not begin until the Coniacian (Wagner and Pletsch 1999). Moreover, a deep connection and circulation did not exist until during the Santonian (Moullade et al. 1998; Pletsch et al. 2001).

The connection to the Tethys at the East side of the proto-North Atlantic is similar in both our simulations. It is thought that the connection from the proto-North Atlantic to the Tethys occurred at a similar time to the opening of the proto-North Atlantic basin itself, in the early Jurassic (Stampfli and Borel 2002). There is clear evidence that a connection existed here across the late Cretaceous (Nouri et al. 2016; Stampfli 2000), with a

deeper connection in the Cenomanian than the Maastrichtian most likely (Stampfli and Borel 2002).

In our Cenomanian simulations we use a relatively shallow panama gateway, however in Figure 3.10 we show oxygen levels in additional simulations with a very shallow and very deep ocean sill. In these, shallowing the sill here further causes oxygen levels in the proto-North Atlantic to reduce, and the reverse occurs when the sill is deepened. However these effects are not as dramatic as the difference seen between the Maastrichtian and Cenomanian here, underlining that both the Panama and Atlantic gateways contribute to the differences observed.

The presence of the more restricted proto-North Atlantic in our simulations, and the resulting circulation changes, precondition the ocean for the onset of an OAE; the background state of the ocean becomes less favourable to the development of an OAE, and less deviation from the background state is required to achieve the OAE towards the Maastrichtian. As the ocean sill deepens over time, and the South Atlantic gateway opens over time, OAE events appear to become less prevalent. By the time of the last recorded Cenomanian OAE: OAE3, the sill has deepened significantly.

We suggest that lack of Pacific-Atlantic circulation and sill are pivotal in causing the reduction in oxygen seen in our Cenomanian circulation. Without a supply of oxygenated bottom water, relatively high benthic oxygen levels seen in the Maastrichtian are much reduced, as seen in the pre-OAE2 simulation and an important precursor to that event. The presence of this gateway is consistent with Donnadieu et al. (2016), but contrasts with the interpretation of Ladant et al. (2020), which suggests that this gateway

is not consistent with Neodymium isotope data. However, Ladant et al. (2020) acknowledge that Neodymium data is difficult to interpret and that the observed changes could also be driven by changes in sources. Until a neodymium-enabled model is run, we can simply note that the currently interpreted Neodymium isotope data is inconsistent with the oxygen concentration and anoxic indicators at the Maastrichtian (Figure 3.2).

Finally, Laugié et al. (2021) studied the Cenomanian ocean oxygen distribution using the IPSCL-CM5A2 Earth System Model. They also found that oxygen distribution is primarily driven by paleogeography and oceanic gateways via ocean circulation, and argued for a deep Panama gateway during pre-OAE2 to better match seafloor anoxia observations. Our model also shows oxygen increasing with a deeper Panama gateway (in our Maastrichtian simulations). Our results agree with Laugié et al. (2021) that the depth of the sill contributes to an increase in anoxia. Here we suggest an alternative that the change in paleogeography can also contribute to a shift in anoxia in that region.

In our simulations, the change in ocean circulation is combined with an increase in upwelling in the proto-North Atlantic in the Cenomanian compared to the Maastrichtian. This is consistent with the suggestion that the proto-North Atlantic acted as a nutrient trap (Trabucho Alexandre et al. 2010), the restricted circulation leading to an accumulation of nutrients unable to leave the basin. The combination of stronger upwelling and nutrient accumulation at the Cenomanian causes an amplification of production at the surface increasing remineralisation in the subsurface, both consuming oxygen and recycling nutrients for further production.

In narrow channels such as the WIS, model resolution of ocean currents is poor. While we model anoxia in the WIS at the seafloor, currents are not resolved well in this area, making evidence for the causes of this lack of oxygen sparse. Modelling of the narrow channels in this area would benefit from higher resolution to achieve clearer results. In addition, we have not modelled the onset of OAE2, modelling only pre-OAE conditions unlike Monteiro et al. (2012). Comparing the effect of warming and nutrients should be done within a higher resolution ocean model, to fully appreciate the effect of ocean currents as an OAE develops.

3.7 Conclusion

We believe we have performed the first simulations of the Cenomanian and Maastrichtian using a full complexity coupled ocean-atmosphere-carbon climate model, at relatively high resolution. The advantage of this model is that the ocean biogeochemistry is fully coupled to the ocean and atmospheric circulation and thus we have a much more comprehensive treatment of the feedbacks between different components of the system. The disadvantage is that the biogeochemical component is simpler than in some intermediate complexity models (such as GENIE) and hence is unable to represent full anoxic conditions. We therefore use low oxygen levels as an indicator of "preconditioning" of the ocean state towards full anoxia.

We have run two sets of simulations, using a Cenomanian and Maastrichtian paleogeography. We selected these periods because a strong OAE occurred during the Cenomanian but no anoxia is recorded in the Maas-

trichtian. Our aim was to investigate how paleogeographic changes alone could impact benthic oxygen concentrations. Hence these are idealised simulations with no changes between time periods, other than the paleogeography.

Our results demonstrate that paleogeography plays a critical role in controlling the ocean circulation and oxygen supply, especially in the Atlantic sector. We find that during the Cenomanian, the bathymetry and geometry of the proto-North Atlantic limit the exchange of high-latitude oxygenated water resulting in low oxygen levels in much of the Atlantic. In the Maastrichtian, the deeper sill across the Caribbean and wider gateway to the South Atlantic result in greater oxygen levels. We thus suggest that the paleogeography "preconditions" low oxygen concentrations in the Cenomanian proto-Atlantic and likely makes the required trigger for a full OAE smaller.

3.8 Acknowledgements

Climate simulations were carried out using the computational facilities of the Advanced Computing Research Centre, University of Bristol.

This work was funded by NERC GW4+ UK Doctoral Training Partnership Studentship.

FMM was supported by a NERC standard grant (NE/N011112/1).

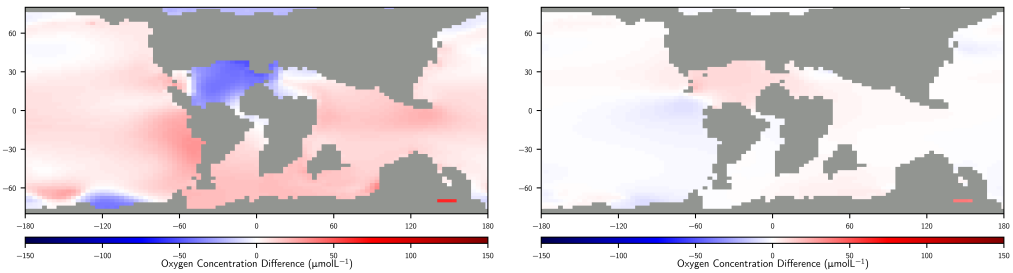

Figure 3.10: Annual mean oxygen concentration at the end of the run shown as a difference from our Cenomanian simulation at 996 meters depth. Two possible scenarios of the Panama sill are shown: very shallow (left), and very deep (right). Shallowing the sill compared to our Cenomanian run reduces oxygen concentration in the proto-North Atlantic further, while deepening it increased the oxygen concentration slightly.

3.9 Supplementary Materials

Figure 3.10 shows two different scenarios for the Panama gateway in the Cenomanian. The first panel shows that without a connection from the proto-North Atlantic to the Pacific, Oxygen levels in the proto-North Atlantic strongly drop, although this also causes a rise in oxygen levels across the rest of the global ocean since low oxygen waters are trapped in the proto-North Atlantic. In the second panel, where the bathymetry across the Panama gateway is significantly deepened the reverse effect is seen, albeit less strongly. While oxygen levels in the proto-North Atlantic are increased by removal of the sill across the Panama gateway, levels in the Pacific are lowered as proto-North Atlantic water spreads through the gateway.

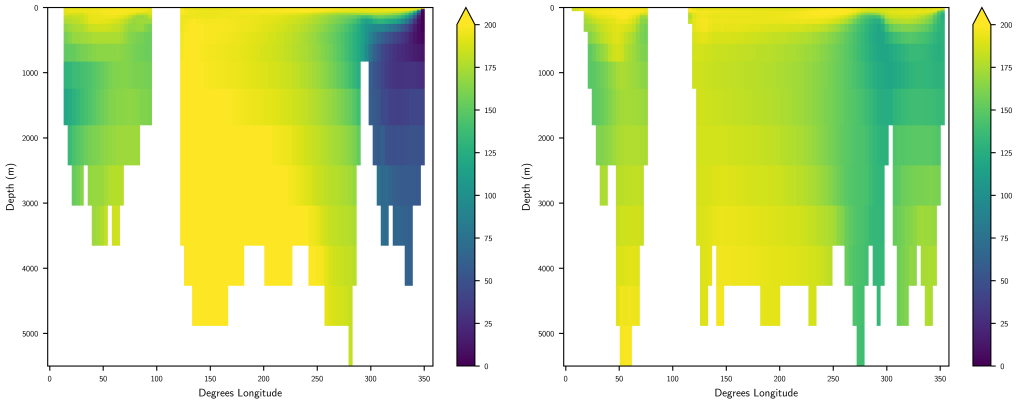

Figure 3.11: Annual mean oxygen concentration at the end of the run, for the Cenomanian (left) and Maastrichtian (right). Cross section of the ocean at fifteen degrees north, intersecting the Panama gateway. Westernmost boundary of the proto-North Atlantic ocean is at 300 degrees east, where a distinct boundary between the more oxygen-rich waters of the Pacific is seen in the Cenomanian, but is much less distinct in the Maastrichtian.

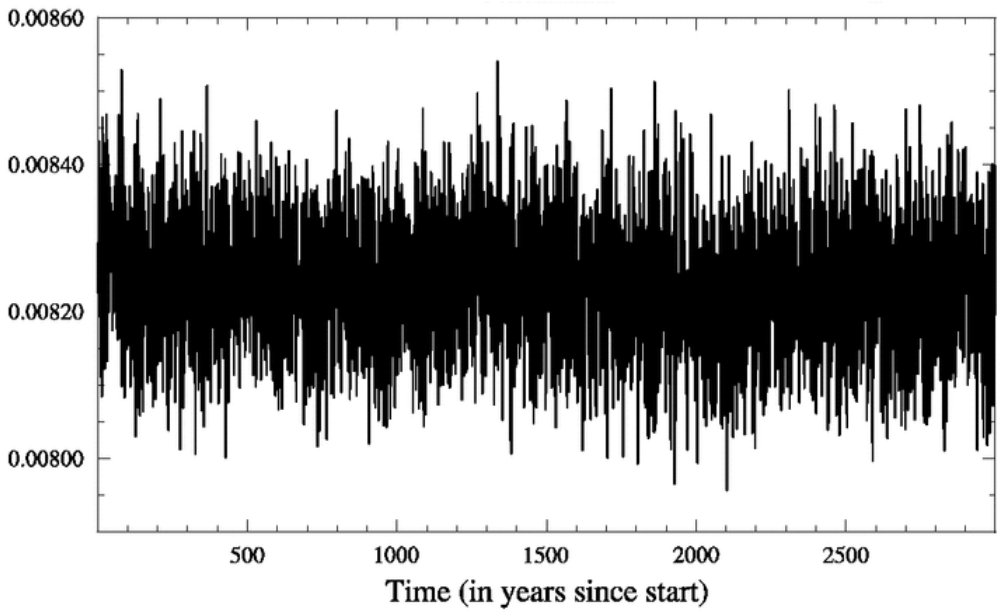

Figure 3.12: Time-series showing change in volume integral ocean nutrient concentration though the model simulation. The ocean ecosystem model is stable as the simulations presented here extended previous simulations with a spun-up Turonian ocean.

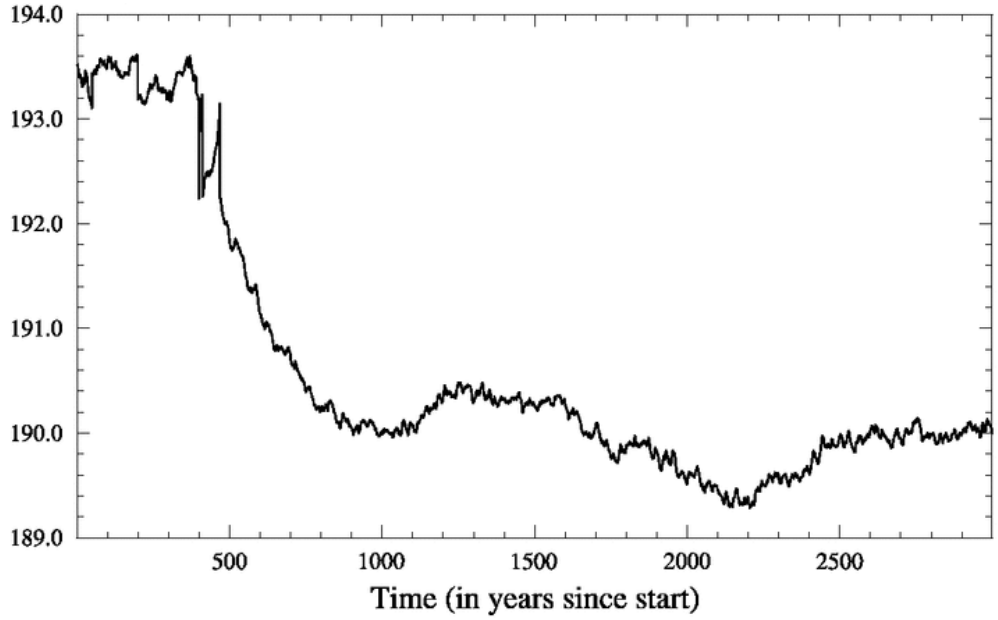

Figure 3.13: Time-series showing change in volume integral ocean oxygen concentration though the model simulation.

Figures 3.14 and 3.15 show HadCM3L simulations of the modern ocean using the Williams et al. (2014) oxygen module used in this paper. Simulated modern ocean oxygen levels are very similar to those observed in HadGEM2 in Williams et al. (2014), with the disparities seen in FAMOUS in Northern Mid-Latitudes and west of Equatorial American noticeably not present (Williams et al. (2014) Figure 1). The predicted zonal mean also compares well, with a slightly less intense equatorial minimum zone than FAMOUS, which again mirrors HadGEM2.

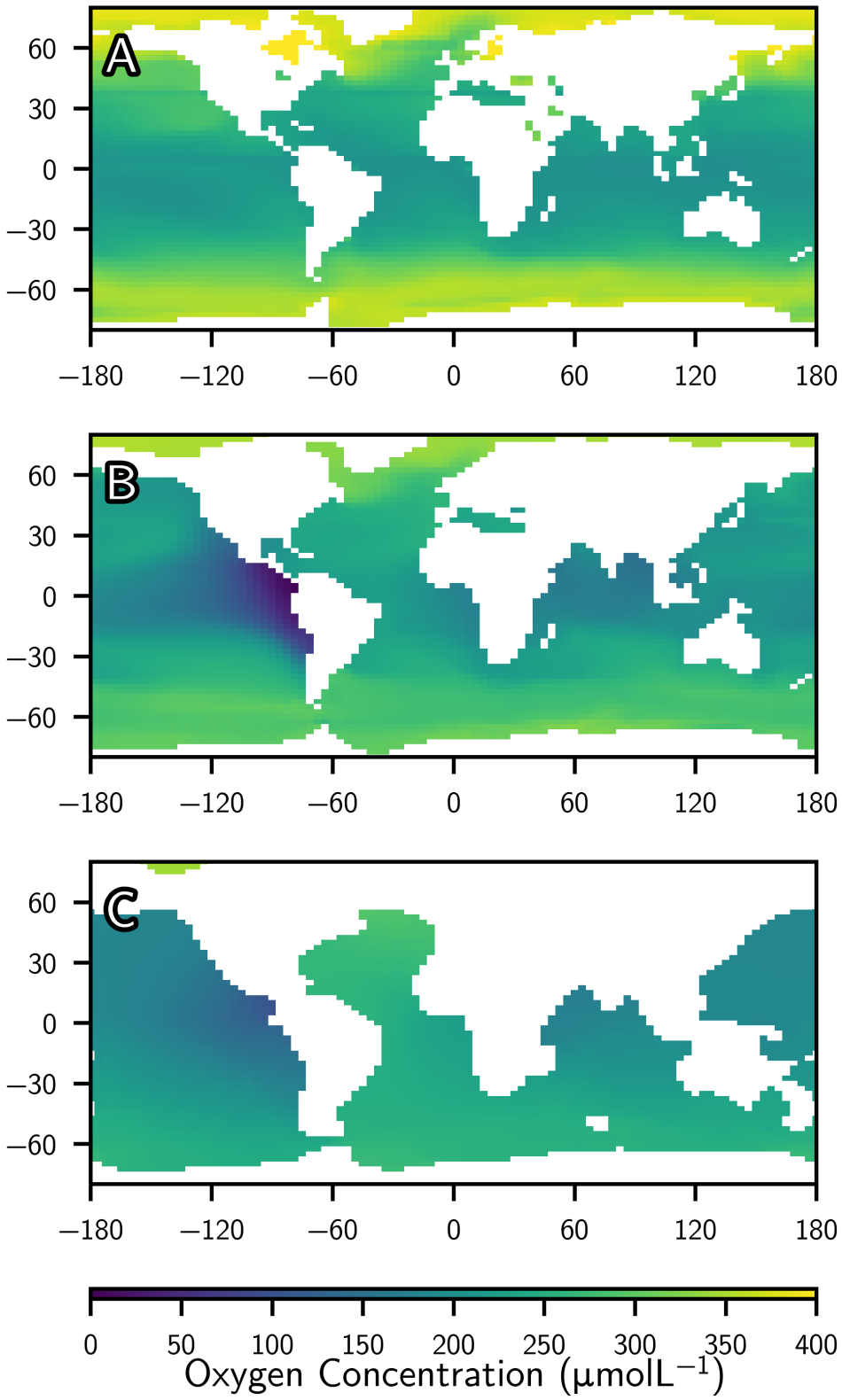

Figure 3.14: Simulated modern ocean oxygen levels, at the surface (A), below the euphotic zone (B) and at 3000m.

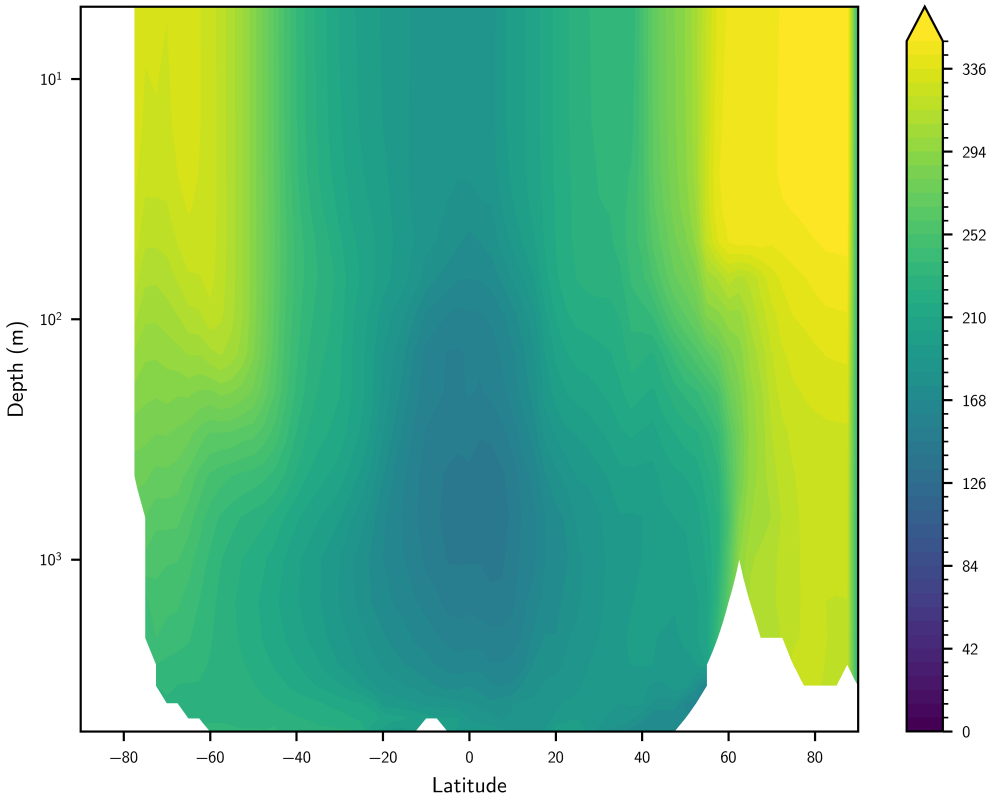

Figure 3.15: Simulated modern zonal mean ocean oxygen levels.

Chapter 4

The Effect of Orbital Cycling on the Development of OAE2

4.1 Preface

This chapter has been written as a paper, to be to submitted to Climates of the Past. This chapter builds on Chapter 3 to continue the study of the combination of physical and biogeochemical effects which lead to OAE2. For the completion of this work, Alexandra Ashley and Jim Harris (CGG Roberson) provided the paleogeographies used. In addition, Paul Valdes provided technical assistance with the model simulations, and along with Fanny Monteiro, provided assistance, feedback and advice for all aspects of the study. The final manuscript was written by Alexander Manning with contributions from all co-authors and has been adjusted for inclusion in this thesis in line with the content of the other chapters.

4.2 Abstract

Oceanic anoxic event 2 (OAE2), marking the Cenomanian/Turonian boundary was a large perturbation in the ocean carbon cycle, occurring at ≈100 Ma. Studies have suggested that this event may have been affected by orbital cyclicity, which affects seasonality in the solar radiation the earth receives, and therefore possibly the development of OAE2. However, the mechanisms by which the seasonal variations cause changes in ocean anoxia are poorly understood. In this study we model a number of possible orbital scenarios on a Cenomanian paleogeography, and analyse the effect this change has on the development of the OAE. We show that changes in orbital cycling affect ocean circulation and upwelling, which consequently alters ocean benthic oxygen. This change in ocean circulation is driven by changes in deep water formation, which itself is controlled by supply of fresh water to the high latitude Pacific. The changes shown are achieved by physical effects alone, and are not large enough to prevent the onset of an OAE, but do suggest that orbital cycling could have modulated the OAE and could regionally cause sediment cyclicity.

4.3 Introduction

Orbital, or Milankovitch, cycling is a well-known phenomenon whereby changes in the earth's orbit around the sun cause long-term periodic (approximately 20 ka, 40 ka, and 100 ka periods) variations in the amount and distribution of incoming solar radiation to the Earth's atmosphere (Berger

1978). This cycling is an important control on the Earth's climate, with the resultant changes in incoming radiation widely attributed to extensive changes in the Earth's climate (Barron et al. 1985; Lowe et al. 2013; Vacher and Rowe 2004). Annually, orbital cycling results in relatively small changes to total incoming radiation, but far larger changes to it's temporal distribution. This has marked implications for many parts of the climate system, on account of the effects of seasonal heating for ocean productivity, ocean circulation, riverine discharge and the monsoon (Beaufort et al. 1997; Beckmann et al. 2005; Brookfield and Hannigan 2021; Cheng et al. 2021). Therefore, any changes to these orbital forcings have a vast impact across the Earth's climate system and it's key mechanisms, from the rainfall inputs to deep ocean currents (Herbert 1997; Mollier-Vogel et al. 2013). Of particular interest for paleoceanography is the effect of orbital cycling on sedimentation, and consequently the sedimentary record we can see today.

The orbital system consists of a number of orbital parameters which together combine to control the incoming solar radiation that the earth receives. Firstly, eccentricity depicts how circular the earth's orbit is and has orbital periods of approximately 100 and 400 thousand years. It changes both the total amount of solar radiation and how pronounced the earth's seasonality becomes (Berger et al. 1992; Berger et al. 2006). Secondly, obliquity, the tilt of the earth, has a period of approximately 40 thousand years (Williams 1993). Increases to obliquity cause higher developed seasonality in both hemispheres by tilting the earths poles further from the sun in winter and closer in summer (Ferreira et al. 2014). Finally, the precession of the season is caused by the combined precession of the earth's orbit

around the sun and the earth's axis of rotation (Merlis et al. 2013). It acts to redistribute solar radiation but does not affect the annual global mean of incoming radiation (Berger et al. 2006). While these parameters are well understood and known for the recent past (and indeed near future), the timing of points in the Milankovitch cycle beyond ≈58 million years ago cannot be calculated with accuracy (Laskar et al. 1993, 2004; Waltham 2015; Zeebe and Lourens 2019). This lack of uncertainty is amplified by the chaotic nature of the solar system, which causes random behaviour in orbital cycling (Olsen and Kent 1999). Despite this, it is still widely understood that orbital cycling affected the climate beyond ≈58 million years ago, and numerous studies attribute sedimentary cycling and other climatic effects to this cause (Ma et al. 2017; Meyers et al. 2012).

On account of the long, well-defined time scale that can be produced, orbital climate cycling can be an immensely powerful tool to aid the dating and analysis of the sedimentary record (Peterson 2012; Weedon et al. 1999). As a result, orbital climate cycling can also be used to estimate sedimentation rate (Waltham 2015), particularly when cycling occurs at a large spatial scale. One example of cyclic variability interpreted as orbital cycles are within OAEs (Boer and Smith 2009). OAEs are extreme climatic events of the Mesozoic era, characterised by widespread black shale sediments indicative of global ocean deoxygenation (Schlanger and Jenkyns 1976). As a large perturbation in the global carbon cycle, with widespread mass extinction and climatic change (Joo et al. 2020), OAEs are hugely important and interesting events that are pivotal in aiding our understanding of the global carbon system, both in terms of how it has developed in the

past and also how it will develop in the future.

OAE2 represents one of the more recent OAEs events, with a global significance on account of the global scale spread of ocean anoxia (Jenkyns 2010). During OAE2, it is thought that widespread ocean anoxia caused massive change in the earth's carbon cycle (Eldrett et al. 2014), perturbed ocean circulation (Zheng et al. 2016), and caused mass extinction of ocean species (Forkner et al. 2021). Carbon rich sediments associated with OAE2 have been found worldwide (Frijia et al. 2019). OAE2 has been widely studied, both in terms of its genesis and its development (Flögel et al. 2011; Jenkyns 2010; Monteiro et al. 2012; Nederbragt et al. 2004; Schlanger and Jenkyns 1976). Cyclical sediments have been identified before, during and after OAE2, with a wide range of potential causes and effects put forward (Elderbak and Leckie 2016; Elrick et al. 2009; Kuhnt et al. 2005) for their presence in the record. However, despite growing evidence regarding the development and effects of OAEs, modelling of changes in the orbital parameters on the onset of OAE2 is somewhat more limited (Beckmann et al. 2005; Dummann et al. 2021; Sarr et al. 2022). It has been observed on many occasions that the layered pattern of black shale sediments characteristic of OAE2 may indicate orbital cycling activity (Batenburg et al. 2016; Charbonnier et al. 2018; Mitchell et al. 2008). However, there is a lack of scientific modelling evidence that has explored this, particularly at a high enough resolution to analyse how the development of OAE2 may have been affected by orbitally induced changes (Sarr et al. 2022).

The role and impact of orbital variability has been frequently attributed to the timing of the OAE2 onset (Batenburg et al. 2016; Kuhnt et al. 2017;

Mitchell et al. 2008). Moreover, the development and very existence of OAE2 has also been attributed to the orbital conditions during the event (Charbonnier et al. 2018; Mitchell et al. 2008). For example, Charbonnier et al. (2018) argued that the orbital effect of perturbed orbital cycle was important in amplifying the supply of volcanic nutrient to the ocean. There is a broad consensus in the literature that the obliquity cycle is a key control on OAE2 development, with many studies (Batenburg et al. 2016; Charbonnier et al. 2018; Meyers et al. 2012) finding that strong obliquity induced seasonality was present at the start of OAE2. To date, these conclusions have typically been made using cyclostratigraphic techniques, for example where Meyers et al. (2012) identified a strong obliquity signal in the sediment intervals of the Demerara Rise. Elsewhere, studies have suggested that the obliquity signal was weak at the OAE2 onset, for example by Li et al. (2017) and Mitchell et al. (2008) who conducted analysis using sediment cores from Tibet and Italy, respectively. Li et al. (2017) concluded that the orbital configuration did not influence the onset, whilst Mitchell et al. (2008) suggested that periods of dampened seasonality across geological time were a major controlling factor on OAE2 and other OAEs.

A further key hypothesis in the literature is that orbital variability did not induce OAE2 alone and that other conditions were required for an OAE development (Li et al. 2017). The onset of OAE2 has most often been attributed to periods of volcanism (Jenkyns 2010; Sullivan et al. 2020), where there is to date, a lack of consensus in the literature that orbital variability was an important factor in the development of the OAE. Indeed, many of the cycles in orbital variability are shorter in timescale than the length

of the OAE, and while it is broadly understood that orbital variability is present in OAE sediments, it's impact on the OAE as a whole remains unclear.

Alongside this range of literature depicting the possible drivers of OAE2, including the potential effects of orbital forcing, there is also an increasing array of evidence for the number of mechanisms linking orbital variability to OAE black shales' cyclicity (Poulton et al. 2015; Ruddiman 2006). These mechanisms include changes to the hydrological cycle (Behrooz et al. 2018; Charbonnier et al. 2018) or weathering in general (Poulton et al. 2015), along with the alteration of ocean currents and upwelling (Batenburg et al. 2016; Meyers et al. 2012). Hydrological cycle intensification has been widely suggested to cause increased weathering and therefore nutrient supply to the ocean (Charbonnier et al. 2018; Chen et al. 2022; Helmond et al. 2014, 2015). Furthermore, additional rainfall at high latitudes has the potential to change ocean circulation itself, by supplying greater freshwater at high latitude and suppressing deep water formation (Charbonnier et al. 2018; Sarr et al. 2022). This suppression in deep water formation can act to slow ocean circulation as a whole (Scopelliti et al. 2004).

A key methodological linkage across the current literature on the drivers of OAE2, is that our knowledge is typically based on sediment core analysis, by stratigraphically analysing the sedimentation rate and composition through time (Meyers et al. 2001). Changes in many different proxies laid down in the sediment are used, including organic carbon content, carbon changes, oxygen isotope composition and degree of magnetisation (Du Vivier et al. 2014; Eldrett et al. 2015; Elrick et al. 2009; Hasegawa et al.

2004; Kolonic et al. 2005; Li et al. 2017; Meyers et al. 2001; Tsikos et al. 2004). Analysis of sediment cores is one of the few ways we can get a real picture of the conditions which occurred during OAE2, enabling both the timing of OAE2 and the cycles within it. However, in general, sediment core analysis can only give a picture of OAE development in the local conditions at the seafloor of a single or few locations. Many samples must be analysed to extrapolate a worldwide picture and ensure that conditions at a single core were not anomalous. In addition, it is important to note that other possible explanations exist (other than orbital cycling) for sediment layering, for example cycling in the availability of ocean trace nutrients such as iron (Owens et al. 2012).

Despite the complexity of processes that lead to a signal in the sediment core, there has been a lack of scientific development in modelling methods, particularly the use of higher resolution models which combine simulations of ocean circulation and oxygen distribution (Sarr et al. 2022). The use of models to simulate orbital scenarios and investigate their effects for OAE2 development offers a number of advantages for giving a wider picture on how orbital scenarios may have affected the ocean-earth system as a whole (Price et al. 1995). Testing multiple orbital scenarios is particularly advantageous when considering the uncertainty present during the OAE2 time period (Laskar et al. 2004). Using a coupled model allows the effects on the whole ocean system to be analysed.

The benefits of using modelling-based methods to investigate the effects of orbital variability in the Cretaceous has been highlighted by Park and Oglesby (1991). This study modelled a number of orbital scenarios using

NCAR CCM1, an early GCM with a zonally averaged ocean. Results here highlighted that of the orbital scenarios, precessional changes were the most important, with obliquity changes presenting a lower overall effect with strong changes in the hydrological cycle. Whilst Park and Oglesby (1991) presents a useful early example of the application of a GCM to analyse orbital change during OAE2, it is important to stress that recent model developments and our growing capabilities in this research field now allow for us to expand on this work, to include a far higher resolution and better representation of the ocean, as well as ocean geochemistry. It is appropriate to revisit this issue with a state-of-the-art model.

Recognition in how we may be able to use modelling methods to understand the effects of orbital variability on OAE2 is expanding, with recent work by Sarr et al. (2022) using the IPSL-CM5A2 Earth System Model with a coupled ocean and atmosphere and ocean biogeochemistry. This study, similar to Park and Oglesby (1991), showed that hydrological changes were able to cause small changes in ocean circulation and lead to deoxygenation of parts of the ocean, particularly the proto-North Atlantic (Sarr et al. 2022). To expand on these emerging modelling methodologies that are examining the potential causes and impacts of orbital forcing on OAE2 (Sarr et al. 2022), and more broadly on other orbital driven changes in the Earth's climate history (Ruvalcaba Baroni et al. 2018; Sellwood and Valdes 2006; Valdes et al. 1995), there is a need for further studies of the potential key mechanisms impacted by orbital forcing. This is essential for aiding our understanding of the causes and effects of atmospheric and ocean dynamics changes in Earth's history.

Therefore, this paper aims to investigate the effects of orbital cycling on the development of OAE2, using a state-of-the-art model to consider the extent to which key mechanisms are impacted by orbital forcing, and to subsequently assess whether these effects are the cause of sediment cyclicity. HadCM3L is used for these applications as it offers an excellent trade-off in complexity versus compute time, being a fully coupled GCM including a representation of ocean biogeochemistry (Valdes et al. 2017). Firstly, we simulate, using pre-OAE2 model parameters, a number of different orbital configurations (principally: real historical orbits, eccentricity and obliquity ranges), and assess the effect of these changes to alter solar insolation at the top of the atmosphere. Secondly, the impacts of these orbital configurations are examined with regard to benthic oxygen, enabling the role in the orbital parameters in controlling the spread of the anoxic event to be analysed. Finally, a particular focus is placed on the key mechanisms acting to cause extreme global ocean deoxygenation, specifically: primary production, ocean circulation and freshwater supply. Overall, this paper offers a new and exciting examination of the mechanisms by which changes in benthic oxygen occurred as a result of the occurrence of OAE2, applying new model developments, whilst building on important existing concepts formed from sediment analysis in this field.

4.4 Methods

The methodological approach taken in this paper comprised of using the HadCM3L model with paleogeography for the Cenomanian, configured with

a number of different orbital forcings to examine their impact on key mechanisms behind the induction of OAE2. The role and impact of primary production, ocean circulation and freshwater supply is subsequently explored, including their interactions as key mechanisms, to examine the effect of orbital cycling on OAE2 development.

4.4.1 Model description

To simulate the ocean-earth system at relatively high resolution, the Earth-System model HadCM3L was used. For the purpose of this study, HadCM3L was configured with a NPZD biogeochemical scheme (Palmer and Totterdell 2001), and with the ocean oxygen cycle (Williams et al. 2014) turned on. This model is known as HadCM3LB-M2.1Da and is subsequently referred to as HadCM3L in this paper.

HadCM3L is fully described by Valdes et al. (2017). Briefly, HadCM3LB-M2.1Da consists of the 3.75^o x 2.5^o atmospheric model used in HadCM3 (Pope et al. 2000), coupled to an ocean model at the same resolution. Both the atmospheric and ocean models have unequally spaced vertical levels, 19 and 20 respectively, both with more densely spaced levels near the surface. In addition, levels in the atmospheric model are also thinner at the tropopause. HadCM3L is coupled to terrestrial and ocean carbon cycle models, TRIFFID (Cox et al. 1998) and HadOCC (Palmer and Totterdell 2001). Williams et al. (2013) further tuned the ocean carbon cycle using the FAMOUS model (low resolution version of HadCM3). We use the same parameter set since the ocean model of FAMOUS is the same resolution

and configuration as the ocean component of HadCM3L. TRIFFID simulates vegetation growth and decay and carbon storage in soil, excluding peat and permafrost. HadOCC is a biogeochemical ocean ecosystem NPZD model, which accounts for the interactions between Nutrients, Phytoplankton, Zooplankton and Detritus, in addition to total alkalinity and carbon dioxide. This ocean ecosystem model represents phytoplankton limitation by nitrogen availability, light and temperature, allowing a basic simulation of the response of the model's ocean ecosystem to changes in orbitally driven nutrient supply, temperature and light. The biogeochemistry is relatively simple compared to some models (e.g. Ridgwell et al. (2007)) but the physical climate system is much more comprehensive and the NZPD model is a more complex representation of biological processes.

We configure HadCM3L using a high-resolution Cenomanian paleogeography provided by CGG Robertson using methods described in Markwick and Valdes (2004), using a compilation of data from tectonic, lithological, and DSDP/ODP records and the literature. We do not account for the climate feedback of CO_2, assuming a fixed atmospheric CO_2 of 3x pre-industrial concentrations. We do not include interactive CO_2 because the ocean carbon cycle component does not include the long term sources and sinks (e.g. volcanism, weathering, sedimentation). 3x pre-industrial concentrations is a typical (maybe low) value for the Cenomanian (Foster et al. 2017).

To sum up the model selection for this study, HadCM3L was chosen on account of it's combination of relatively high spatial resolution and full representation of ocean physics, representation of ocean ecosystem and oxygen,

and manageable simulation times.

4.4.2 OAE2 and orbital model configuration

This study explored the effect of various orbital parameters for the development of OAE2. For this model configuration, we imposed a number of varying orbital parameters, which were chosen to consider a range of effects for OAE2 development. Using different combinations allowed for a range of extremes in orbital configuration to be studied, importantly considering the uncertainty of the true orbital parameters for this period (Laskar et al. 2011).

Each of the differing orbits causes a differing pattern in solar radiation when compared to the control orbit across a model year (see Figure 4.1). This Figure demonstrates how the orbital parameters used translate into incoming solar radiation in the model across the yearly cycle. Within Figure 4.1, panel A shows the control (modern) incoming radiation supplied to the model, whilst panel B-G shows how each of the tested orbital scenarios differed. The pattern in solar radiation is the key difference between simulations used; simulations are otherwise identical. Pairings of orbital parameters were chosen to gain a strong contrast between the two scenarios, with an almost inverted change between one scenario and it's partner. In all cases these orbital parameters were chosen as extreme end members, due to the problem of unknown orbital parameters during the Cenomanian time period in question.

The selected orbital parameters and their justification for use are pre-

sented as follows:

1. A control run with a modern orbit

Firstly, a control run was selected using modern orbital parameters to correspond with modern day orbit, with the pattern of solar insolation in a year shown in Figure 4.1A. The control simulation corresponds to the pre-OAE2 Cenomanian configuration of the model. This modern orbit control run is the control simulation from which we will compare the results of the subsequent three pairings of changes. See Figure 4.1A for the solar insolation pattern this corresponds to. The pattern of solar insolation in this run is the same as the modern, with northern-hemisphere summer in June, July and August and winter in December, January and February.

2. Real orbits with altered seasonality

The first of the pairings of changes to be applied were changes to seasonality. Previous studies have made idealised changes to precession, obliquity and eccentricity. Such changes are useful for discussing theoretical mechanisms but likely do not correspond to any real orbit. Therefore, we decided to utilise "real" orbital configurations corresponding to those that occurred 216 thousand years ago, with enhanced seasonality (compared to the control, modern orbit) and a "real" orbit from 228 thousand years ago, with reduced seasonality (compared to the control, modern orbit). Both of these time periods correspond to the largest perturbation in seasonal solar insolation during the last 800,000 years (as measured by the 65N summer insolation) (Berger and Loutre 1991).

The 216 ka real orbit (see Figure 4.1B) shows a strong strengthening of the Northern Hemisphere Summer, and a decrease in the Northern Hemisphere Autumn and Winter. This causes an increase in seasonality, particularly in the northern hemisphere. In contrast, the 228 ka orbit (see Figure 4.1C) shows a reduction in seasonality, with cooler northern hemisphere summers and warmer winters. This distinction is not as clear cut in the southern hemisphere, where the effects are still strong but fall mainly in spring and autumn.

There are marked differences in seasonal solar forcing between the two orbits (see Figure 4.1A and B). The two orbits have nearly identical eccentricity, leading to similar total annual solar insolation values when comparing the two simulations; $339.90\,\mathrm{W\,m^{-2}}$ and $339.80\,\mathrm{W\,m^{-2}}$ respectively. Their obliquity difference (with the 216 ka orbit having slightly more than the control 24.30° and the 228 ka having slightly less 22.40°) leads to the 216 ka simulation having slightly more pronounced seasonality than the 228 ka simulation. Moreover, their procession is entirely opposing with the 216 ka simulation receiving much more marked northern-hemisphere seasonality compared to the 216 ka simulation.

We use 'real orbit' configurations as plausible, heavily perturbed end-members which are nonetheless known to be realistic, representing known configurations from the recent past. Representing near identical eccentricity but with seasonal cycles very different from the modern (control) simulation, they allow us to understand how greatly modified seasonality might look as a combination of parameters.

3. Obliquity

The second of the pairings of changes to be applied were changes to obliquity only. This utilised firstly an orbit with high obliquity and secondly, an orbit with low obliquity.

The main effects of obliquity (see Figure 4.1d-e) are centred at latitudes greater than 30 degrees north or south. The high obliquity scenario causes a large increase in radiation at the surface in summer for both hemispheres: increasing by $50\,\mathrm{W\,m^{-2}}$ compared to the control while winters are slightly cooler, with a reduction of $20\,\mathrm{W\,m^{-2}}$. Due to the increased tilt of the earth in the high obliquity run, the high latitudes therefore experience an enhanced seasonal cycle (Williams 1993).

In summary, from changing obliquity alone, this second pairing of changes has increased or decreased seasonality, as a result of using high or low obliquity, respectively. Notably however, there is little overall change in incoming radiation across the year, with both presenting a mean insolation of $338.80\,\mathrm{W\,m^{-2}}$.

4. Eccentricity

The third and final set of pairings of changes were applied with firstly, a highly circular (no eccentricity) orbit, and secondly, an highly elongated (non-circular, high eccentricity) orbit.

Changing eccentricity (see Figure 4.1F-G) causes changes in the magnitude of solar insolation in summer and winter, but does not move them temporally within the year. A circular orbit has less intense summers and

winters, since solar insolation does not change through the year (Figure 4.1F), with a mean insolation of 338.70 $\mathrm{W\,m^{-2}}$. In comparison, a more eccentric orbit (Figure 4.1G) has an increased summer-winter difference, with warmer summers and cooler winters compared to the control, and a mean solar insolation of 339.90 $\mathrm{W\,m^{-2}}$.

Unlike the other simulations, eccentricity acts across the whole earth surface in a relatively uniform way: in the circular orbit acting to reduce the difference between summer and winter worldwide, and increasing it in the high eccentricity orbit.

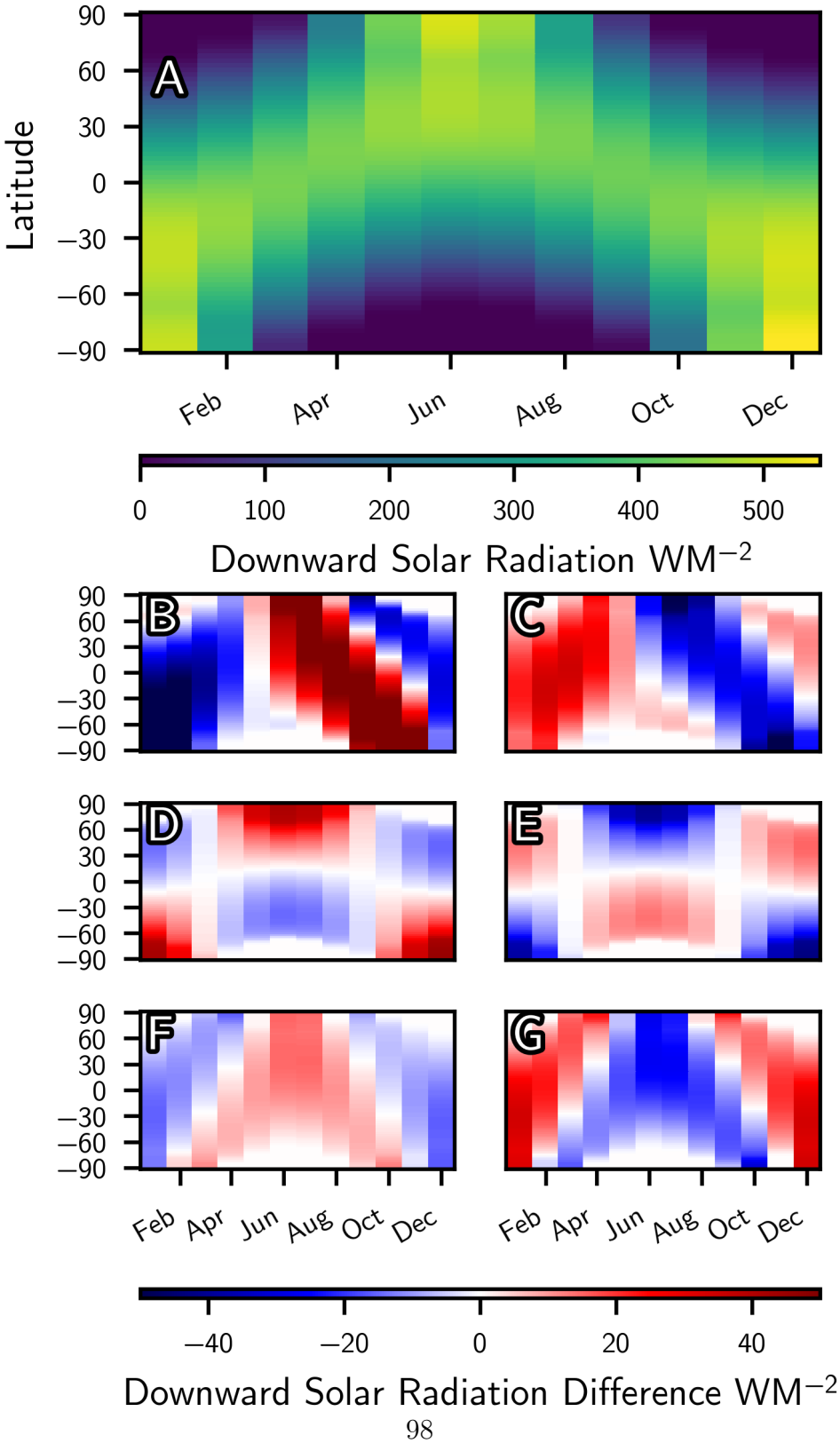

Figure 4.1: Solar radiation at the top of the atmosphere. The selected orbital parameters are detailed, firstly showing Panel A: the modern control orbit. This modern control orbit is then compared with a 216 ka orbit (Panel B), a 228 ka orbit (Panel C), a high (Panel D) and low obliquity orbit (Panel E), and a high (Panel F) and low (Panel G) eccentricity orbit.

4.4.3 Impact of orbital changes on benthic oxygen

Using these outlined orbital forcings, we firstly look at the variation in benthic oxygen concentration with orbital change, since oxygen depleted bottom waters are an important indicator for when deposition of anoxic sediments would have occurred (Schlanger and Jenkyns 1976; Turgeon and Creaser 2008). The variation in benthic oxygen concentration importantly indicates the potential for black shale deposition, as high levels of organic carbon preservation is generally possible only for oxygen levels as low as or smaller than $10\,\mu mol\,L^{-1}$ (Monteiro et al. 2012; Zhou et al. 2017). We then examine primary productivity, ocean circulation, and freshwater supply in order to understand the key mechanisms that drive the changes in benthic oxygen.

To examine these changes we configure HadCM3L runs with contrasting orbital forcings, outlined in section 4.4.2: real 216 ka and 228 ka orbits, obliquity and eccentricity and then highlight the impact of these ranges on benthic oxygen concentration, as the key chosen indicator for the onset of OAE2.

4.5 Results

4.5.1 What is the effect of orbital configurations on benthic oxygen?

To assess the impacts of various orbital configurations for the onset of OAE2, the effects of configuring HadCM3L runs with various orbital forc-

ings: real 216 ka and 228 ka orbits (Figure 4.2), obliquity (Figure 4.3) and eccentricity (Figure 4.4) ranges on benthic oxygen concentrations were examined.

Firstly, Figure 4.2 shows the effects of the orbital perturbations on benthic oxygen concentration for the real 216 ka and 228 ka orbits. All of these simulations show an area of low benthic oxygen centred on the proto-North Atlantic This somewhat enclosed area results in oxygen levels being reduced to as little as $0\,\mu mol\,L^{-1}$, before spreading to the rest of the world's ocean. The area with the strongest orbitally driven changes in benthic oxygen (percentage difference) is the proto-North Atlantic area. In the 216 ka orbit runs, oxygen concentration in this area is markedly reduced with respect to the control run, by as much as a 51.90 % reduction. In contrast, in the 228 ka orbit there is an increase in oxygen concentration, by up to 21.70 %. Changes in the proto-North Atlantic are mirrored by changes in the Pacific in both the 216 ka and 228 ka orbital runs. Whilst a reduction is seen in Pacific benthic oxygen in the 216 ka run, the reverse occurs in the 228 ka run, with the effect particularly seen in the north where the simulations see changes of up to -25 % and 5 % respectively. However, it is important to note that this change is not reflected across the entire global ocean. In both real orbit runs, the Tethys sea is a reverse of the proto-North Atlantic, with increases of up to 14.10 % and increases of up to 16.20 %, respectively. Despite this, the changes in the global mean reflect the dominance of the proto-North Atlantic, where in the 216 ka run the global mean drops $15.82\,\mu mol\,L^{-1}$ compared to the control. Moreover, despite much of the global ocean seeing a reduction in benthic oxygen of

around 5 %, the 228 ka run sees a small increase of 0.31 µmol L^{-1} in the global mean.

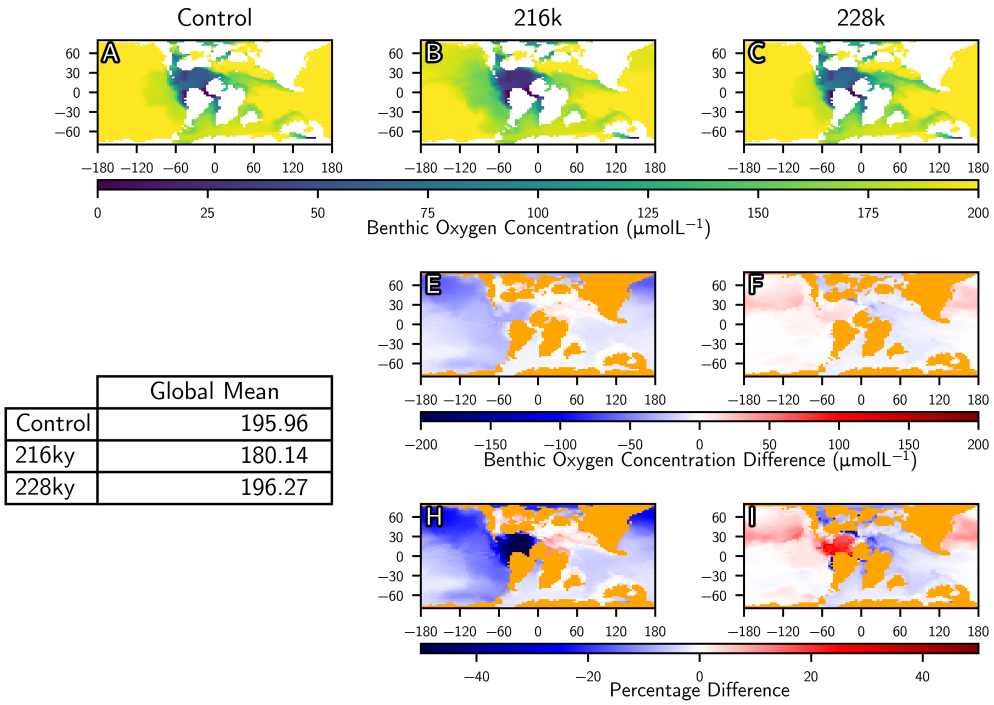

	Global Mean
Control	195.96
216ky	180.14
228ky	196.27

Figure 4.2: Changes in benthic oxygen concentration for the 216 ka and 228 ka orbit configurations, compared to the control (modern) orbit. Panels A-C: Benthic oxygen concentrations at the end of the model run for each of the three orbital scenarios. Panels E and F: Difference between each orbital scenario and the control run. Panels H and I: Percentage difference between each orbital scenario and the control run.

Secondly, changing obliquity has a similar, yet not identical effect to the two real orbital scenarios (see Figure 4.3). This is expected since the changes in incoming radiation across a model year are fairly similar at high latitudes (for example, when comparing panels B and C of Figure 4.1 to D and E). Indeed, the changes in the 216 ka and 228 ka runs have a strong obliquity signal. The most important difference between benthic oxygen levels from Figure 4.2 and Figure 4.3 is the lack of change in the high lati-

tude Pacific in the obliquity scenarios, and the uniformity across the global ocean with which these simulations differ from the control. In the high latitude Pacific, the reductions seen in the 216 ka simulation are smaller and more consistent with the Pacific as a whole ($-11.10\,\%$). These simulations achieve bigger differences from the control simulation than the 'real orbit' simulations ($-16.03\,\mu mol\,L^{-1}$ and $8.96\,\mu mol\,L^{-1}$), but the changes are more evenly distributed across the global ocean.

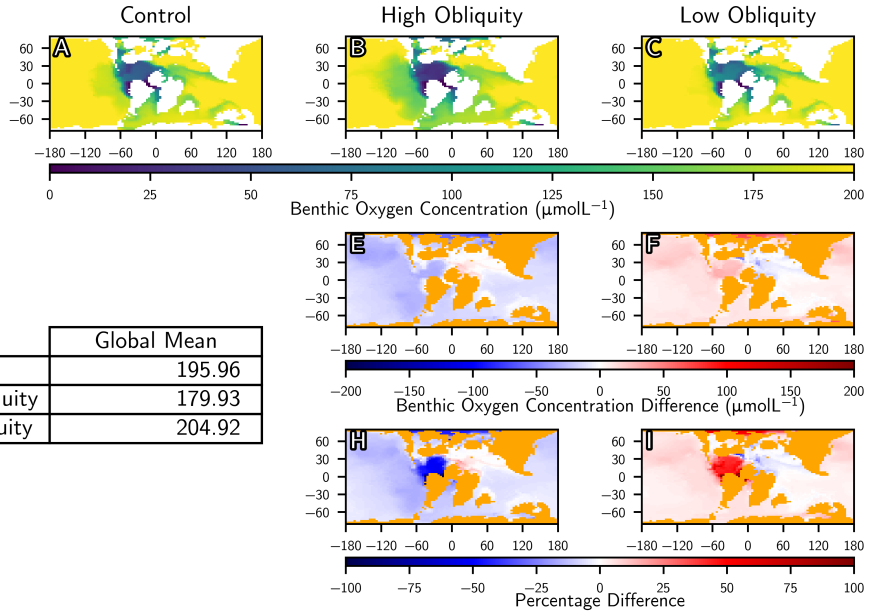

	Global Mean
Control	195.96
High Obliquity	179.93
Low Obliquity	204.92

Figure 4.3: Changes in benthic oxygen concentration for a high and low obliquity orbit, compared to the control (modern) orbit. Panels A-C: Benthic oxygen concentrations at the end of the model run for each of the three orbital scenarios. Panels E and F: Difference between each orbital scenario and the control run. Panels H and I: Percentage difference between each orbital scenario and the control run.

Finally, the eccentricity scenarios show more muted changes (see Figure 4.4), particularly in the proto-North Atlantic, when compared with the real orbital scenarios (see Figure 4.2) and with simulations where obliquity was

altered (see Figure 4.3). Figure 4.4 predominantly shows that a weakening (circular orbit) or strengthening of the seasonal cycle as a whole appears to have little effect on benthic oxygen in the important proto-North Atlantic, where levels barely change with respect to the control simulation (a small increase of 20 % is seen in the high eccentricity simulation). In this simulation, small reductions are seen across the Tethys, but the impact is small and the areas of benthic anoxia are not greatly deepened (Figure 4.4).

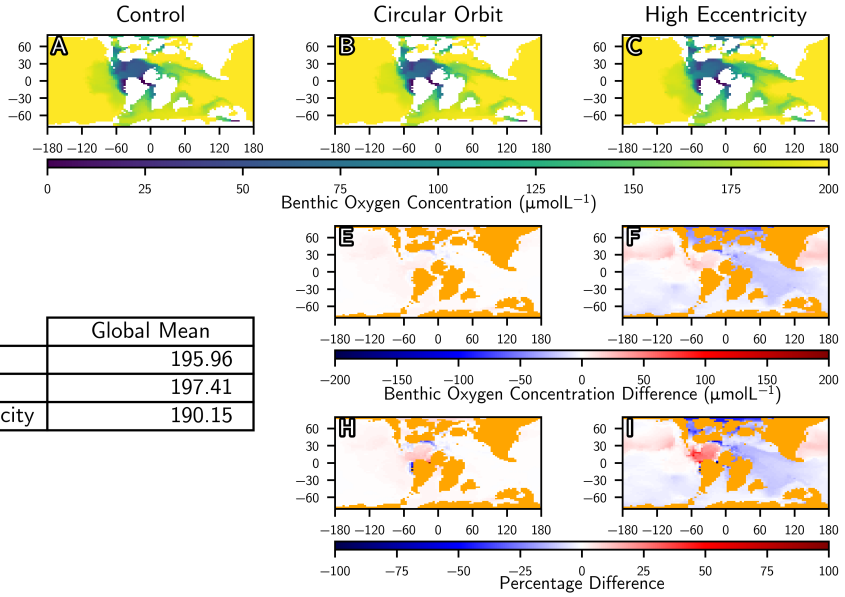

	Global Mean
Control	195.96
Circular	197.41
High Eccentricity	190.15

Figure 4.4: Changes in benthic oxygen concentration for a circular and very eccentric orbit, compared to the control (modern) orbit. Panels A-C: Benthic oxygen concentrations at the end of the model run for each of the three orbital scenarios. Panels E and F: Difference between each orbital scenario and the control run. Panels H and I: Percentage difference between each orbital scenario and the control run.

While changes in orbital cycling cause variations in benthic oxygen up to 16.13 $\mathrm{mmol_{O_2}}$ L, concentrated in the North proto-Atlantic basin (see Figure 4.2), none of the modelled orbital scenarios cause a dramatic deoxygenation

as observed during OAE2. Our results support the idea that orbital cycling cannot trigger OAE2 alone.

Comparing the real orbit simulations (Figure 4.2), obliquity simulations (Figure 4.3) and eccentricity simulations (Figure 4.4) shows that the changes to the seasonal cycle seen in the former two simulations are more important in controlling benthic oxygen levels than the strengthening in the latter. The driving forces in the "real orbit" and obliquity simulations: namely seasonal cycle changes (a strengthening and weakening of the winter and summer seasons) are similar. We therefore focus on our real orbit simulations with strong and weak seasonality for the remainder of the analysis, with reference to the other scenarios where appropriate.

4.5.2 What is the impact of primary production on benthic oxygen concentration?

A first key, identified mechanism, linked for its role in altering ocean oxygen, is primary production. It has been widely cited that enhanced primary production in the surface ocean, causes deoxygenation (Poulton et al. 2015; Ruvalcaba Baroni et al. 2014), since remineralisation of the extra carbon exported from the euphotic zone consumes oxygen (Van Cappellen and Ingall 1994).

To identify areas of high primary production in the model, surface phytoplankton concentration from the NPZD ecosystem model was examined. Areas with increased phytoplankton concentration highlight higher primary production is present. We examine changes in surface primary production

(Figure 4.5) and changes in below photic zone upward nutrient flux (Figure 4.6). Comparisons were made between a 216 and 228 ka orbit, relative to a control run.

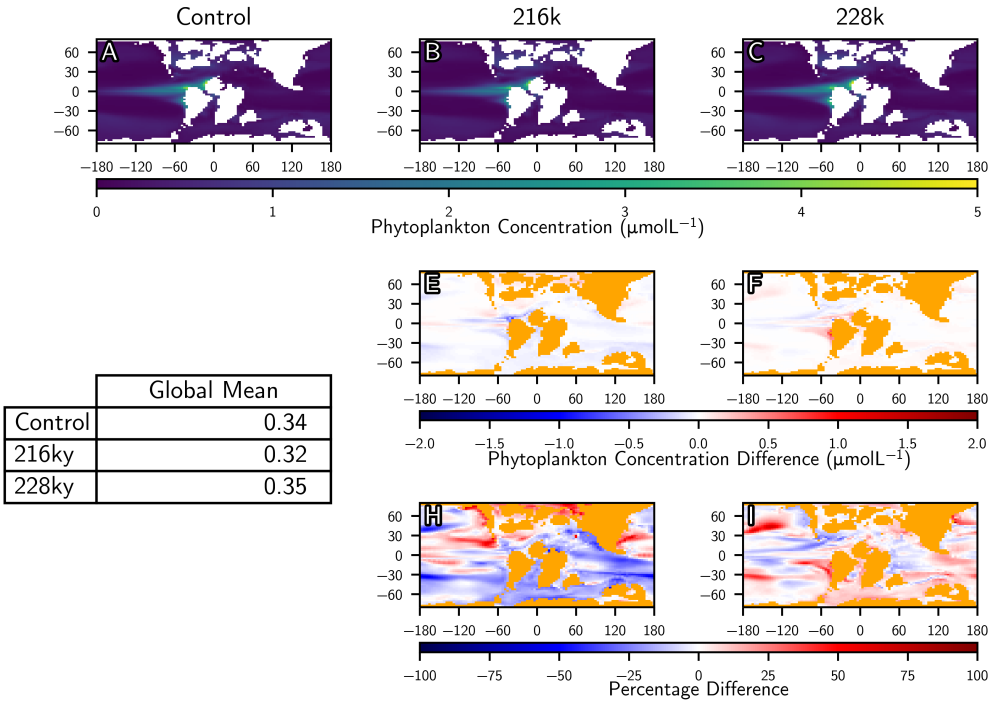

	Global Mean
Control	0.34
216ky	0.32
228ky	0.35

Figure 4.5: Changes in surface primary production for a 216 ka and 228 ka orbit, compared to the control (modern) orbit. Panels A-C: Primary Production at the end of the model run for each of the three orbital scenarios. Panels E and F: Difference between each orbital scenario and the control run. Panels H and I: Percentage difference between each orbital scenario and the control run.

In the 216 ka model run, global mean primary production is slightly reduced, by $0.02\,\mu\text{mol}\,\text{L}^{-1}$, whilst in the 228 ka model run it is increased by $0.01\,\mu\text{mol}\,\text{L}^{-1}$ (see Figure 4.5). In both model runs these changes are largest in absolute terms at the south side of the proto-North Atlantic, and on the equatorial Pacific, with difference values in the Atlantic of up to $-0.43\,\mu\text{mol}\,\text{L}^{-1}$ (216 ka) and $0.28\,\mu\text{mol}\,\text{L}^{-1}$ (228 ka). In both simulations

the changes in primary production are largest in areas where the control simulation shows non-zero primary production; in neither simulation does primary production meaningfully spread from the equatorial east Pacific and proto-North Atlantic.

These changes highlight that primary production does not drive the changes in benthic oxygen seen in in the proto-North Atlantic. Indeed, an increase in benthic oxygen would be expected from a reduction in primary production (eg. seen in the 216 ka run), however, a reduction of $0.02\,\mu mol\,L^{-1}$ globally is seen. Similarly in the 228 ka run, the increase in primary production seen would be expected to cause a lowering of benthic oxygen, however the opposite is seen as benthic oxygen increases by $0.01\,\mu mol\,L^{-1}$.

Elsewhere in the global ocean, moderate percentage changes of up to 25 % in the 216 and 228 ka runs are shown. While the global mean change in both these runs correspond with the changes seen in the proto-North Atlantic, there is significant spatial variation worldwide. Areas of particular interest are those where the sign of change in primary production correlates with that expected in benthic oxygen. This is true in the Arctic ocean in the 216 ka run, and perhaps some areas of the Tethys Sea in both runs, although patterns here are complex.

The observed primary production changes with orbital cycling result from perturbations on nutrient vertical flux, with the primary production decrease associated with a decrease in nutrient vertical flux and primary production increase associated with an increase in nutrient vertical flux (Figure 4.6). The largest changes in upward nutrient flux (Figure 4.6)

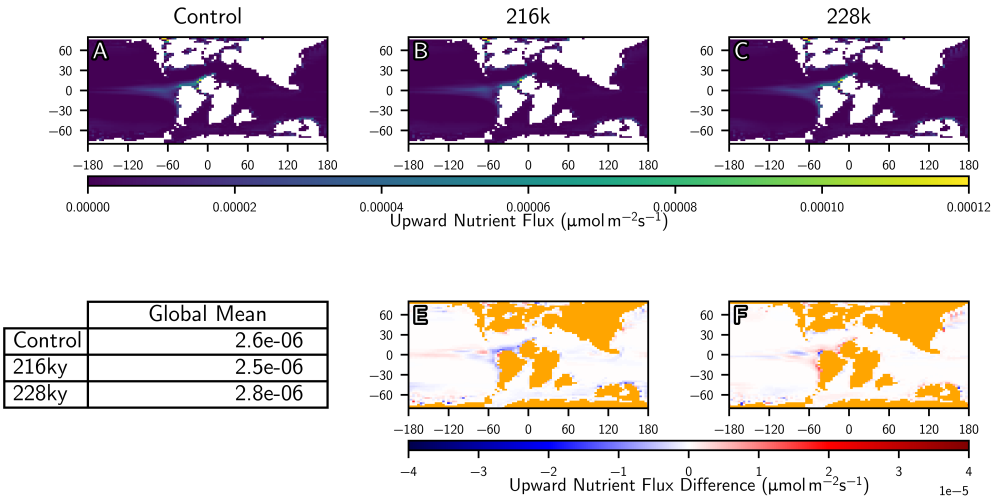

	Global Mean
Control	2.6e-06
216ky	2.5e-06
228ky	2.8e-06

Figure 4.6: Changes in below photic zone upward nutrient flux for a 216 ka and 228 ka orbit, compared to the control (modern) orbit. Panels A-C: Upwelling at the end of the model run for each of the three orbital scenarios. Panels E and F: Difference between each orbital scenario and the control run.

correlate well with the highlighted changes in ocean primary production (Figure 4.5). The largest changes in upwelling are again in the equatorial Pacific and south proto-North Atlantic, with the sign of the change in nutrient fluxes being generally that which would be expected to cause the changes in primary production. These changes in upwelling are caused by seasonal changes in surface wind, manifested as a winter northward shift of the ITCZ in the 216 ka run and an opposite shift in the 228 ka run, with this shift reversed in the winter months.

Overall, primary production does not explain the orbital changes in benthic oxygen. Another source of deoxygenation is a slowing down in ocean circulation. We investigate this further now.

4.5.3 What is the impact of ocean circulation on benthic oxygen concentration?

Ocean circulation is able to change ocean oxygen concentration both by changing how often ocean waters are brought to the surface and equalised with the atmosphere, and by changing the supply of nutrients and altering phytoplankton growth (Van Cappellen and Ingall 1994), as seen through changes to primary production. Ocean circulation was examined based on three different variables: water age, overturning circulation and mixed layer depth.

Firstly, a water age tracer was used, whereby the model calculates how long ago a virtual tracer was last exposed to the ocean surface. When this occurs and water is mixed to the ocean surface, it's water age is reset to zero; on leaving the ocean surface, water age is increased as the water remains away from the surface. Through these calculations we can understand the time since water masses were at the ocean surface as if water age increases in ocean as a whole it can demonstrate a slowdown of the ocean circulation.

Secondly, the ocean overturning circulation is analysed. The overturning circulation is the transport of deep water from the poles toward the equator, and surface water towards the poles. This circulation is very important for the transport of heat away from the equator, and is particularly controlled by deep water formation and the meridional temperature difference (Ladant et al. 2018; Zhang et al. 2020).

Finally, mixed layer depth was used to identify areas where deep water formation was occurring in the model ocean. In deep water forming areas

the mixed layer depth deepens (Holte and Talley 2009), as more dense surface water falls away from the surface and is replaced. This means high latitude areas where deep water is forming have deep mixed layer depths compared to the remainder of the world ocean.

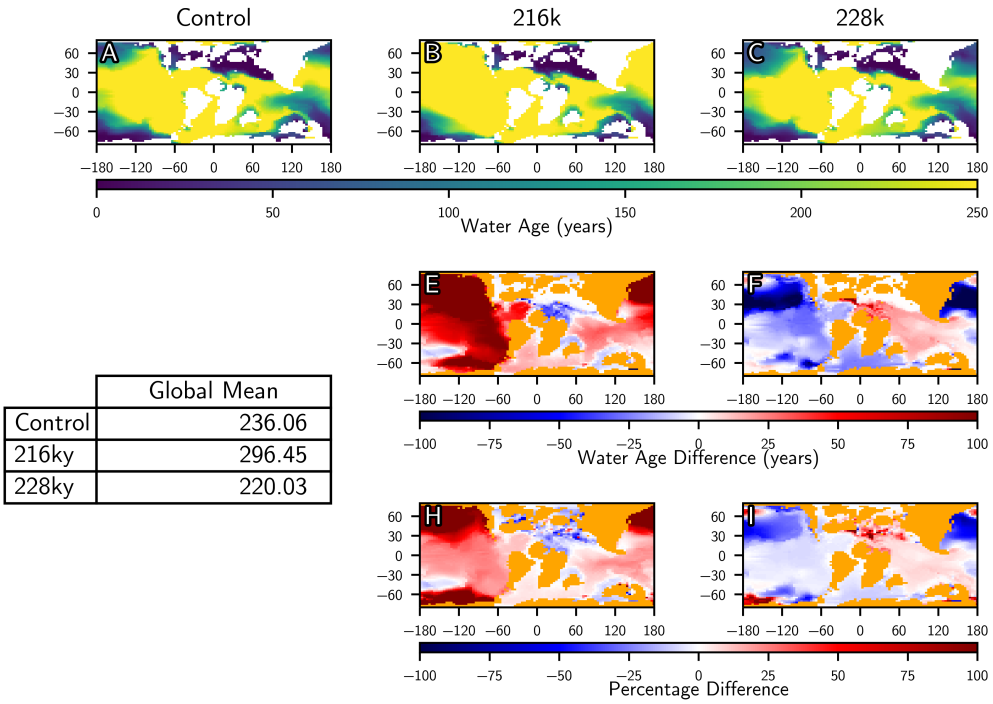

	Global Mean
Control	236.06
216ky	296.45
228ky	220.03

Figure 4.7: Changes in benthic ocean water age for a 216 ka and 228 ka orbit, compared to the control (modern) orbit. Panels A-C: Water age at the end of the model run for each of the three orbital scenarios. Panels E and F: Difference between each orbital scenario and the control run. Panels H and I: Percentage difference between each orbital scenario and the control run.

In contrast to our results demonstrating the impact of primary production on benthic oxygen concentration (section 4.5.2), changes in deep ocean water age do correlate well with changes in benthic oxygen, suggesting ocean circulation may be an important mechanism. Deep ocean water is generally older in the 216k run, where benthic oxygen is also reduced,

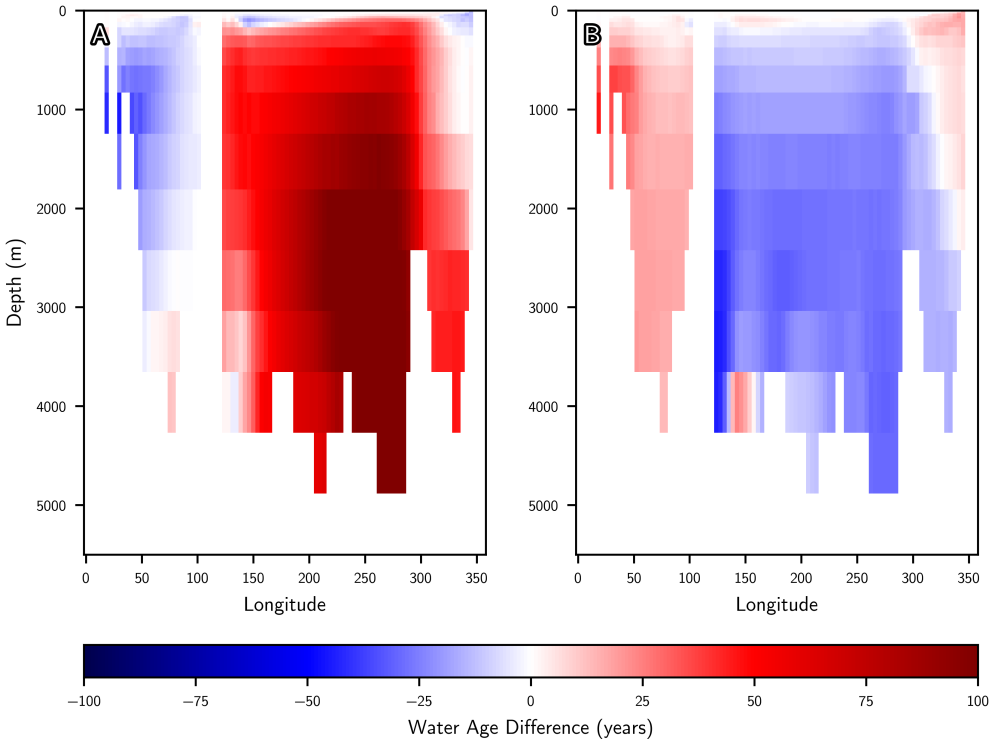

Figure 4.8: Difference in ocean water age from the control simulation, in section along 10 degrees latitude north, in the 216 ka (A) and 228 ka (B) simulations.

particularly in the proto-North Atlantic, and across the Pacific (see Figure 4.7). Figure 4.8 shows older water in the Pacific to be supplying older water to the proto-North Atlantic (Figure 4.8A), with the increase in water age in the Pacific causing an increase in the North Atlantic through the Panama gateway.

The 216k run shows a general reduction in ocean overturning circulation (Figure 4.9, panel D), whilst the 228k run shows an increase in overturning in the Northern hemisphere only, and a reduction in the south (Figure 4.9, panel E). This change in ocean circulation is caused by a slowdown in deep water formation in both the North and South Pacific (Figure 4.10). North-

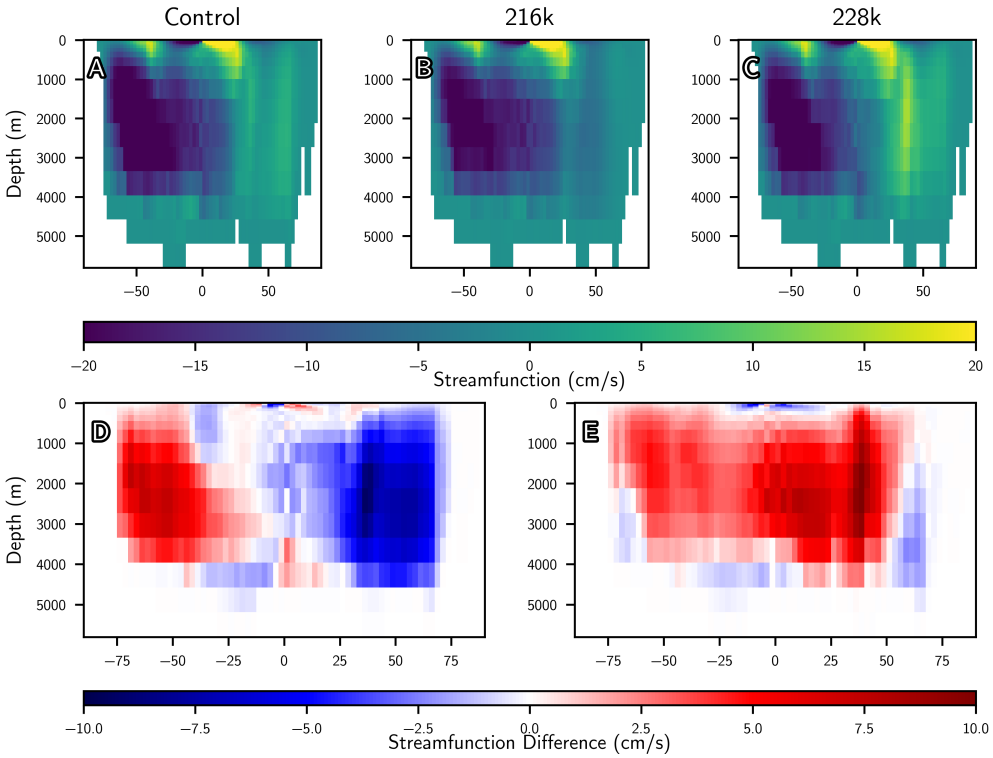

Figure 4.9: Global stream function across a model year, in the control, 216k and 228k runs (panels A-C). The difference with the control (panels E and F).

ern Hemisphere circulation (coming toward the reader out of the page from Figure 4.9) is fairly weak in the control run, and further weakened in the 216 ka run. Southern Hemisphere circulation is stronger than the Northern Hemisphere circulation in all of the model runs, but is also weaker in the 216 ka run. The picture in the 228 ka run is more complex, with this run seeing a similar reduction in the southern hemisphere but an increase in the North. These patterns in northern hemisphere circulation help in explaining the highlighted patterns in water age, with the reduced overturning in Figure 4.9D reflecting a broad increase in water age here as water is mixed

to the surface less frequently.

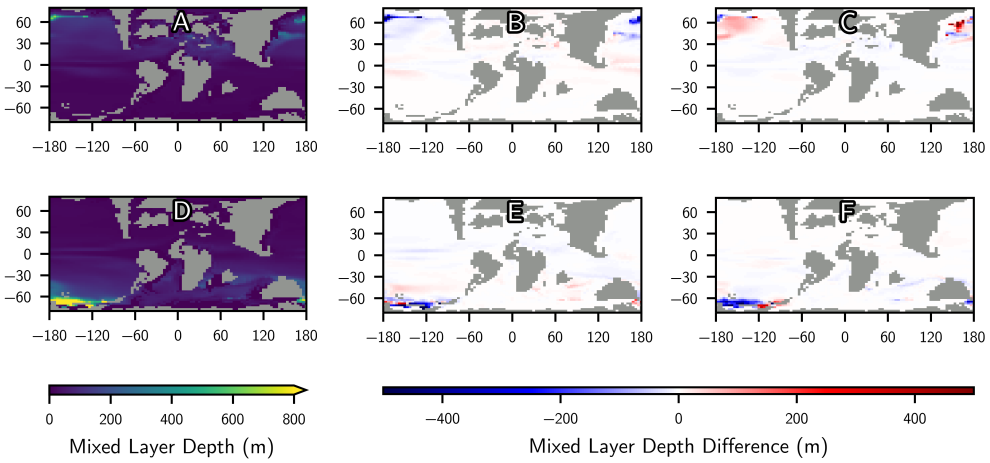

Figure 4.10: Mixed layer depth, used to show areas of deep water formation. A and C show the mixed layer depth in the control simulation. B and E the difference with the 216k simulation and C and F with the 228k simulation. Northern winter (seasonal mean for December, January and February) shown in the top row (A, B and C), southern winter (June, July and August) below (D, E and F).

The changes in ocean circulation which can be seen in Figure 4.9 are a direct result in the change in intensity of deep water formation in the Pacific. In Figure 4.10 we use mixed layer depth (MLD) as a proxy to identify areas where winter deep water formation occurs. As the largest ocean and only area with notable deep water formation, the Pacific dominates the overturning circulation previously discussed. In our control simulation, deep water formation occurs in both the north (4.10A) and south (4.10B) of the Pacific, with a particularly strong signal in the south: this is also reflected in the dominance of the southern hemisphere in Figure 4.9A. In the northern hemisphere deep water formation is nearly completely suppressed in our 216k simulation (4.10B), while in the 228k simulation it is

strengthened, particularly in the North West Pacific: enough to generate noticeably stronger overturning in Figure 4.9. Southern Pacific deep water formation is reduced in both simulations. Unlike in the north, the 216k retains weakened deep water formation in the south. The change in the 228k simulation is both a reduction in area of deep water formation and a shift eastwards, and since it is smaller in magnitude it has less dramatic effect on the total circulation.

These changes in deep water formation are caused by a complex picture of ocean surface temperature and salinity changes. Temperature has a minor contribution in this when compared to salinity. Ocean surface water in the 216k simulation is on average 0.65 °C warmer than that of the 228k, a result of the warmer summer in the 216k simulation (Figure 4.1 B compared to C). The effect of this on deep water is felt most strongly in the southern winter (June, July and August), where the surface water surrounding the south pole is ≈1 °C warmer in the 216k year simulation compared to the 228k simulation. A lowering of ocean surface salinity is seen in our 216k simulation, by 0.30 psu globally, and the reverse is true in our 228k simulation, with a 0.20 psu rise seen there.

In both simulations, these salinity changes are caused by both the P-E budget (PE) changes seen in Figure 4.11 and the consequent riverine runoff, which along the north coast of the Pacific (above 40 North) is increased by 72 % in the 216k simulation compared to 228k. The PE balance in both the northern and southern Pacific Ocean upwelling areas (Figure 4.11) reflects the suppression and intensification of deep water formation. In the 216 ka simulation (Figure 4.11A), rainfall is intensified in the north, east, and south

Pacific, suppressing upwelling. In the 228 ka simulation (Figure 4.11B), the reverse is true in the northern hemisphere, but redistributed in the south, causing the movement in deep water formation there. The large changes in PE seen at the equator result from intensification of the monsoon. Of these changes, the most interesting is the intensification (216 ka) and suppression (228 ka) of rainfall to the north of South America, which further acts to freshen the supply of water from the proto-North Atlantic to the Pacific in Figure 4.11.

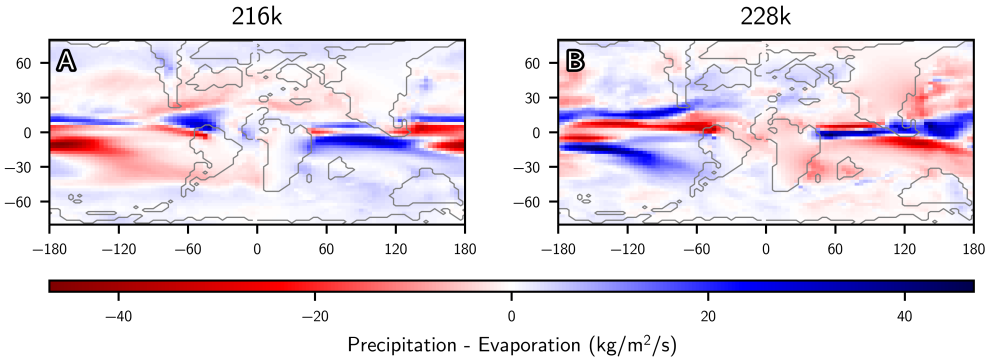

Figure 4.11: Difference in water balance (precipitation minus evaporation) from the control simulation in the 216 ka simulation (A) and 228 ka simulation (B), in $kg/m^2/s$.

4.6 Discussion

4.6.1 The onset of OAE2 was not triggered exclusively by changes to orbital cycling

Our examination of the effects of orbital forcings on benthic oxygen concentration highlighted firstly that no singular orbital configuration modelled

caused a large enough change to either remove or significantly reduce the spread of the area of low oxygen seen to develop in the proto-North Atlantic. This is in agreement with much of the literature (Charbonnier et al. 2018; Voigt et al. 2007) where the consensus is that the major perturbation which caused OAE2 was not orbital cycling (the major cause is generally attributed to vulcanisim), but that orbital cycling caused variations in deposition throughout the OAE.

Despite this, our orbital perturbations do induce changes in benthic oxygen concentration as demonstrated in section 4.5.1 and Figures 4.2, 4.3 and 4.4. This has marked implications for identifying cycling relating to this in the sediment record, and how orbital variability affected the onset and development of the OAE. Indeed, many studies suggest that orbital forcing had an important role in triggering the onset of OAE2 (Kuhnt et al. 2017; Meyers et al. 2012; Mitchell et al. 2008). In our pre-OAE2 model, orbitally induced changes primarily act to make the developing area oxygen in the proto-North Atlantic more or less pronounced. Our results show higher obliquity simulations cause benthic deoxygenation in line with Charbonnier et al. (2018) and Meyers et al. (2012), who also suggested strong obliquity at the OAE onset. Indeed, Charbonnier et al. (2018) suggest, using cyclostratigraphy, that there was high obliquity at the onset of OAE2 and show obliquity as a dominant driver of climate This is in line with our results showing obliquity can cause large changes in benthic oxygen concentration.

4.6.2 Primary production does not account for the orbital changes in benthic oxygen for development of OAE2

We achieve a reduction in benthic oxygen without an increased supply of nutrient to the surface ocean, either from the deep ocean (Figure 4.6), or from riverine input (the latter is not included in our model). This means we achieve the discussed oxygen changes without the continental weathering arguments used in much of the literature (Charbonnier et al. 2018; Meyers et al. 2012; Mitchell et al. 2008; Mort et al. 2007) and instead find them to be caused by ocean circulation changes alone.

Examining the series of key mechanisms for their effects as a result of orbital changes demonstrated that variability in primary production did not generate changes in benthic oxygen concentration. Indeed, surface primary production is seen to be reduced in model simulations where benthic oxygen is decreased (see Figures 4.5 and 4.6). This is the opposite to what might be expected if primary production was the driving force for benthic oxygen in this instance, and is at least partially a result of our model not incorporating the weathering mechanism used to explain an increased nutrient supply in much of the literature (Charbonnier et al. 2018; Kuhnt et al. 2017; Mitchell et al. 2008; Poulton et al. 2015). Notwithstanding this omission, the circulation changes shown in section 4.5.3 do not result in the supply of nutrient rich waters to the surface in a way which triggers increased primary production, in disagreement with Meyers et al. (2012) who suggest this as a mechanism for orbital impact on the OAE.

We suggest a logical extrapolation of our precipitation and runoff results (section 4.5.2) is that continental weathering would have increased in our simulations due to the changes in runoff observed. Therefore, while in this paper we show that large changes can be achieved using only physical effects, we suggest that any biological effects from this mechanism may have acted in tandem with the circulation effects, albeit it is possible they would be suppressed by the upwelling changes shown in Figure 4.6.

4.6.3 Ocean circulation is an important control on benthic oxygen for the development of OAE2

In contrast to our analysis of primary production, we see that changes in ocean circulation can markedly explain the changes seen in benthic oxygen concentration and therefore the onset of OAE2: a finding in alignment with Sarr et al. (2022). The strong control that ocean circulation has on benthic oxygen here is highlighted through the increases in the age of water in the benthic proto-North Atlantic, which is the driving factor behind the reduction in oxygen in our 216 ka-orbit run. This process can be accounted for as this water is supplied from the Pacific, and it's increase in age is caused by a general slowdown of the ocean circulation which results from the changing patterns of solar warming.

We show that these ocean circulation effects (for example, a slowdown in the 216 ka simulation) are driven primarily by high latitude deep water formation changing the supply of new bottom water to the Pacific. In our simulations deep water formation is quite dramatically suppressed by fresh-

water inputs at high latitudes. This is similar to the mechanism found by Sarr et al. (2022) who find high-latitude deep water formation to be important in the ocean circulation as a whole, and suggest that these changes in deep water formation are caused by precipitation differences. Our results build on those by Sarr et al. (2022), where we suggest in addition that high-latitude riverine inputs of freshwater input are also important.

The ocean oxygen changes demonstrated in our simulations are predominately a result of ocean circulation changes. This is important in lending weight to other studies who found ocean circulation and high latitude deep water formation to be similarly important in controlling the spread of ocean anoxia (Sarr et al. 2022; Wagner et al. 2013). These results do not preclude the nutrient-runoff mechanism more commonly discussed in the literature (Charbonnier et al. 2018; Poulsen et al. 2001), but do suggest that ocean circulation is important in it's own right.

It is important to note the associated limitations of our modelling study. As discussed above, our model does not include an interactive weathering flux and it is possible that orbital forcing could cause variations in weathering. However, it should be noted that there are a lot of regional variations in runoff fluxes and hence the overall sign of weathering changes are difficult to assess.

The modelling does not include any changes in the atmospheric carbon dioxide (or methane) concentrations. This is common to almost all modelling studies of orbital variability within the Cretaceous. However, during the late Quaternary we know that orbitally induced changes to greenhouse gases can greatly amplify the physical climate response (e.g. Singarayer

and Valdes (2010)). The precise mechanisms by which the orbit modifies carbon dioxide concentrations are still poorly understood and hence cannot currently be included here.

4.7 Conclusion

The results in this paper are a key contribution to understanding how orbital effects contributed to ocean anoxia during OAE2. We show the impact of different orbital configurations on benthic oxygen concentrations and examine the mechanisms by which this oxygen change was caused by changes in solar insolation resulting from the orbital changes we defined. The ocean anoxia changes we show are caused by changes in ocean circulation, rather than primary production, highlighting the importance of this mechanism. We show that ocean circulation in our simulations was controlled by deep water formation in the high latitude Pacific, where different orbital scenarios were able to cause big changes in the extent and location of deep water formation. In our simulations, this deep water formation was controlled by high-latitude freshwater supply, through both runoff from rivers and precipitation. This control was particularly clear in the north Pacific where orbital changes were able to almost completely suppress deep water formation in some simulations. We show that while the changes caused by orbital cycling in our study are not dramatic enough to prevent the reduction in oxygen in a pre-OAE2 ocean, they do show that orbital cycling is likely to have affected the development of OAE2 and could be the cause of variation seen during the OAE.

Although our study lends considerable strength to a ventilation mechanism for orbitally induced controls on benthic oxygen, it does not preclude this acting in tandem with orbital changes causing an additional supply of nutrients to the ocean. Further simulations are necessary to study these nutrient effects in detail, and analyse the relative importance of this nutrient supply when compared to ocean circulation.

These results are highly applicable to advancing our understanding of how orbital cycling affects the development of OAE2. They highlight that orbital changes are able to exert an important control on anoxia though ocean circulation alone, even without an additional supply of nutrients to the ocean.

Chapter 5

The role of physical and biological complexity in modelling OAE2

5.1 Preface

This chapter focuses on how the representation of ocean biology within models affects our understanding of how the OAE developed. For the completion of this work, Alexandra Ashley and Jim Harris (CGG Roberson) provided the paleogeographies used. Fanny Monteiro ran the cGENIE model experiments to compare the behaviour seen in that model with that of HadCM3. In addition, Paul Valdes provided technical support in incorporating this into HadCM3 and with the wider model simulations and along with Fanny Monteiro, provided assistance, feedback and advice for all aspects of the study.

5.2 Abstract

Oceanic anoxic event 2 (OAE2), marking the Cenomanian/Turonian boundary (≈93.50 Ma ago), was a time of huge change in the ocean carbon cycle. A large increase in ocean primary production is thought to have occurred during this event, leading to extensive burial of carbon-rich organic matter in sediments. Consequently, this event has been investigated in many modelling studies, many of which include representation of ocean primary production as an important control on how ocean anoxia developed. However, the ocean carbon cycle (and earth system more generally) is represented differently in different models, and the effects of this on their representation of OAE2 remains unexplored. In this study, we compare the results of OAE2 simulations using HadCM3L and cGENIE. We show that the two models produce different increases in the spread of ocean anoxia when subjected to an increase in nutrient inventory: a result of different ocean productivity and ocean circulation representation. In HadCM3L, grazing pressure acts to suppress the export of detritus from the euphotic zone; an effect which occurs less in high production areas due to a Holling-III functional response of zooplankton. This concentration of export in high production areas means a smaller spread of anoxia is seen in HadCM3L, when compared to cGENIE. This means HadCM3L sees a much smaller reduction in ocean anoxia than cGENIE, which highlights that ocean ecosystem differences should be a key focus when designing modelling studies for OAE2.

5.3 Introduction

OAEs were important events in the past climate, during which large parts of the ocean experienced intense deoxygenation (Schlanger and Jenkyns 1976). Most of the OAEs studied occurred in the Cretaceous and Jurassic periods of the Mesozoic era (Schlanger and Jenkyns 1976), where OAE2 represents one of the most recent OAE events, occurring at the Cenomanian-Turonian boundary (93.5 Ma) (Jarvis et al. 2011). It has been widely suggested that the quantity and spatial distribution of nutrients in the ocean is a dominant control on the development of OAE2 (Jenkyns 2010; Joo et al. 2020; Monteiro et al. 2012). Indeed, an increase in ocean nutrient supply is thought to have caused a dramatic increase in ocean production during OAE2, followed by a subsequent increase in burial causing the resultant layer of black shale seen in modern sediments (Schlanger and Jenkyns 1976).

This nutrient supply increase at the onset of OAE2 is thought to have been derived from an increase in weathering, resulting from increased volcanism (Adams et al. 2010; Jenkyns 2010; Mort et al. 2007). The generally understood mechanism is that a higher nutrient supply to the ocean should stimulate ocean primary production, as phytoplankton that were previously nutrient limited are able to grow more (Joo et al. 2020; Tyrrell 1999). This primary production increase then enhances organic matter export from the euphotic zone, where dead phytoplankton, zooplankton and other particulate organic matter settle down as particles into the ocean interior (Anderson and Ducklow 2001; Flögel 2001; Turner 2015). The majority of export production is remineralised into dissolved inorganic matter:

a process which consumes oxygen (or another elector acceptor if oxygen is not available) (Lam and Kuypers 2011). It is through this process of higher production and remineralisation by which ocean oxygen levels are thought to have been lowered during OAE2. A consequence of reducing the ocean oxygen level is to reduce the remineralisation rate; an effect seen in modern oxygen minimum zones which causes elevated export production from these areas compared to the rest of the ocean (Devol and Hartnett 2001). This effect is thought to be caused by bacteria using other less efficient electron acceptors such as nitrate or sulphate, although other processes such as ecosystem change and changes in composition of sinking material may contribute (Cavan et al. 2017; Devol and Hartnett 2001). Regardless of the cause in this increase in export production, the overall effect results in higher organic matter burial in the sediments (Jenkyns 2010).

5.3.1 Physical controls on nutrient supply

Our current understanding of the controls on nutrient supply as a key control of ocean oxygen concentration, can be broadly defined according to key physical and ecosystem processes. Firstly, the physical ocean exerts an important control on nutrient supply to the surface ocean (and therefore on ocean production) (Berger et al. 1989). Important processes in controlling the ocean circulation include deep water formation, wind-driven upwelling and vertical mixing (Kuhlbrodt et al. 2007). In this section, we outline these processes and the ways in which they affect the distribution in the modern and Cenomanian oceans.

Wind-driven upwelling is caused by a combination of ocean surface wind stress and the Coriolis force. Whenever the transport resulting from surface wind stress is divergent, the effect of this transport is to replace surface waters with water from the deep ocean (Marshak 2012). In the modern ocean, wind-driven upwelling occurs at the equator (Wyrtki 1981), in the Southern ocean around Antarctica (Harrison and Cota 1991) and along the West coasts of continents (Small and Menzies 1981), and this upwelling drives surface primary production wherever it occurs, as surface waters are replaced with more nutrient-rich waters from below (Richardson 2008). In the Cenomanian, equatorial upwelling was particularly strong in the equatorial region of the proto-North Atlantic (Musavu-Moussavou and Danelian 2006), causing high primary production in this crucial region, known for its euxinic conditions. Similarly to the modern ocean (Kuhlbrodt et al. 2007; Marshall and Speer 2012), upwelling is also known to have occurred around Antarctica, driving primary production here like it does in the modern day (Marshall and Speer 2012).

The mixing of nutrients to the surface is an effect caused by internal ocean turbulence, particularly surface winds (Kuhlbrodt et al. 2007) and other internal ocean processes such as tides and friction (Munk 2005; Waterhouse et al. 2014). This turbulence causes deeper ocean waters to mix from below the thermocline into the surface layer, where they are available for primary production. Ocean freshwater input or an increase in temperature act to make the surface layer of the ocean less dense, suppressing this mixing. As a result of these effects, nutrient supply though ocean mixing is most prevalent at high latitudes, where surface waters are cooler and a sea-

sonal mixed layer develops. In the modern ocean, this supply of nutrients through mixing is strongest in the subpolar North Atlantic and the Southern Ocean (Tatebe et al. 2018). It has been suggested that ocean stratification was stronger during the period when OAEs occurred due to warmer temperatures (Corbett and Watkins 2013; Elderbak and Leckie 2016; Erbacher et al. 2001), reduced mixing (Elderbak and Leckie 2016; Hetzel et al. 2011) and reduced ventilation of the deep oceans.

A final important ocean circulation process is deep water formation, which is an important factor in determining the strength of the global thermohaline circulation as a whole (Marshak 2012). This process occurs at high latitudes where water becomes more dense through cooling and brine rejection from sea-ice formation, and sinks away from the surface to spread towards lower latitudes across the ocean floor (Dickson and Brown 1994). Deep water formation at the time of OAE2 is likely to have occurred in the North Pacific and Southern Oceans (Ladant et al. 2020; Poulsen et al. 2001), leading to a more dominant overturning circulation in the Pacific (Laugié et al. 2021; Trabucho Alexandre et al. 2010; Uenzelmann-Neben et al. 2017) than in the modern ocean, where the North Atlantic is also important (Richardson 2008).

In summary, these processes act together to ventilate deep ocean waters and bring nutrient from the deep ocean to the euphotic zone where it is able to be used for production and potentially play a role in regulating OAEs.

5.3.2 Ecosystem controls on primary production

While the effect of higher export production on ocean anoxia development is well-established (Jenkyns 2010; Monteiro et al. 2012), less is clear about the effects of ocean ecosystem dynamics in controlling production during OAEs. Controls on phytoplankton populations can be split into two groups: bottom up, and top down. Firstly, the availability of nutrient, light and the ocean temperature constitute the bottom-up control, and when this control is dominant phytoplankton populations are primarily controlled by the supply of nutrient to the ocean surface (as discussed in section 5.3.1). Secondly, top down control is when consumption of phytoplankton by zooplankton is the primary control on production: the effects of this are explored in this section.

One aspect relevant to high nutrient supply in the modern ocean is that high nutrient regimes tend to have higher zooplankton biomass and higher grazing pressure (Banse 1995), where phytoplankton growth is top-down controlled more than in low nutrient regimes (Vanhoutte-Brunier et al. 2008). This is a particularly complex set of interactions, with different groups of zooplankton becoming dominant depending on the amount of nutrient. However, the net effect is to suppress ocean primary production compared to that which might be expected in high nutrient areas. Because of this, more recycling of organic matter occurs in the surface ocean and less production is exported (Cavan et al. 2017).

This effect is seen in many places in the modern ocean, and has been extensively discussed (Ducklow 2000; Lam and Kuypers 2011; Raven and

Falkowski 1999). Grazing pressure is thought to be an important control on phytoplankton in the subpolar North Atlantic (Banse 1992; Sherr and Sherr 2002), with the effect more strongly observed in the Summer when the mixed layer shallows and phytoplankton are able to grow (Lindemann and St. John 2014). In the equatorial Pacific, grazing rates are high and account for a significant proportion of production (Chavez et al. 1991; Stukel et al. 2011), which contributes, along with micro-nutrient limitation, to suppression of production and export here (Landry et al. 2011). A very similar effect is seen in the Southern Ocean (Martin et al. 1989), and although iron limitation is thought to be most important here (Edwards et al. 2004; Pitchford 1999), there is a bulk of evidence to suggest that when iron becomes available, zooplankton grazing pressure continues to suppress production (Edwards et al. 2004; Halfter et al. 2020; Tsuda et al. 2007).

There has been little-to-no discussion on how zooplankton grazing pressure might have differed during the period of OAE2, despite many studies showing change in zooplankton populations during this time (Coccioni 2004; Coccioni et al. 2006) and indeed use that change to infer other changes in the ocean environment (e.g. Coccioni and Luciani (2005)). In a more stratified ocean, which may have existed during the period of OAE2 (Corbett and Watkins 2013; Sepúlveda et al. 2009), grazing pressure is thought to have increased (Lindemann and St. John 2014; Rose and Caron 2007), simply as a result of the increased density of prey for zooplankton. However, it is unknown how other differences in the zooplankton and phytoplankton populations which existed at the time would have been affected by this pressure.

5.3.3 Model Representation of OAE2 grazing pressure

Modelling studies have been used to assess the interactions between climate, biogeochemistry and ocean anoxia during OAEs, with different degrees of representation of the coupling between nutrient supply, ocean production, warming and ocean currents (Everett et al. 2017; Valdes et al. 2017).

The choice of model used in studies is invariably a trade-off between model computational cost and complexity, on account of the contrasting representation of physical and ecosystem controls (eg. see sections 5.3.2 and 5.3.1) between different models. It is therefore highly advantageous to compare simulations between differing models to firstly, improve our understanding of how the differences in model representation may affect produced results, and secondly to gain information on which processes have the greatest impact on the observed results. HadCM3L and cGENIE are two models of differing complexity which have been applied to simulate OAEs, and their representation of OAE2 will be compared in this study.

The HadCM3 model family sees extensive continued use as a tool for the modelling of paleoclimates (Valdes et al. 2017), primarily due to the niche they fill between computational speed and model complexity. While these models have relatively low resolution and complexity compared to more recent models, they remain a valuable tool combining a simple NPZD marine ecosystem (Fasham et al. 1990), a fully coupled atmosphere-ocean GCM and run-times which are acceptable and useful when undertaking the long simulations required when modelling paleoclimate. The cGENIE model (Ridgwell and Hargreaves 2007) is an Earth System model of intermediate

complexity, which has also been previously used in OAEs studies (Adloff et al. 2021; Monteiro et al. 2012; Naafs et al. 2019). cGENIE makes use of simplified and parameterised ocean circulation physics and marine ecosystem representation. cGENIE typically runs at a lower resolution than HadCM3 meaning it offers greater speed and efficiency than that of HadCM3, making it a useful tool for studying long-term climate events like OAEs (Monteiro et al. 2012). Unlike HadCM3L, cGENIE does not include any plankton dynamics but represents surface production as a biogeochemical flux dependent on nutrients and temperature limitations, capturing the net organic matter export from the surface due to phytoplankton and zooplankton interactions. This omission means that ecosystem dynamics are simplified in cGENIE.

While work has been done to explore changes in the nitrate cycle during OAE2 (Higgins et al. 2012; Jenkyns et al. 2007; Naafs et al. 2019), little has been done to explore how the ocean ecosystem might have differed overall, and still fewer studies have explored zooplankton grazing for both OAE2 and paleoclimates in general (Lenton 2020; Lovecchio and Lenton 2020). Lovecchio and Lenton (2020) explored the response of the ocean biological pump to differing remineralisation rates and sinking speeds, and suggested that ocean particle size (and consequent sinking speed) changes through time may have resulted in less export production in the past. This suggests marked implications for paleoclimate model simulations such as those done using cGENIE. Lenton (2020) undertook a wide-ranging comparison of how models might be misrepresenting biogeochemistry across the Proterozoic. While they did not focus on OAEs specifically, they suggested that the

efficiency of the ocean biological pump is likely to have been different in the past and is particularly important in controlling anoxia.

Despite increasing developments within the literature on the modelling of OAE2, no studies were identified that have investigated how differences in ecosystem representation between contrasting modelling frameworks affect how OAE2 is represented when modelled. This is particularly important when considering the key physical and ecosystem processes outlined here, which ultimately are represented markedly differently between different models. These are vitally important issues to understand within the context of OAE2 modelling as they ultimately underpin how well our models represent paleoclimate worlds and the conclusions that we are able to draw from our simulations. Moreover, this is important to further aid our future model experimental design, along with our understanding on how the ocean ecosystem impacted OAE development itself.

Therefore this chapter aims to examine the differences in HadCM3L and cGENIE when modelling OAE2; exploring how each of the models responds to a doubling in ocean nutrient inventory. Firstly, the response of each model to this perturbation will be explored, particularly in terms of how the modelled ocean ecosystem responds. Secondly, the differences in representation of model ocean circulation will be compared. This will allow a discussion of the similarities and differences between the two models, and of how a differently represented ocean ecosystem affects our representation of OAE2.

5.4 Methods

We compare the response of a model with well-captured physics and plankton dynamics (HadCM3L) and a model with simplified physics and ecosystem representation (cGENIE) to an increased ocean nutrient inventory (mimicking supply) in the context of OAE2. The different outputs were examined, with a particular focus on the key physical and biological effects altered as a result of this increased nutrient supply.

5.4.1 Model descriptions

HadCM3L is described in section 2.1, and further outlined in chapters 3 and 4, along with a full description by Valdes et al. (2017). HadCM3L was selected for it's comparatively good representation of ocean physics and ecosystem balanced with relatively fast simulation speed.

cGENIE is described in section 2.2, and fully described in Ridgwell et al. (2007). Briefly, it is a fast earth system model of intermediate complexity (EMIC) with simplified frictional-geostrophic physics, atmosphere and marine production and a complex set of ocean biogeochemical tracers. cGENIE was selected both as a model which has been frequently used for modelling of OAE2, and because it has a contrasting treatment of ocean production to that used in HadCM3L (Adloff et al. 2021; Hülse et al. 2016; Naafs et al. 2019; Ridgwell et al. 2007).

The differences that are most key to this chapter are outlined in sections 5.4.3 and 5.4.4.

5.4.2 Model Configuration

HadCM3L and cGENIE were configured with similar paleogeographies and ocean bathymetries, taking into account their different resolutions and model grid sizes. The HadCM3L bathymetry (Figure 5.1 A) is able to capture significantly more detail than that of cGENIE, particularly above 35 degrees north, however their ocean basins and gateways are the same.

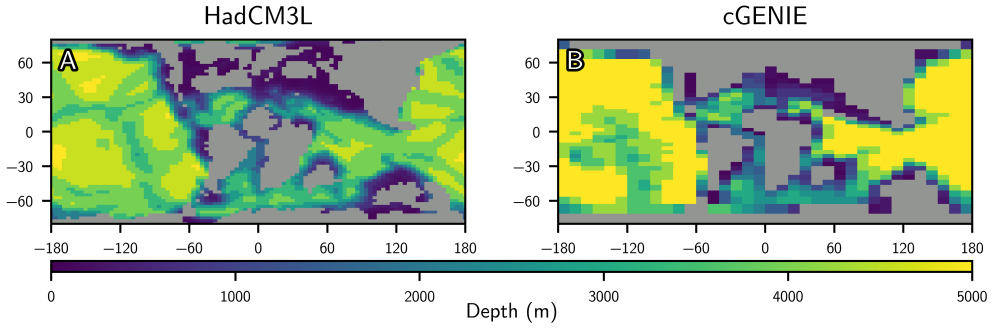

Figure 5.1: Ocean bathymetry for HadCM3L (A) and cGENIE (B).

Using the outlined model configurations for HadCM3L and cGENIE, comparisons were made based on model responses to an increased ocean nutrient inventory. These were assessed according to key biological (ocean ecosystems) and physical (ocean physics) processes.

5.4.3 Ocean biological controls in HadCM3L and cGENIE

NPZD Ecosystem in HadCM3L

Ocean biogeochemistry and carbon modelling in HadCM3L uses an optional ocean ecosystem module called HadOCC. HadOCC is described in

Palmer and Totterdell (2001) and represents a NPZD ecosystem (Nutrient-Phytoplankton-Zooplankton-Detritus). The main state variables used in HadOCC's ecosystem are nutrient, phytoplankton, zooplankton and detritus; these are represented in terms of nitrogen units (Palmer and Totterdell 2001). Alkalinity and TCO_2, in units of carbon, and stored, and converted from nitrogen units using the Redfield ratio (Palmer and Totterdell 2001). These variables are transported in the ocean model grid as tracers, with biological processes occurring at each time step. The ecosystem in HadOCC assumes a nitrogen-limited ocean; the carbon content of phytoplankton, nutrient and detritus are calculated at a fixed ratio (Palmer and Totterdell 2001) based on the Redfield ratio of 106:16 carbon:nitrogen.

In the surface ocean, primary production is limited by nutrient, light and temperature. Detritus is produced by mortality of both phytoplankton and zooplankton, together with excretion from zooplankton. Phytoplankton and detritus are consumed by zooplankton using a Holling-type-III relationship (Holling 1965; Palmer and Totterdell 2001). Zooplankton do not have a preference between phytoplankton and detritus, and simply consume both in the same proportion as their availability. Detritus sinks at a fixed velocity and is remineralised back to nutrient at two fixed rates: faster in the surface ocean (above 164.80 m) and slower below.

HadOCC as described by Palmer and Totterdell (2001) does not include a representation of dissolved oxygen; Williams et al. (2014) added oxygen to FAMOUS and this work is used to provide the simulation of oxygen in HadCM3BL. Oxygen is added as a tracer in the ocean, and the production or consumption of oxygen is calculated proportionally to the flows of

DIC in HadOCC. Oxygen is produced in the ocean by primary production, and subsequently removed by remineralisation and other biological processes. These biological processes directly produce DIC as a result of the excretion, mortality and respiration of zooplankton and phytoplankton, respectively (Williams et al. 2014). Of these, only remineralisation occurs outside the euphotic zone, since all the others are associated with biological production. Also at the surface, air-sea gas exchange occurs with the atmosphere, and oxygen is transported into the ocean interior when oxygen-rich water is mixed away from the surface. It is important to note that this does not change the amount of remineralisation occurring in the HadOCC model ocean, which remains at a fixed rate, dependent only on a single depth threshold: a lack of oxygen does not prevent remineralisation from occurring.

Comparison of export representation in the two models

The NPZD model included in HadOCC allows us to dynamically represent interactions between the environment (nutrient, temperature and light), phytoplankton, zooplankton and export. On the other hand, cGENIE assumes a fixed interaction between phytoplankton, zooplankton and export, while capturing environmental controls (nutrient, temperature and light).

Figure 5.2 illustrates a conceptualised comparison of ocean model ecosystems between HadCM3 and cGENIE, highlighting how ocean nutrient is converted to detritus (particulate organic matter) and exported from the surface ocean. Most of the additional process that HadCM3L represents are parameterized in cGENIE as nutrient uptake.

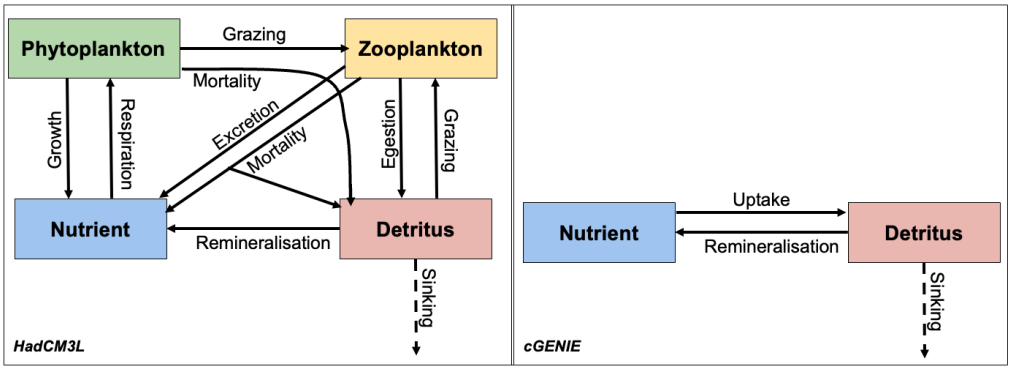

Figure 5.2: Conceptual diagram showing the NPZD model in HadCM3L and the primary production scheme in cGENIE. Based on Palmer and Totterdell (2001) and Ridgwell et al. (2007)

.

cGENIE calculates export of organic matter in proportion to the available nutrient, taking into account light and temperature limitations (Ridgwell and Hargreaves 2007). This parameterisation represents grazing as a constant fixed proportion of the total primary production, and does not represent any spatial or temporal distribution in grazing. Because of this cGENIE parameterisation, a doubling in nutrients broadly produces a doubling in export production (Monteiro et al. 2012), which has marked implications for ocean oxygen concentration.

5.4.4 Ocean physical controls in HadCM3L and cGENIE

The ocean model in cGENIE is a frictional-geostrophic simplification of the basic equations of flow dynamics included in HadCM3L. This geostrophic balance approach means that the tropical ocean circulation is less well represented than in HadCM3L (Edwards et al. 1998). In addition, momentum-

advection is replaced with a simpler frictional term and this leads to distortion in tropical Kelvin waves (Edwards and Marsh 2005). However, these optimisations allow cGENIE to use a significantly longer time step (3.8 days) than HadCM3L's hourly time step, which is required to solve the non-linearity of the full equations of motion (Marsh et al. 2011). This is a key contributor to cGENIE's increased speed compared to HadCM3L. A marked outcome of this difference is that cGENIE sees more convective mixing at high latitudes (Marsh et al. 2011), while equatorial upwelling is reduced.

In addition, cGENIE represents the atmosphere as a 2D energy-moisture balance model (Ridgwell et al. 2007), in contrast to the dynamic atmosphere in HadCM3L (Valdes et al. 2017). This notably means that wind stress and planetary albedo needs to be specified in cGENIE. This is either using some form of idealised assumptions (e.g. that they are similar to present) or are extracted from an equivalent higher resolution GCM simulations, though this may have slightly different paleogeographies. The wind stress and albedo are zonally averaged leading to reduced longitudinal variations. The 2-D energy-moisture balance model does not transport enough moisture between the Atlantic and Pacific. Hence, there is an additional arbitrary scaling factor of net freshwater flux between the ocean basins. For the modern, it was tuned to ensure a good simulation of the AMOC. However, it is unclear what that factor should be for alternative paleogeographies.

cGENIE's lower resolution is the final key physical difference. This low resolution has the effect of increasing mixing effects by increasing the proportion of grid cells which are exposed to boundary conditions such as

gateways and topography. This means that high-latitude geostrophic flows are more poorly represented than in HadCM3L (Marsh et al. 2011). For this reason, cGENIE representation of the ocean circulation at high latitudes could be somewhat improved by increasing resolution (Lenton et al. 2007). However, this is considerably more computationally expensive and does not improve the model's representation of equatorial upwelling (Marsh et al. 2011).

In summary, compared to HadCM3L, the physics in cGENIE is expected to lead to more mixing at high latitudes, a less developed representation of upwelling at low latitudes and smaller longitudinal variations.

5.5 Results

The following results represent an examination of the response of HadCM3L's (Figures 5.3 to 5.7) and cGENIE's (Figures 5.8 to 5.11) ocean biological productions to an increased nutrient inventory. This is followed by an assessment of a number of key, identified differences in model representation (Figures 5.12 to 5.14).

5.5.1 The response of HadCM3L to an increased nutrient inventory

Firstly, doubling the ocean nutrient level in HadCM3L causes a global increase in primary production (Figure 5.3) of 23 % (table 5.1). Although most of the global ocean experiences a moderate primary production in-

crease (Figure 5.3C), the biggest primary production increases occur in areas where phytoplankton concentration was already high in the control simulation. The biggest increases are seen in equatorial upwelling areas of the equatorial Pacific, and the north and west of South America (Figure 5.3C), with increases of up to 3.48 µmol L^{-1} to the north of South America.

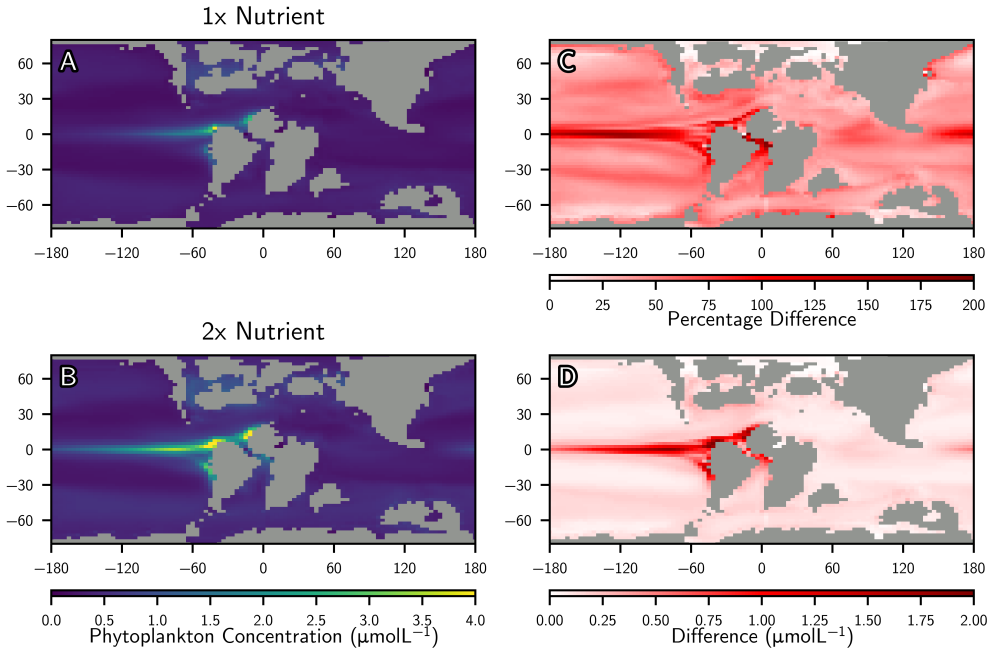

Figure 5.3: HadCM3L surface phytoplankton concentration at the end of the simulations, used as a proxy for primary production. Showing the control simulation (panel A), the double nutrient simulation (panel B) and the difference (C) and percentage difference (D) between the two.

Under doubling nutrient, zooplankton concentration increases much more strongly globally, with a near full global doubling worldwide (table 5.1). While the areas of highest zooplankton concentration occur in high primary production areas (comparing Figure 5.4A and B with Figure 5.3), the pattern of increase in response to increased nutrient inventory is quite differ-

ent. Zooplankton increases are largest where the area of primary production has expanded, particularly in the equatorial Pacific (Figure 5.4 D), with increases of up to $1\,\mu mol\,L^{-1}$. There are smaller increases (a maximum of $0.60\,\mu mol\,L^{-1}$, typically $\approx 0.50\,\mu mol\,L^{-1}$), seen across the rest of the global ocean. In areas where primary production is particularly high in the control run (Figure 5.3A), zooplankton increases are distinctly suppressed (Figure 5.4C), with the high productivity area at the South of the proto-North Atlantic seeing little or no zooplankton increase. The only other areas with little or no zooplankton increase are the oligotrophic ocean gyres, where there is little or no primary production or zooplankton production.

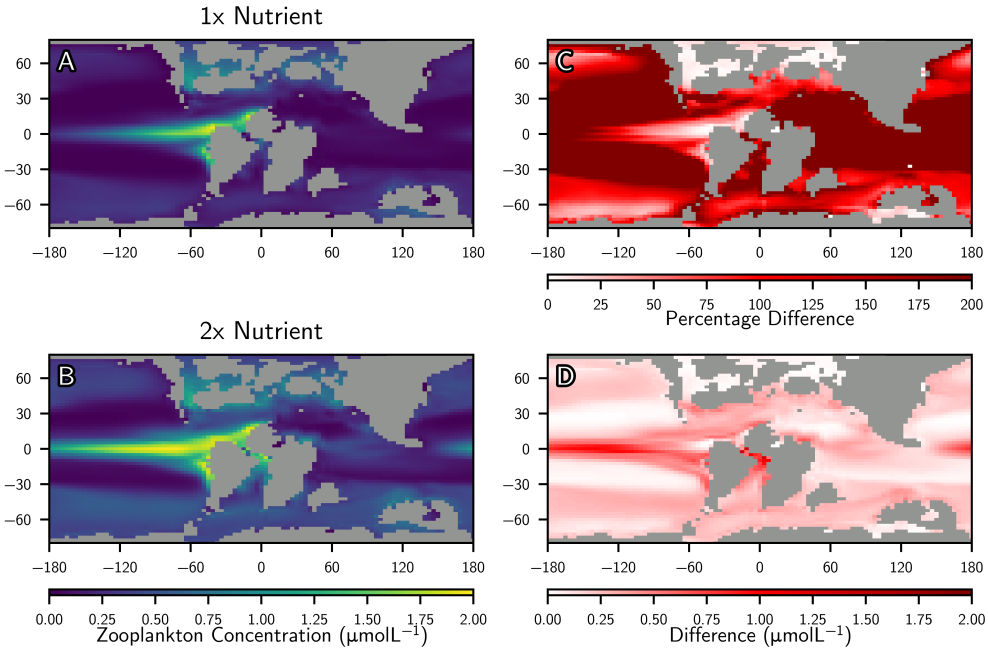

Figure 5.4: HadCM3L surface zooplankton concentration. Showing the control simulation (panel A), the double nutrient simulation (panel B) and the difference (C) and percentage difference (D) between the two.

These changes in phytoplankton and zooplankton combine to change

the amount of detritus exported from the euphotic zone. Subsurface ocean detritus increases the most (by up to $0.18\,\mu\text{mol}\,\text{L}^{-1}$) south of the proto-North Atlantic (Figure 5.5D), where primary production was most increased but zooplankton was not. Elsewhere, most areas of the ocean with an increase in primary production have a small increase in detritus export, although the pattern of detritus is more complex than than that of primary production. Increases in detritus are smaller than might be expected across the high latitude oceans, and particularly across the equatorial pacific where zooplankton levels are high (Figure 5.4). The oligotrophic gyres see change only at their periphery (Figure 5.5), since detritus levels in their centre are very low regardless of the change in nutrient inventory.

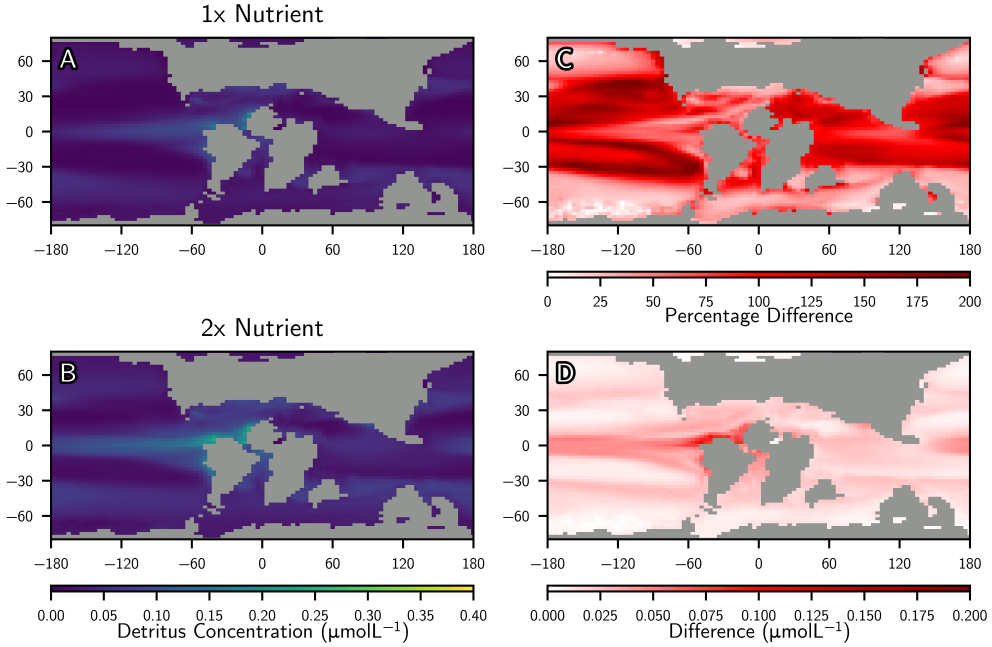

Figure 5.5: HadCM3L detritus levels at the base of the euphotic zone (200m) at the end of the simulations, showing the control simulation (panel A), the double nutrient simulation (panel B) and the difference and percentage difference between the two (D and C).

Increasing detritus levels cause an increase in remineralisation, which consumes oxygen and increases anoxia. The response of oxygen levels below the photic zone to this increased supply of organic matter is a increase in anoxia, confined particularly to areas close to high primary production in the surface ocean (Figure 5.6C). Oxygen is particularly reduced in two areas. Firstly, in the upwelling areas around the perimeter of the proto-North Atlantic: a manifestation of the deep oxygen minimum zone shown in Figure 5.7B expanding upwards. Indeed, oxygen is lowered by $\approx$50 µmol L^{-1} along the north and south coasts of the proto-North Atlantic. Secondly, oxygen is notably lowered across the Pacific, where deep water is less anoxic and the lowered oxygen is centred around the photic zone itself. Here oxygen is lowered by 89 µmol L^{-1}. However, little or no difference is seen in the confined waters between and close to the north of South America and Africa where oxygen levels have already reached zero. In summary, below the euphotic zone, oxygen levels are particularly reduced in areas where primary production was seen to be very high.

At the seafloor is a limited expansion of ocean anoxia, but this does not clearly follow areas of high production as it does at the surface. Across nearly the whole ocean floor (Figure 5.7C), a drop in oxygen levels are seen when the nutrient inventory is doubled, where mean benthic oxygen levels are reduced by 36 µmol L^{-1}. This effect is noticeably reduced to the north of the Tethys sea, where the ocean is particularly shallow (less than 100 m, Figure 5.1 A), and well mixed, with particularly young bottom water of around 20 y. Indeed here, benthic oxygen levels are reduced by only small amounts (less than $\approx$20 µmol L^{-1}. The strongest reductions in oxygen

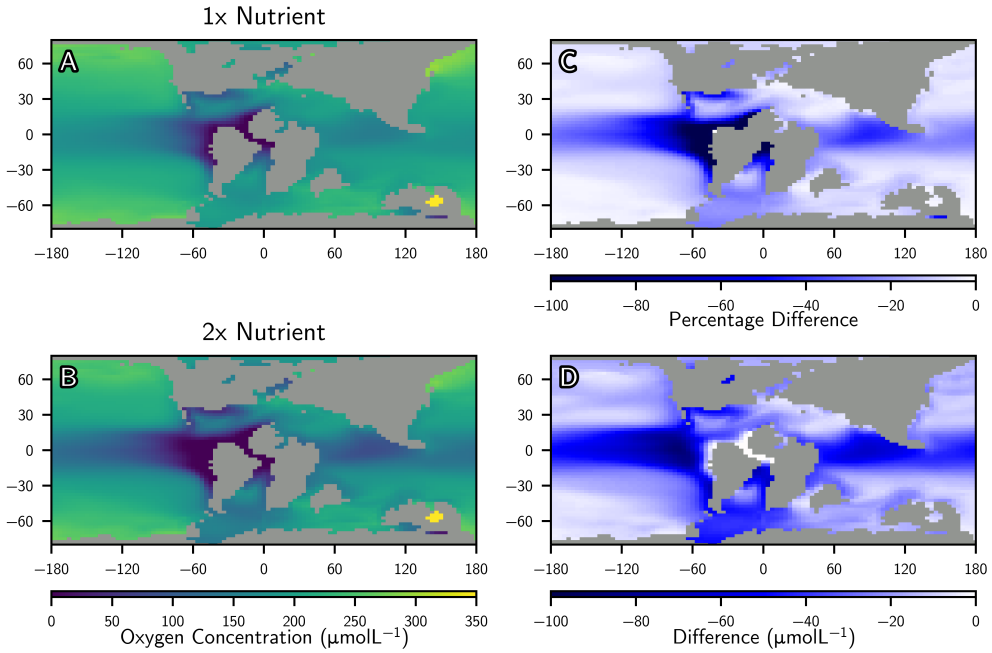

Figure 5.6: HadCM3L oxygen levels at the base of the euphotic zone (200m) at the end of the simulations, showing the control simulation (panel A), the double nutrient simulation (panel B) and the difference and percentage difference between the two (D and C).

concentration are seen along the western edge of the proto-North Atlantic and into the eastern Pacific, where the benthic low oxygen of the proto-North Atlantic expands to cover a wider area to the west. Here oxygen levels drop as much as 79.76 µmol L^{-1} and typically drop ≈60 µmol L^{-1}. Within this area two anomalies are seen to the west of both South America and Africa. These areas have very low oxygen levels (≈0 µmol L^{-1}) in the 1x nutrient simulation, and a further reduction in oxygen concentration is not possible here.

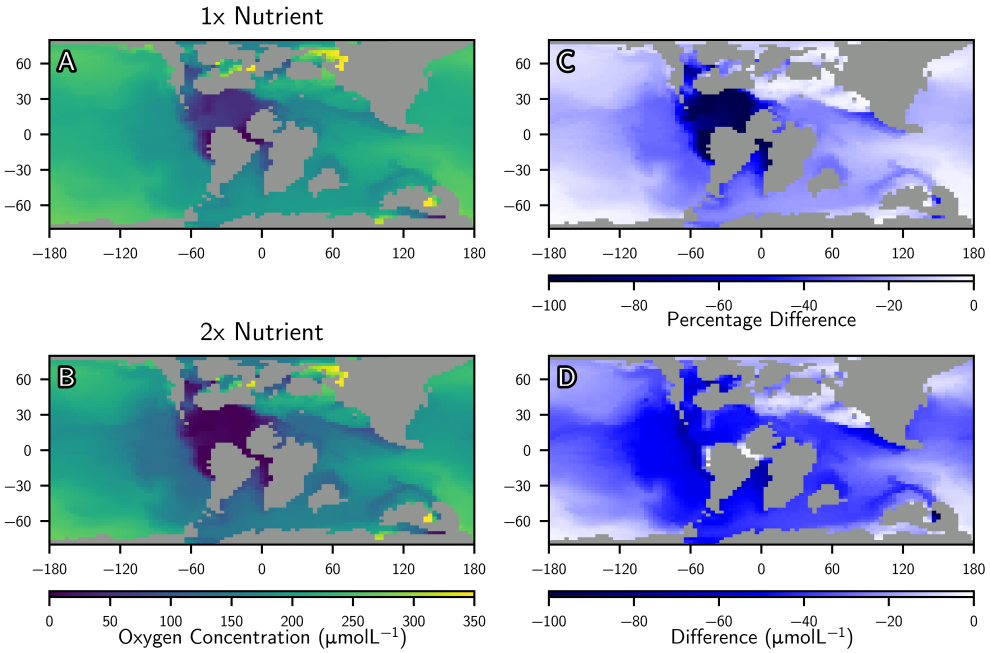

Figure 5.7: HadCM3L benthic oxygen at the end of the simulations, showing the control simulation (A), the double nutrient simulation (B) and and the difference and percentage difference between the two (D and C).

5.5.2 The response of cGENIE to an increased nutrient inventory

The response of primary production in cGENIE to a doubling of nutrient inventory is a relatively uniform doubling across the whole ocean (Figure 5.8C), with the biggest absolute changes simply seen in areas where primary productivity was already high (Figure 5.8). Indeed, these areas show increases in uptake of 2.06 µmol L^{-1} y^{-1}. The only areas in which primary production does not increase are high latitude areas of downwelling, an effect also seen in HadCM3L (see Figure 5.3). The subtropical gyres also see very small absolute changes, since while they undergo a doubling of

production, very little occurs here in either simulation. cGENIE has larger areas of high primary production in the high-mid latitude Pacific compared to HadCM3L, both in the north and south (Figure 5.9A and B), which also see increases in production of up to 1.42 µmol L^{-1} y^{-1}.

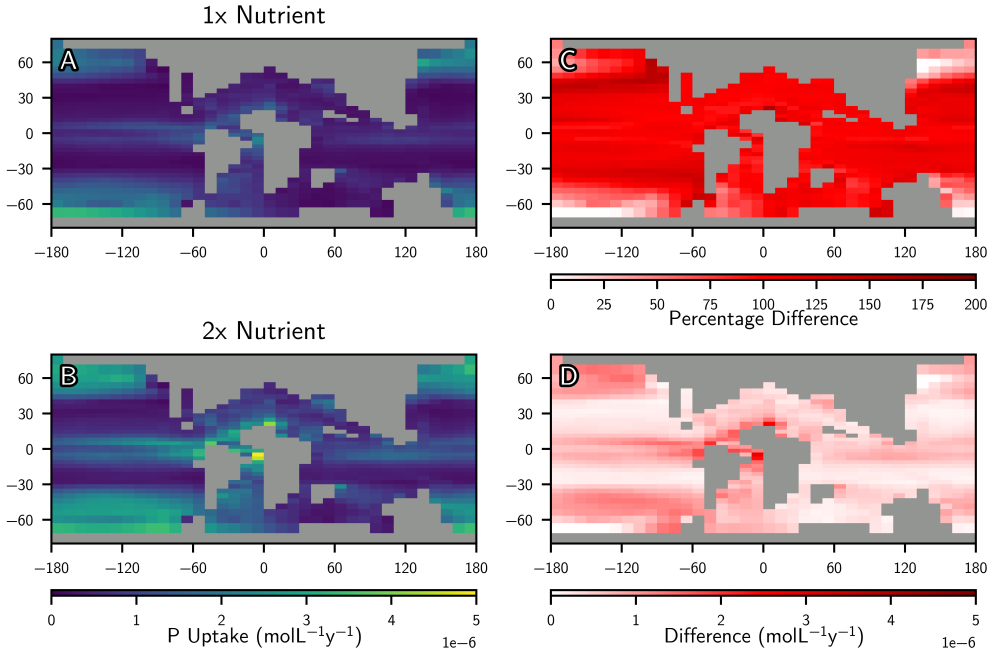

Figure 5.8: Ocean phosphate uptake, used as a proxy for primary production, in cGENIE 1x Nutrient simulation (A), 2x Nutrient simulation (B), with the percentage difference (C) and difference (D).

cGENIE does not hold the NPZD model state variables described for HadCM3L; export production into the deep ocean is calculated as a proportion of nutrient uptake in the surface ocean (Ridgwell et al. 2007). Nutrient uptake is limited by temperature, light availability and ice coverage, but otherwise scales in proportion to nutrient availability up to a theoretical maximum consumption. For this reason, cGENIE's change in detritus flux mirrors change in primary production (Figure 5.8) exactly and occurs

across the whole global ocean (Figure 5.9C) with the biggest absolute differences concentrated in areas where primary production is already high (Figure 5.9D).

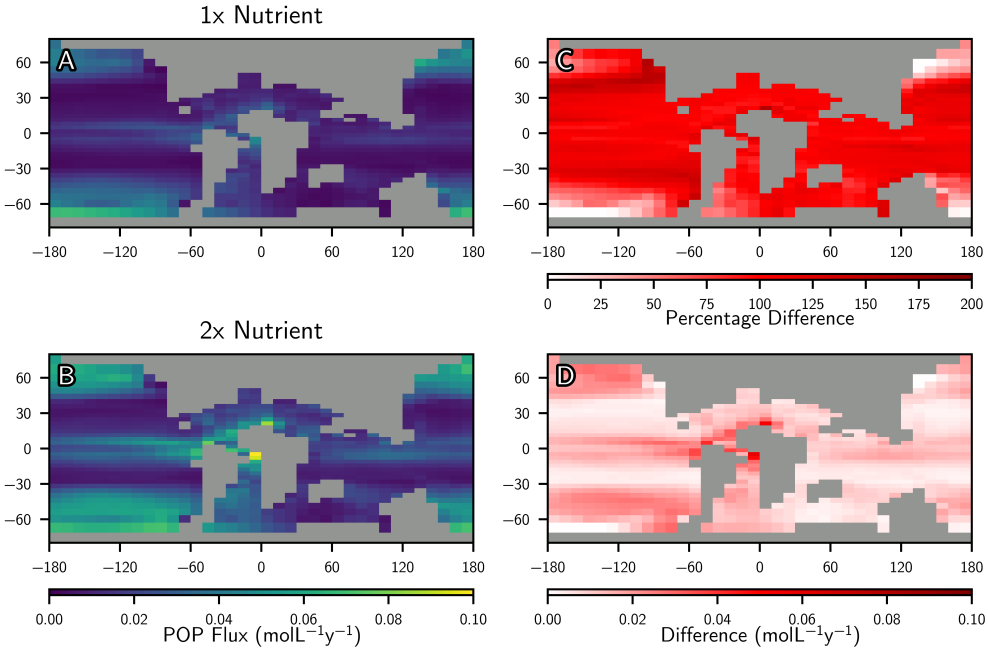

Figure 5.9: Ocean export flux in cGENIE 1x Nutrient simulation (A), 2x Nutrient simulation (B), with the percentage difference (C) and difference (D).

As a result of a larger ocean production increase with doubling nutrient, cGENIE shows lower oxygen levels across the board in the control simulation (Figure 5.11 A), compared to HadCM3L (Figure 5.7 A), with a ocean mean oxygen concentration 88.77 µmol L^{-1} lower. Oxygen reductions below the euphotic zone are spread in a ≈30° wide band around the equator (Figure 5.10), with an area around the south of the proto-North Atlantic where no reductions are seen due to oxygen reaching it's lower limit. This is similar to the area seen in HadCM3L but expanded somewhat into the

Pacific. Reductions are seen at much higher latitudes than in HadCM3L; reflective of the increased primary production here.

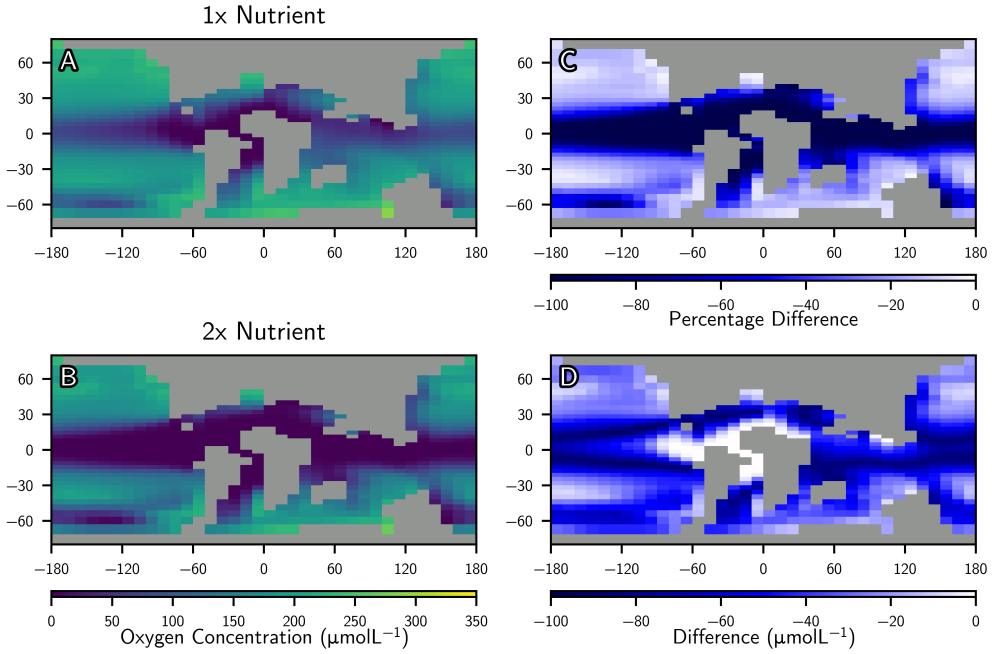

Figure 5.10: cGENIE below photic zone (200m) oxygen at the end of the simulations, showing the control simulation (panel A), the double nutrient simulation (panel B) and the difference between the two.

At the ocean floor, oxygen levels across the benthic proto-North Atlantic are already at the limit of ≈0 in the cGENIE 1x nutrient simulation. In the cGENIE 2x nutrient simulation (Figure 5.11B), anoxic waters have spread across the entire ocean floor, with much of the Pacific and Tethys having reached the lower limit of zero. This is reflective of the more pronounced dramatic decrease in overall ocean oxygen compared to HadCM3L.

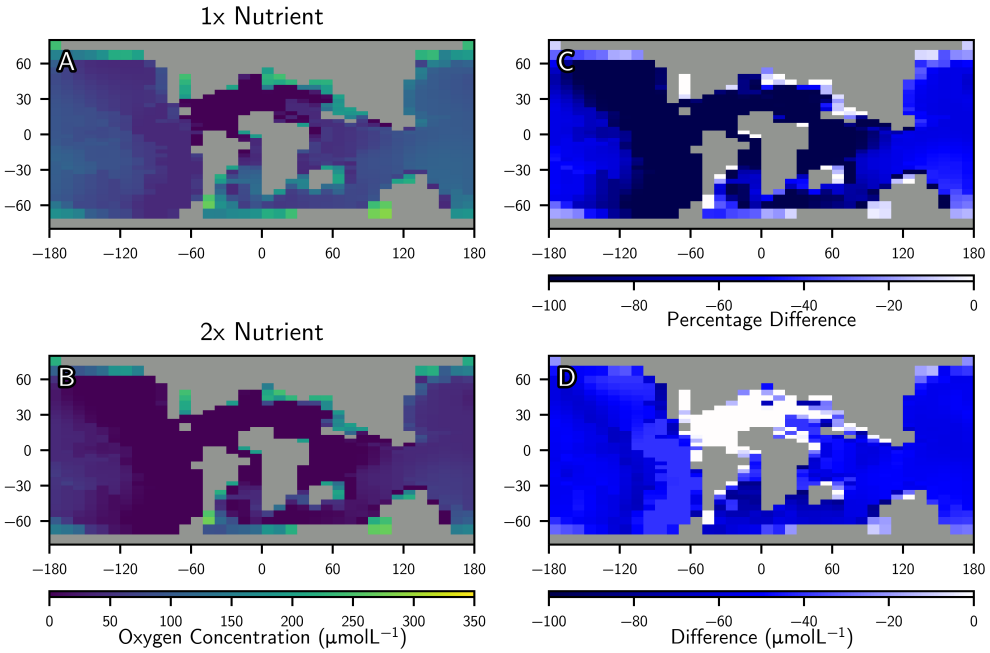

Figure 5.11: cGENIE benthic oxygen at the end of the simulations, showing the control simulation (panel A), the double nutrient simulation (panel B) and the difference between the two.

5.5.3 Differences in model ocean circulation

In addition to the ways in which the models represent ocean biological production, the models differ in physical resolution, affecting the ocean circulation, which in turn impact ocean production (via nutrient supply to the surface) and oxygen distribution. In this section, the model ocean circulations in cGENIE and HadCM3L will be compared.

Figure 5.12 compares the vertical advection in HadCM3L and cGENIE, which show similar patterns. Advection in cGENIE has noticeably less detail, a result of it's coarser model grid, but captures much of the spatial variation seen in HadCM3L. However, there are a number of potentially important differences. In HadCM3L, areas of wind-driven upwelling are

stronger, including the key area to the south of the proto-North Atlantic and equatorial region in general. Indeed here, values in cGENIE are as high as $10.73\,\mathrm{cm\,s^{-1}}$ while in HadCM3L values are as high as $20.15\,\mathrm{cm\,s^{-1}}$. In contrast, cGENIE has a stronger band of upward advection across the mid latitude (≈50° South) Pacific, which is noticeably stronger than HadCM3L along the whole Pacific Antarctic coast. This causes an increase photic zone nutrient and consequent export (Figure 5.9A and B) in this area.

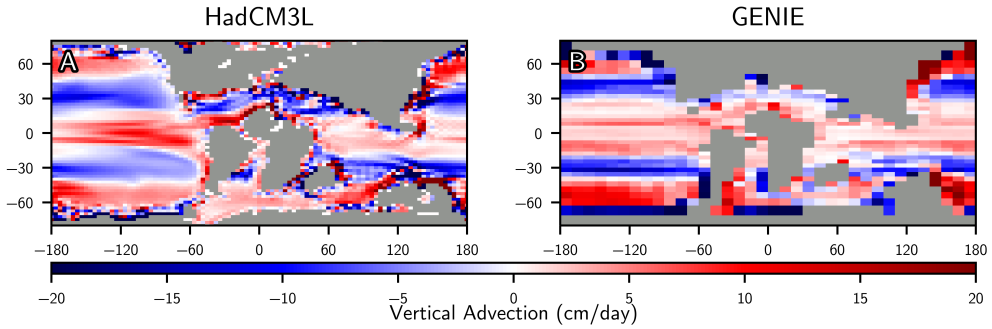

Figure 5.12: Annual mean vertical advection at the base of the euphotic zone (200m) at the end of the simulations, showing the HadCM3L control simulation (panel A), and cGENIE control simulation (panel B).

Areas of deep water formation in both models are shown by Figure 5.13, showing the difference in the spatial distribution (but not intensity) of deep water formation in HadCM3L and cGENIE. Deep water formation along both the Pacific Antarctic and East Arctic coasts is much more coherent in cGENIE, and, unlike HadCM3L also present in the South Atlantic. cGENIE sees a more widespread area of deep water formation in both the north and the south, consistent in both Figure 5.13 and the increased downward advection seen in cGENIE in Figure 5.12. However, areas of particularly strong deep water formation are very similar in the two models; in both the

North and South Pacific at 180 degrees longitude.

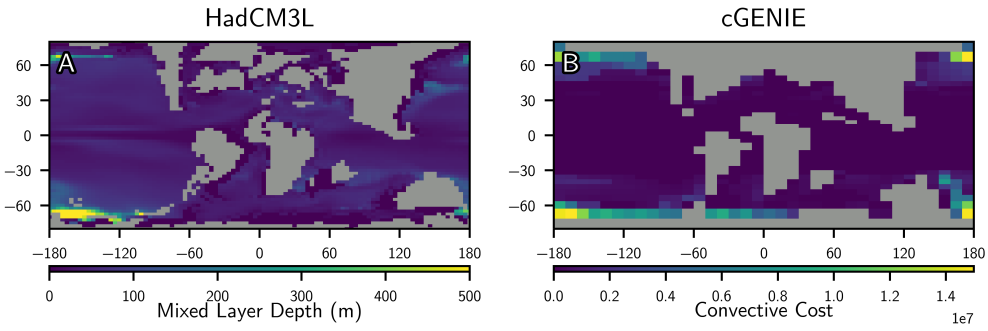

Figure 5.13: Deep water formation in HadCM3L (A) and cGENIE (B). In HadCM3L mixed layer depth is used as an indicator of deep water formation, while in cGENIE convective cost is used.

In Figure 5.14, equatorial upwelling is reduced when compared to HadCM3L. In HadCM3L, water upwelling to the surface at the equator can be clearly identified in a plume spreading and widening downwards from the surface. In contrast, in cGENIE this upwelling does not reach the ocean surface due to the model's parameterisation of geostrophic motion to frictional mixing.

In summary, while cGENIE and HadCM3L have a similar circulation in general and most differences are small, there are key contrasts which are likely to cause differences in nutrient supply to the euphotic zone. The most important of these is the reduced upwelling at low latitudes in cGENIE compared to HadCM3L.

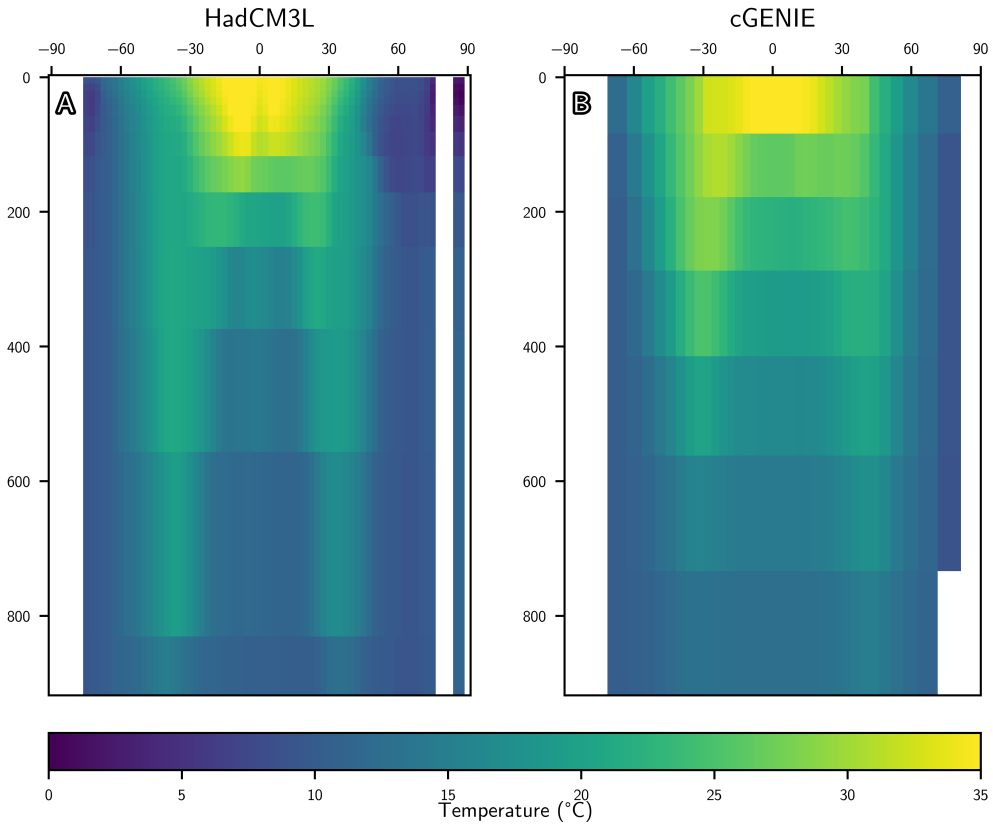

Figure 5.14: Transect of ocean temperature from South to North at 180° longitude, in HadCM3L (A) and cGENIE (B).

5.5.4 Differences in global response of model ecosystem and anoxia

In HadCM3L, a doubling of ocean nutrient has a limited effect on export production and consequent increase in detritus, and lowering of oxygen. When compared with the control simulation, HadCM3L's double nutrient simulation produced a 23 % increase in phytoplankton growth, together with a somewhat larger (95 %) increase in zooplankton (see table 5.1). In cGENIE, the 92 % increase in primary production caused by doubling nu-

trient inventory causes exactly the same (92 %) increase in detritus export. In HadCM3L the response is more complex, with an increase in detritus of 82 % resulting from the combined primary and zooplankton production increases.

Names	Oxygen	Detritus	Phytoplankton	Zooplankton
HadCM3L 1x N	189.66	1.05e-02	8.32e-03	4.37e-03
HadCM3L 2x N	151.73 -20%	1.91e-02 +82%	1.02e-02 +23%	8.50e-03 +95%
cGENIE 1x P	41.37			
cGENIE 2x P	12.81 -69%	+92%	+92%	

Table 5.1: Total ocean means of key model state variables for the HadCM3L and cGENIE simulations. Percentage change from the control simulation shown for simulations where nutrient (Nitrate in HadCM3L and Phosphate in cGENIE) was doubled. All units µmol L^{-1}. cGENIE percentages for Detritus and Phytoplankton are included for comparison, they are the change in detritus export from the euphotic zone and change in nutrient uptake (rather than total inventory shown for HadCM3L).

cGENIE responds more strongly to this increase in detritus than HadCM3L, with a 69 % decrease in oxygen compared to HadCM3L's 20 %. In HadCM3L, detritus is increased in areas which already have low oxygen levels (Figures 5.5 and 5.7), compared to cGENIE where the increase is seen more widely across the global ocean. In both models, oxygen is constrained and cannot fall below zero; therefore an increase in detritus in areas that already have low oxygen levels would not be expected to cause a further decrease in oxygen. Thus in HadCM3L, where detritus increases are more confined to areas which are already anoxic in the 1x nutrient simulation, the increase in anoxia is reduced.

5.6 Discussion

5.6.1 Biological controls on ocean productivity

In HadCM3L, zooplankton grazing pressure acts to suppress the increase in primary production with increases in nutrient (Figure 5.3D and F), particularly in areas of moderate production: a well known effect in the modern ocean (Aksnes and Wassmann 1993; Fasham et al. 1990). In areas of particularly high production, a top-down control prevails, as zooplankton reach the saturation expected from the functional response (Figure 5.4C): an effect also observed in the modern ocean (Morozov 2010).

These effects are thought to be caused by HadOCC's modelling of the ocean surface ecosystem. In HadCM3L, zooplankton consume both phytoplankton and detritus using a Holling-type three functional response: grazing first increases slowly with prey density, then increases linearly until high prey density, where grazing rate increases no further and becomes saturated (Holling 1965; Palmer and Totterdell 2001). This explains why we do not see much increase in zooplankton in very high productivity areas; grazing pressure increases most in areas where our perturbation to the model causes a transition from low to high productivity.

In cGENIE, the response of ocean biogeochemistry to increased nutrient inventory is much more straightforward, with a doubling in production seen near-worldwide (see Figure 5.8). The less complex ecosystem in cGENIE translates an increased availability of nutrient near-directly to increased production. Unlike HadCM3L, which allows the grazing rate to vary both spatially and temporally, cGENIE's fixed parameterisation of grazing means

regional differences in grazing are not modelled.

Le Quéré et al. (2016), in a modern model comparison study found that models which did not include macro-zooplankton grazing consistently overestimated summer phytoplankton biomass. This result suggested that zooplankton dynamics were able to explain the low phytoplankton levels observed here in summer. While this is consistent with our results, showing suppressed phytoplankton growth in HadCM3L when compared to cGENIE, this study used a far more complex ecosystem model than HadCM3L includes, with many phytoplankton and zooplankton functional groups. Gusha et al. (2019) showed in a modern, in-situ study that in high temperature high nutrient systems like those which occurred during OAE2s, top down grazing is unable to keep up with an increase in phytoplankton, which reflects the effect we see in equatorial HadCM3L. However, this and many other studies (Anneville et al. 2019; Landry et al. 2011; Stukel et al. 2011) acknowledge that zooplankton exert a top-down control on phytoplankton populations in the modern ocean.

These differences in spatial distribution in primary production, and consequent export, cause the differences in response of ocean oxygen concentration between the two models. In HadCM3L, primary production is increased in areas where primary production is high in the 1x nutrient simulation. These areas of high production are the areas in which the ocean is already anoxic; with very low or zero oxygen concentration in the 1x nutrient simulation (Figure 5.6A). However, in cGENIE, production increases across the global ocean and is not confined to anoxic areas (Figure 5.8C). Since oxygen concentrations are unable to fall below zero (in both HadCM3L and cGE-

NIE), further addition of detritus in already anoxic areas does not lower oxygen levels further. Therefore, the product of these effects is to reduce the amount that the global ocean oxygen concentration falls in HadCM3L when compared to cGENIE.

5.6.2 Physical controls on ocean productivity

While cGENIE and HadCM3L simulate the physical climate differently they produce a similar global ocean circulation with a few key differences, particularly in equatorial upwelling, which are discussed in this section.

In both models, the physical ocean circulation is critical in determining where nutrients are supplied to the ocean surface and therefore controlling the areas of primary production. In particular, our cGENIE simulations have less intense equatorial upwelling and downwelling compared to HadCM3L (Figure 5.14), but stronger supply at higher latitudes (figure 5.12), the sub-polar Pacific gyres, leading to more primary production at high latitudes (Figure 5.8). These effects reduce the importance of the proto-North Atlantic in determining global trends when compared to cGENIE. However, at the highest latitudes, the relatively strong deep water formation in cGENIE along the Arctic and Antarctic coasts acts to suppress production, with cGENIE's lower resolution grid not capturing the more detailed spatial distribution shown in HadCM3L.

Previous work by Trabucho Alexandre et al. (2010) ran the CCSM3 model with a vertical velocity pattern more similar to HadCM3L than cGENIE. This similarity is explained by the resolution of this model (100 x 122

grid) being slightly higher than that of HadCM3L. In Trabucho Alexandre et al. (2010), this is noticeable particularly at high latitudes, where they show even less upward flow than our HadCM3L simulation. This is also noticeable in the proto-North Atlantic and Equatorial Pacific where Trabucho Alexandre et al. (2010) show upwelling that is notably centred on the North African coast and on the equator. Another modelling study by Topper et al. (2011) focused on the proto-North Atlantic, running a regional climate model, MOMA, at much higher resolution (0.50° x 0.50°). Their simulations also show a similar pattern to HadCM3L with upward velocities seen only close to coasts, particularly of South America and Africa, and downward movement across the centre of the basin.

The main effect of differences in physical oceans between the two models is that cGENIE supplies more nutrients to the ocean surface at Pacific high latitudes than HadCM3L, causing higher production in these areas (Figure 5.8). A possible impact of this difference is that higher production in the North Pacific may be important in supplying detritus into newly formed deep waters in these areas, allowing a greater supply of detritus to the ocean interior and supporting the more widespread lowering of ocean oxygen on cGENIE than HadCM3L.

5.6.3 Implications for OAE2 modelling

The large differences in ocean benthic oxygen predicted by HadCM3L and cGENIE result from a combination of differing physical and ecosystem representations. These contrasting ecosystem dynamics are particularly impor-

tant in setting how much carbon is exported from the euphotic zone and importantly for controlling the detritus differences we show in table 5.1. The suppression of production by zooplankton, and consequent suppression of the reduction in ocean anoxia seen in HadCM3L suggest that higher nutrient supplies to the ocean than previously thought may be required to achieve the widespread anoxia of OAE2.

Compared to the modern ocean, ecosystem dynamics and the effects of grazing during OAE2 are much less well studied and discussed. Most studies of OAEs that refer to the ocean ecosystem, are sedimentary studies, which use ecosystem change as a proxy to gain insight into other changes in the ocean (Caswell and Coe 2013; Erba 2004; Erba et al. 2019; Gangl et al. 2019), particularly the presence or absence of anoxia (Caswell and Coe 2013). However, the way the surface ocean ecosystem may affect the development of an OAE is remarkably understudied. Fossil records show that plankton populations have undergone great change during anoxia events (Coccioni et al. 2006; Leckie 1989). Indeed, this is the basis which countless proxy studies use to identify the development of OAE2s (Coccioni 2004; Friedrich 2010; Gebhardt et al. 2010; Petrizzo et al. 2021). It is clear that the ocean ecosystem was very different during the OAE2s period, relative to today, for example with diatoms being a much less important primary producer (Harwood et al. 2007). However, there is little work to date that has touched on how these changes in both zooplankton and phytoplankton concentrations would have affected how much primary production occurred. As a result, OAE modelling is forced to assume that modern ecosystem dynamics may be applied to the period. While this is a reasonable assumption,

it makes it all the more important to understand how differences in representation affect the the results of simulations, to ensure we fully understand the mechanisms by which results are produced.

To follow up on this study, it would be useful for further comparisons to be made, particularly with further additional models which treat the problem of ocean production differently. It may be interesting to tackle the problem using a modern plankton ecosystem model, such as that used by Le Quéré et al. (2016), which contains plankton functional groups such as diatoms and coccolithophores. However this model would have to be adjusted to account for ways in which the Ceonomanian ecosystem are known to differ from the modern (e.g. the reduced importance of diatoms). Indeed, it remains uncertain whether there is enough information available to effectively tune models such as this for paleoclimates. A particular area to focus upon would be to identify how ocean ecosystem change which has been identified in sediment core studies might have impacted on the ocean ecosystem. This is particularly relevant since both HadCM3L and cGENIE in this study make the assumption that ecosystems responded in similar ways to modern ecosystems during OAE2. HadCM3L perhaps performs stronger in this area in that it allows zooplankton grazing rates to change based on the nutrient and production regime of the Cenomanian. cGENIE on the other hand assumes constant grazing at a rate tuned for the modern. However, importantly, many assumptions are still made as to the similarity of the modern and the past, which should be a key focus of future works.

5.7 Conclusions

In this study we have shown the effect on OAE2 of doubling nutrient inventory in two different models, selected for their contrasting complexity. In both models, this doubling causes an increase in ocean anoxia, but with a different magnitude. cGENIE, a model with fixed plankton dynamics and a frictional-geostrophic ocean model coupled to a 2D atmosphere, shows a decrease of 69 % in ocean oxygen. HadCM3L, which has more complex physics and a much more dynamic NPZD ocean ecosystem dynamics, sees a smaller decrease of 20 %.

This study suggests that differences in grazing pressure from zooplankton are important in causing this effect. Indeed, these processes lead to the export of organic matter increasing most in areas where it was already high in HadCM3L, whereas in cGENIE export increases across the global ocean. cGENIE's more intense mixing at high latitudes also compliments this, leading to more primary production occurring here than in HadCM3L.

Neither of our two models fully represents the complex dynamics of how zooplankton grazing affects export production, or how export production itself is affected by changes in remineralisation caused by anoxia. However, it is clear that the response to an increase in nutrient of the two models was substantially different, and that this was a result of both differences in nutrient supply processes and in surface ocean ecology. These results highlight that model ecosystem representation is an important factor in defining the amount of anoxia which is achieved during OAE2, and this should be taken into account when interpreting model results.

Chapter 6

Conclusions, Scientific Contributions and Recommendations

6.1 Introduction

This thesis has investigated the interaction between the physical climate system and biogeochemistry in the context of OAE2. Using the HadCM3L model, it has focused on how the ocean biogeochemical system of OAE2 is affected by the physical climate, and how improvements or changes in modelling aid our understanding of OAE2. This final and concluding chapter will synthesise and collate the modelling results of this thesis, the methods of which were introduced in chapter 2, and then were detailed in chapters 3-5. This chapter will explore and highlight how the aim of this thesis has been achieved. In addition, based on the knowledge we have evaluated in

this thesis, areas for recommended further research will be highlighted.

6.2 Synthesis

This project investigated the role of paleogeography, orbital cycling, and marine ecosystem in a comparatively comprehensive and high-resolution Earth System model: HadCM3L. The following section will summarise the key findings and contributions of the three presented research chapters of this thesis (chapters 3-5), drawing on their applicability and ultimately how they have each contributed to answering the aim of this thesis. In addition, whilst this thesis has made a number of key scientific contributions in our understanding of the physical and biogeochemical causes of OAE2, this in turn, has drawn out a number of key areas in which future research in this field should now be targeted.

6.2.1 Paleogeographical Preconditioning of the Late Cretaceous Oceanic Anoxic Event (OAE2)

Chapter 3 examined how paleogeography affected the development of OAE2 by comparing model simulations of the Cenomanian with that of the Maastrichtian. This assessment showed that Cenomanian paleogeography has an important impact on the circulation of the ocean, and consequently benthic ocean oxygen, and is a necessary pre-conditioning for OAE2 to develop. The change in physical ocean dynamics due to the paleogeography was found to be less important than nutrient input for the development of a full OAE.

However, this was still an important control and instrumental in determining the geographical spread of an OAE, since they determine patterns in ocean currents and ultimately how fast the deep ocean is replenished with oxygen from the surface. This information may also help provide limits on the time periods when OAEs were able to occur as some paleogeographic configurations may have prevented OAEs from developing.

Our conclusions that the sill between the Americas contributes to the pre-conditioning of an OAE is important but there remains uncertainty about the depth of such a sill. However, the purpose of the chapter is to show that, if a sill exists, then it is likely important. It represents a challenge to the paleogeographic reconstruction community to improve and reach consensus about the depth.

This chapter builds upon previous modelling such as Donnadieu et al. (2016) and Monteiro et al. (2012) which have investigated the affect of paleogeography on the development of OAE2. It does this by tackling the problem in the first high resolution GCM simulations which included ocean biogeochemistry, improving upon the frictional-geostrophic low-resolution ocean modelling of cGENIE and the low resolution purely physical modelling using FOAM (Donnadieu et al. 2016). Simulating problems such as this in multiple contrasting models is extremely important since all models represent the ocean-earth system in different ways. Tackling problems such as this in as wide a variety of models, with processes represented in a variety of ways, with different paleogeographies and at contrasting resolutions is vital in order to be sure that behaviours exhibited are not an artefact of model or experiment design. Tackling this problem in a model

which includes ocean biogeochemistry and a good representation of ocean physics allows the affects of the latter on the former to be discussed in more detail, and including these two together is incredibly important when studying OAE2: an event resulting from a combination of both. As such, this work is a major modelling advance for OAE2 but needs to be repeated with other high resolution GCM simulations with biogeochemistry explicitly represented.

To develop our understanding of how paleogeography ocean circulation and ocean biogeochemistry came together to cause OAE2, is is important for this problem to be tackled in further studies, using a variety of models in combination with available proxy data. This area of research has started to get more attention, with Ladant et al. (2020), published at a similar time to this chapter's first submission as a paper, using the CCSM4 earth system model. This expansion of knowledge is likely a result of increasing computational power making simulations of this problem easier to tackle in more complex models. However, tackling the problem in a variety of models is as equally important as simply improving resolution or model representation.

Aside from this, continuing work in HadCM3L or another model could be forced with other paleogeographies in the Cretaceous and with a variety of nutrient inventory to see if more widespread anoxia was able to develop under these conditions or if, as we suggest, the changing ocean circulation will prevent this. This would help us to understand more fully to what extent paleogeography is able to aid or completely prevent OAE2 development, and whether other features of the OAE ocean circulation contributed

to this.

Ultimately, it would be good to develop modelling to represent the nutrient flux from land to ocean so that nutrients become less of an input and more a response to the climate system. Some aspects would be relatively straightforward to address (e.g. coupling nutrient input to surface runoff) but other aspects (such as the flux from volcanic sources and the extent of weathering fluxes) require considerable development

6.2.2 The Effect of Orbital Cycling on the Development of OAE2

Chapter 4 presents a number of Cenomanian simulations forced with different orbital parameters, to compare how orbital changes over time may have affected the development of OAE2. A key conclusion from Chapter 4 is that, similarly to paleogeography but with a less pronounced effect, orbital cycling is able to cause change in ocean oxygen levels during OAE2. It was able to impact these changes observed in ocean oxygen concentration through only physical changes to the ocean system. Ocean nutrient inventory was not changed in our simulations, and in fact, observed changes in primary production were the reverse of that expected when compared to the change in ocean oxygen levels. These changes in ocean oxygen levels were achieved instead by mediation of the Pacific overturning circulation by freshwater inputs. However, increases in precipitation align with the ocean circulation reduction to make it likely that more nutrient would have been supplied to the ocean in this scenario, further lowering oxygen levels, as

explored in chapter 5.

The changes in ocean oxygen level we observed were relatively small, and they are not large enough to cause the whole ocean, particularly the proto-North Atlantic, to switch from a wholly oxic to wholly anoxic mode. Therefore, despite being extreme end member simulations, the results presented do not lend weight to arguments that orbital forcing might have been a driving cause for OAE2 overall. However, it seems likely that changes in ocean oxygen level would be large enough to cause observable changes in sediments, particularly in areas where they cause an expansion or contraction of the oxygen minimum zone.

This chapter is one of very few modelling studies to tackle the question of how orbital cycling may have affected OAE2 development, building on a number of proxy studies (e.g. Eldrett et al. (2015), Meyer and Kump (2008), and Voigt et al. (2007)). Indeed, at the time of writing, this chapter represents the only recent, high resolution simulations of these effects. Moreover, the finding that we are able to see variation in ocean oxygen level caused by changes in orbital parameters is important, albeit expected considering the large body of cyclostratigraphic work which relies upon it (Meyers et al. 2001; Mitchell et al. 2008; Poulton et al. 2015). Finding that ocean circulation is the mechanism which causes this in our simulations underlines the importance of representing OAE2 with models which have good representation of this important driver of ocean primary production. However, a very interesting experiment might be to conduct similar simulations in a lower-resolution model such as cGENIE, to compare what effect these model's representation of ocean circulation has on the development of

OAE2. This ocean circulation mechanism is replicated in the recent Sarr et al. (2022), which lends weight to this diagnosis and suggests that scientific interest in this area is continuing to develop.

It should be noted that in both this work and the work of Sarr et al. (2022), only the orbit was changed. In the late Quaternary, we also know that there are related changes to the carbon, methane, and nitrogen cycles which act to amplify the response to orbital change. There are no fully reliable proxy data for orbitally driven Cretaceous CO_2 (and CH_4 and N_2O) variability and, although there is some quantitative modelling understanding of the methane and nitrogen cycles (Valdes et al. 2005), it still remains difficult to fully quantify the mechanisms that cause the orbitally driven CO_2 changes. Hence our simulations remain a likely underestimate of the full orbitally driven changes but it currently is difficult to assess in more detail.

While the approach of keeping the ocean nutrient inventory constant between the different simulations (a configuration shared in Sarr et al. (2022)) has had the great advantage of allowing us to clearly separate the circulation effects from that of additional supply, it would also be highly advantageous in the future to undertake further simulations of different orbital scenarios where nutrient inventory in the ocean was increased. This may be possible in HadCM3L or similar models (eg. cGENIE) by increasing ocean nutrient artificially, essentially combining aspects from 5 with 4. However, it would be challenging to gain enough confidence in the appropriate amount of nutrient to add, and this would loose any spatial effects associated with new areas of primary production at the ocean surface. Although most models

omit the riverine input of nutrient completely, this problem has started to be tackled in the modern ocean in studies such as Tivig et al. (2021), which uses a much more complex ocean ecosystem model than HadCM3L. However, in this study the riverine inputs were forced using measured river inputs, rather than being coupled to an atmosphere or land surface model, and the application of this to paleoclimate studies would be particularly difficult.

6.2.3 The role of physical and biological complexity in modelling OAE2

Chapter 5 presents a comparison of OAE2 simulations using HadCM3L and cGENIE, to explore how model differences, and in particular their respective treatments of the ocean ecosystem, affect OAE2 simulation. Key differences between the two models are discussed in terms of ocean biology: the ocean biological system itself and how ocean circulation affects primary production. Given the same perturbation (a doubling of ocean nutrient inventory), HadCM3L produces a significantly smaller reduction in ocean oxygen. It is suggested that a combination of two factors act to cause this difference: stronger mixing in cGENIE at high latitudes when compared to HadCM3L, and grazing pressure differences in HadCM3L which particularly affect areas of the ocean outside the south proto-North Atlantic and Equatorial Pacific.

The response of the ocean ecosystem is particularly interesting; grazing pressure as a control on ocean anoxia has not seen detailed discussion in

the current literature. When combined with the ocean circulation and the fact that some areas of the ocean are more important for the development of anoxia that others, small changes in primary production and grazing pressure appear to be able to exert non-negligible controls on the whole ocean system.

This chapter furthers our understanding of how cGENIE and HadCM3L represent OAE2 (and high nutrient conditions more generally). In finding that the ocean ecosystem may be important in helping to control ocean oxygen levels it suggests that the large body of work tackling this area in the modern ocean (Caddy and Bakun 1994; Dauvin 2012; Price et al. 1994; Tsuda et al. 2007) is likely to be important to take into consideration when modelling the OAE2 ocean and that all previous modelling studies of the OAE underestimated the complexity of biological feedbacks. It also highlights that studies need to also consider the correct model representation of export production to ensure that the assumptions that our models make are as much as possible appropriate for the time period we are studying. The differences shown in ocean circulation underline that model representation and resolution can have substantial effects on the ocean biogeochemistry and, to get a true picture of the past, models must be compared and the reasons for their difference understood.

The fact that the two models compared in this study differed in both ocean circulation and ecosystem made their comparison more complex. To better decouple the two effects it may be useful for a future study to examine different ecosystem schemes within model oceans that are more similar. However, the implementation of this would likely represent a significant

amount of work, which may not be justified unless it can be suggested that this will represent an improvement in model representation.

To gain confidence in the grazing pressure mechanic and the type of functional response used in HadCM3L, it would be helpful to determine if this effect is present in other modelling studies or if any proxy evidence can be drawn upon to reinforce it. It may be possible to do this by making comparisons to modern literature, where there is much discussion of different plankton ecosystems and how they respond to perturbation.

6.3 Summary

This thesis is one of the first studies to use a high resolution GCM fully coupled with a representation of biogeochemical processes to simulate OAE2. It has examined how physical and biogeochemical processes combine to cause the ocean anoxia characteristic of this time period. Findings in chapters 3 and 4 concluded that changes to the physical climate system were important in defining the magnitude and extent of ocean anoxia, but were not large enough to be the critical drivers in defining the full onset of OAE2. While factors such as paleogeography and orbital cycling are not strong enough to cause OAE2 on their own, they appear to be necessary conditions for OAE2 to develop, affecting the magnitude and worldwide spread of OAE2. The final research chapter (5) focused on the biogeochemical system, finding that the inclusion of an ecosystem in HadCM3 causes the model to be less responsive to ocean nutrient than cGENIE.

All three research chapters have used high resolution modelling to study

OAE2, analysing how the effects of ocean circulation and biology combine to create low oxygen conditions. By representing the OAE in a different, higher resolution model when compared to previous studies it has also allowed analysis of how modelling differences can change our understanding of how the OAE developed. Continuing growth in computer power allows more comprehensive models to be applied to these problems, and this is likely to lead to further improvements in our understanding of the causes and consequences of OAEs in the coming years.

Appendix A

The role of biology and sulphur in modelling OAE2

A.1 Preface

This section was originally included as chapter 4 of the thesis as a whole, and the ecological effects of the HadCM3L ecosystem discussed here were the foundation of the current chapter 5. It focused on how the representation of the biochemistry within the model affects our understanding of how the OAE developed. My co-authors for this section are from CGG Robertson, who provided the model paleogeographies used; and my supervisors Paul Valdes and Fanny Monteiro who provided feedback, help and advice on all aspects of the study. Fanny provided help and support in understanding the H_2S system and translating the sulphur cycle into a form that could be included in the model. She also ran the cGENIE model on a number of occasions to allow comparison of the behaviour seen in that model with

that of HadCM3. Paul provided technical support in incorporating this into HadCM3 and in running simulations in general.

A.2 Abstract

Oceanic anoxic event 2, which marks the Cenomanian/Turonian boundary was a large perturbation in the ocean carbon cycle which occurred at ≈100 Ma. It is thought that the large reduction in ocean oxygen seen during OAE2 was caused by the addition of large amounts of nutrient to the ocean, which caused an increase in primary production and subsequent burial of organic matter. In this study, we model the importance of two different processes in causing a dysoxic ocean during OAE2: (1) Using a new sulphur cycle module for HadCM3, we show that the sulphur cycle is less important than previously thought in the modelling of OAE2. (2) We show that the inclusion of an NPZD ocean ecosystem in HadCM3 prevents it from achieving a globally dysoxic ocean when ocean nutrient is doubled. This is in contrast to previous studies without an ocean ecosystem which have achieved global anxoia under otherwise similar conditions. These results underline the importance of the inclusion of an ocean ecosystem when modelling OAE2, and show that it is important to use more complex models to gain a full understanding of how the OAE developed.

A.3 Introduction

The HADCM3 family of models sees extensive continued use as a tool for the modelling of paleoclimates (Valdes et al. 2017), primarily due to the niche they fill between computational speed and model complexity. While the HadCM3 family of models have a relatively low resolution compared to more recent models, it remains a useful tool by combining a fully coupled atmosphere-ocean GCM with run-times which are acceptable and useful when undertaking the long runs required when modelling paleoclimate.

Research into OAEs is one area in which HadCM3 is well suited. OAEs, occurring in the Jurassic and Cretaceous periods, were large perturbations in the Earth's carbon cycle (Schlanger and Jenkyns 1976). Identified from the deposition of black shales at a global scale (Jenkyns 2010), these events were some of the largest changes in the global carbon cycle seen in the last 250 Ma. The development of an OAE is thought to have consisted of widespread low ocean oxygen levels, and euxinic conditions in the ocean photic zone. OAE2, one of the more widespread and recent OAEs (Jarvis et al. 2011), occurred at the Cenomanian and Turonian boundary approximately ninety-three million years ago. This OAE has been modelled in a number of different studies, and multiple theories to explain its presence have been put forward (Joo et al. 2020).

To allow the study of OAEs, Williams et al. (2014) developed a module for FAMOUS which allowed the modelling of the oxygen cycle in the HadCM3 family of models. This module has allowed the extensive modelling of Cretaceous OAEs in a full GCM, and allowed the identification of

climatic effects and processes which are not seen at lower resolutions or less comprehensive models. However, modelling using HadCM3 has generally been limited to pre-OAE2 conditions, with ocean nutrient levels and therefore primary production at relatively low levels compared to that thought necessary to achieve a full OAE (Meyer and Kump 2008; Monteiro et al. 2012).

A.3.1 Processes important for modelling an OAE

Remineralisation of organic matter is thought to be an important driver in the consumption of ocean oxygen leading to the development of anoxic conditions (Jenkyns 2010). Organic matter which sinks below the euphotic zone is respired by microorganisms, returning organic matter into inorganic form while consuming oxygen. In this way, increasing production (for example, by the addition of nutrient) in the surface ocean acts to reduce oxygen in the deep ocean, this effect is thought to be an important driver of the low oxygen conditions seen during OAE2 (Joo et al. 2020).

When oxygen levels reach very low conditions, microbes survive on organic matter by using less energetically efficient oxidants (in decreasing order of efficiency): Nitrate, Manganese Dioxide, Ferric Oxyhydroxide, Sulphate and Methane (Thamdrup et al. 1994).

Sulphate reduction is particularly interesting in the context of OAEs, since this reaction produces hydrogen sulphide, which is readily oxidised in the presence of oxygen causing the further removal of oxygen from the water column. In addition, hydrogen sulphide presence in the water column,

a condition known as euxinia, can be observed from specific biomarkers present in sediment cores indicating photic-zone euxinia (Jenkyns 2010). Hydrogen sulphide is then both an important part of the ocean oxygen system, and its inclusion in the model would allow better comparison with sediment proxies.

A.3.2 Remineralisation in HadCM3

In the existing HadCM3 with the oxygen module, remineralisation continues once oxygen has run out, with the rate of remineralisation determined only by depth. In the model, remineralisation is set at two different rates: one fast in the shallow and one slow in the deep ocean, and continues regardless of the presence of oxygen. If oxygen runs out, remineralisation continues, but oxygen is no longer consumed and remains at zero.

In this study we develop an addition to the HadCM3 oxygen module, allowing the production of hydrogen sulphide when oxygen levels are low. We compare the effects of this with the effects of adding such a scheme when oxygen levels are thought to have been low at a global scale during OAE2 and compare the model results with a previously published model of OAE2, cGENIE (Monteiro et al. 2012).

A.4 Model Development

A.4.1 The Sulphur Cycle in HadCM3

The additions to the model described here build upon the oxygen module added to FAMOUS as described in Williams et al. 2014. This is modified to incorporate the production of hydrogen sulphide and its decomposition.

Williams et al. (2014) assumed all remineralisation occurred using oxygen, and artificially prevented oxygen from becoming negative. In cases where oxygen is in abundance there is no change from this scheme, and the calculation with regards to oxygen is exactly the same as before.

However, when there is not enough oxygen to remineralize all the organic matter, the leftover organic matter (having oxidised as much as possible using oxygen) is then oxidised using a new state variable, sulphate. Remineralisation using sulphate produces hydrogen sulphide, which is held in another new state variable. If there is not enough sulphate to remineralize all the remaining organic matter, the remineralisation is still allowed to occur (the total remineralisation rate is not changed from HadOCC). However, this remineralisation will not produce hydrogen sulphide. The process of doing this remineralisation, and consuming either oxygen or sulphate is shown in Figure A.1.

If hydrogen sulphide is present in a grid box, this is oxidised using oxygen, where oxygen is available. This oxidation produces sulphate, ensuring hydrogen sulphide and sulphate are conserved in the model. This process is shown in Figure A.2.

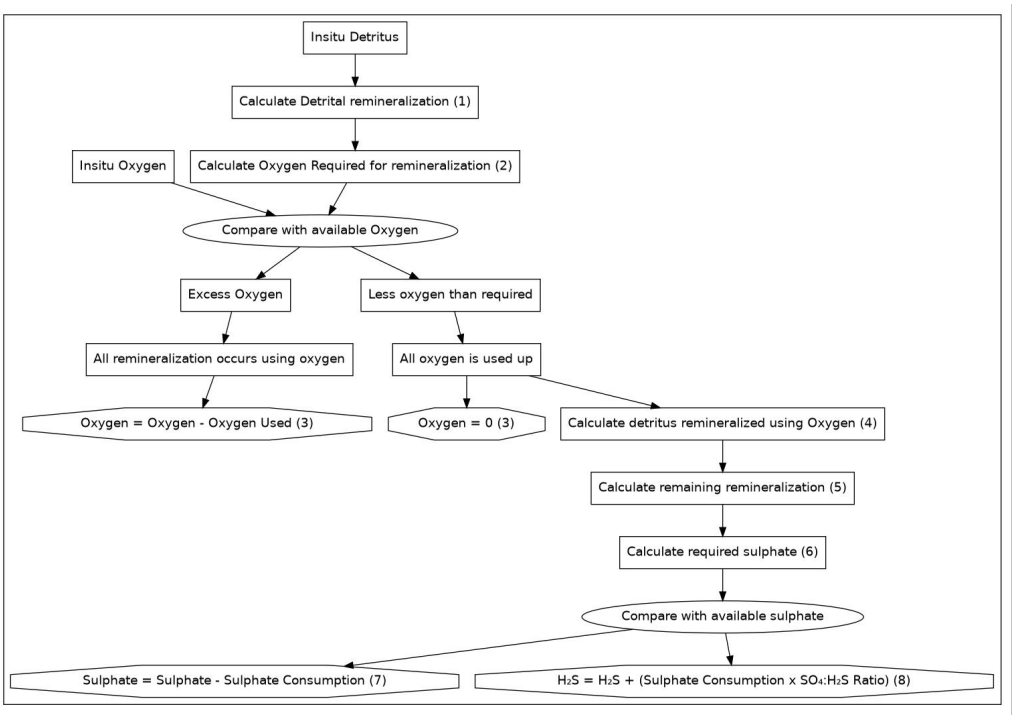

Figure A.1: Diagram showing how oxygen and sulphate are calculated using the new module for HadCM3. Oval boxes denote a comparison of variables, and octagonal boxes denote the output of the calculation to a model state variable. Numbers in brackets indicate the related equation below.

Remineralisation in detail

In detail, the scheme begins by calculating the amount of detrital remineralisation to occur, λD, which is simply the concentration of detritus multiplied by the detrital remineralisation rate ($0.10\,\mathrm{d}^{-1}$ in the shallow ocean, $0.02\,\mathrm{d}^{-1}$ in the deep ocean) (equation A.1).

$$\lambda D = [D] k_{remin} \tag{A.1}$$

The amount of Oxygen required to do this remineralization is then calculated, using the ratio of oxygen to carbon $R_{\mathrm{O_2:CO_2}} = \frac{138}{106}$ (equation A.2).

$$O_{2req} = D_{remin} R_{\mathrm{O_2:CO_2}} \tag{A.2}$$

If the oxygen requirements of remineralization are greater than the oxygen available, it is all used up. Otherwise, the change in oxygen is simply the required amount for remineralization (equation A.3).

$$\Delta \mathrm{O}_2 = \min(O_{2req}, [\mathrm{O}_2]) \tag{A.3}$$

If there was not enough Oxygen for full remineralization, the amount of detritus that was remineralized is calculated, using the O_2:CO_2 ratio (equation A.4).

$$\lambda D_{\mathrm{O}_2} = \frac{\Delta \mathrm{O}_2}{R_{\mathrm{O}_2:\mathrm{CO}_2}} \tag{A.4}$$

To calculate the remineralization yet to occur, this is subtracted from the total remineralization from equation A.1 (A.1).

$$\lambda D_{remain} = \lambda D - \lambda D_{\mathrm{O}_2} \tag{A.5}$$

The amount of sulphate required for remineralization of the remaining organic matter is calculated, using the fixed ratio $R_{{\mathrm{SO}_4}^{2-}:\mathrm{CO}_2} = \frac{59}{106}$ (equation A.6).

$$SO_{4req} = \lambda D_{remain} R_{{\mathrm{SO}_4}^{2-}:\mathrm{CO}_2} \tag{A.6}$$

Similarly to oxygen, the required amount of sulphate is used up, capped at the amount available (equation A.7).

$$\Delta {\mathrm{SO}_4}^{2-} = \min(SO_{4req}, [\mathrm{SO}_4]) \tag{A.7}$$

Sulphate consumption produces hydrogen sulphide, at a fixed ratio of $R_{{\mathrm{SO}_4}^{2-}:\mathrm{H}_2\mathrm{S}} = 1$.

$$\Delta \mathrm{H}_2\mathrm{S} = \Delta {\mathrm{SO}_4}^{2-} R_{{\mathrm{SO}_4}^{2-}:\mathrm{H}_2\mathrm{S}} \tag{A.8}$$

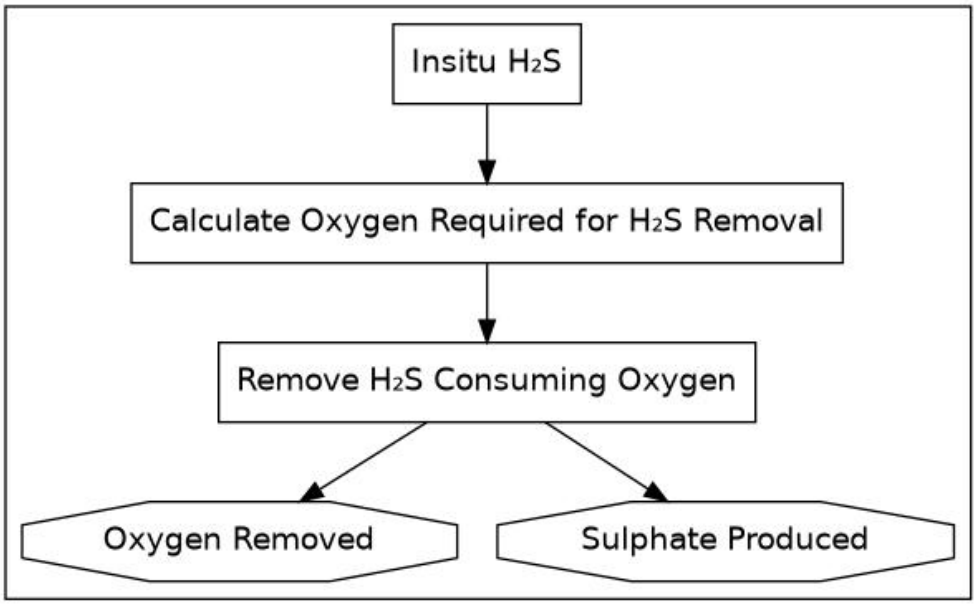

Figure A.2: Diagram showing how hydrogen sulphide produced decomposes, consuming oxygen in the new module for HadCM3. Oval boxes denote a comparison of variables, and octagonal boxes denote the output of the calculation to a model state variable.

H_2S removal in detail

H_2S decomposes in the presence of oxygen, consuming oxygen and producing ${SO_4}^{2-}$ (equation A.9).

$$H_2S + 2\,O_2 \longrightarrow {SO_4}^{2-} + 2\,H^+ \tag{A.9}$$

In the new model scheme, this reaction occurs immediately whenever both oxygen and H_2S are available, removing oxygen and hydrogen sulphide and producing sulphate.

A.4.2 Model Experiment Design

A number of model runs were undertaken in order to both evaluate the additions to HadCM3, and further understand how an OAE could be modelled.

In an attempt to achieve full-OAE conditions in HadCM3, the model was run both in a normal Cenomanian configuration, and with nutrient doubled across the whole ocean. These runs allowed the comparison with experiments using cGENIE, where the doubling of ocean nutrient is known to produce a full OAE (Monteiro et al. 2012).

These runs were mirrored by a further two runs, identical but with the new module adding sulphate to the model, instead of only the oxygen system from Williams et al. (2014).

cGENIE was run in a similar configuration to HadCM3L for pre-OAE2 and OAE2 to enable a comparison with another model which contained a similar sulphur cycle. This configuration, as in Naafs et al. (2019), includes both the sulphur cycle and nitrogen cycle, which is similar to HadCM3 with the new sulphate module, although the latter does not include the nitrogen cycle.

In addition to OAE2 simulations, the model was also run in a modern configuration, to ensure that the results produced were not significantly different to that of the original oxygen module- the modern ocean should not develop significant anoxia or euxinia.

	xokja	xokjb	xokje	xokjf
Nutrient	1x	1x	2x	2x
New Sulphate Mod	No	Yes	No	Yes

Table A.1: Outline of the Cenomanian runs and their configuration.

A.5 Results

The results of the runs using the modern palaeography did not produce areas of euxinia or depleted oxygen, as observed in the real ocean. Indeed, runs using the modern paleogeography showed no significant differences to those using the simple Williams et al. (2014) oxygen module. This is to be expected, as the sulphate cycling added in the module is not thought to be important in the modern ocean, which does not exhibit euxinia and whose oxygen minimum zones are more oxic than the Cenomanian ocean. The remainder of this paper will therefore focus on the Cenomanian results.

	Phytoplankton	Zooplankton
1x Nutrient (Control)	8.32e-03	4.37e-03
1x Nutrient with SO_4^{2-}	7.98e-03 (-4%)	3.79e-03 (-17%)
2x Nutrient	1.02e-02 (+23%)	8.50e-03 (+95%)
2x Nutrient with SO_4^{2-}	9.77e-03 (+17%)	8.33e-03 (+83%)
	Detritus	Oxygen
1x Nutrient (Control)	1.05e-02	189.66
1x Nutrient with SO_4^{2-}	9.82e-03 (-9%)	189.91 (-0%)
2x Nutrient	1.91e-02 (+82%)	151.73 (-20%)
2x Nutrient with SO_4^{2-}	2.06e-02 (+91%)	151.99 (-20%)

Table A.2: Global ocean Nutrient, Phytoplankton, Zooplankton and Detritus values for the four runs, in $\mu mol\,L^{-1}$.

A.5.1 Ocean Ecosystem

When compared with the control run, the double nutrient run (with Cenomanian paleogeography) produced a ≈20 % increase in phytoplankton grown, together with a somewhat larger (≈85 %) increase in zooplankton. This is a result of HadOCC's relatively complex ecosystem, and is quite different from the response of phytoplankton to an increase in nutrient seen in models with less complex ecosystems, such as cGENIE, which sees a full 100 % increase in phytoplankton as a result of a doubling of ocean nutrient. The ecosystem of cGENIE does not include a representation of phytoplankton or zooplankton, instead including a constant biological net uptake of nutrients. However, in HadOCC zooplankton graze using a Holling type three relationship (Holling 1965; Palmer and Totterdell 2001), treating both phytoplankton and detritus as "prey" and consuming them in proportion to their biomass (Palmer and Totterdell 2001). HadOCC shows a clear top-down control on phytoplankton from zooplankton, with zooplankton numbers increasing dramatically in response to the increase in nutrients (and phytoplankton biomass). The increase in detritus seen is also suppressed somewhat below a full doubling to a 85 % increase by grazing pressure from the large numbers of extra zooplankton.

The reduction in ocean oxygen in the double nutrient run compared to the control initially seems somewhat small (20 %) when compared to the increase in available detritus. Oxygen is constrained and cannot fall below zero; therefore an increase in detritus in areas that already have low oxygen levels would not be expected to cause a further decrease in oxygen (at least

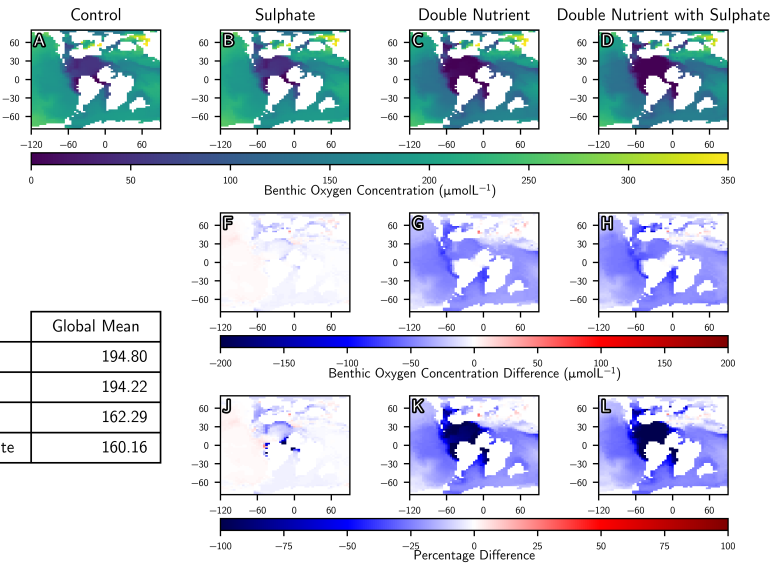

	Global Mean
Control	194.80
Sulphate	194.22
Double Nutrient	162.29
Double Nutrient with Sulphate	160.16

Figure A.3: Model ocean oxygen concentration at ocean bottom. Absolute oxygen concentration (top), difference with control (middle) and percentage difference with control (bottom).

in the no-sulphate mode).

A.5.2 Sulphur Cycle

Benthic oxygen concentrations in the runs with the new sulphate module (Figure A.3 columns two and four) are similarly not depleted as much as was expected; a small reduction in benthic oxygen is seen in both of these runs compared with runs without the sulphate module, but adding the sulphur cycle did not dramatically increase the spread of benthic low oxygen.

The addition of the sulphur cycle only has an effect in areas where benthic oxygen was already very low, which comprises a very small area of the global ocean, particularly in the 1 x nutrient run, where effects of the sulphur module on oxygen are only seen in the equatorial proto-Atlantic

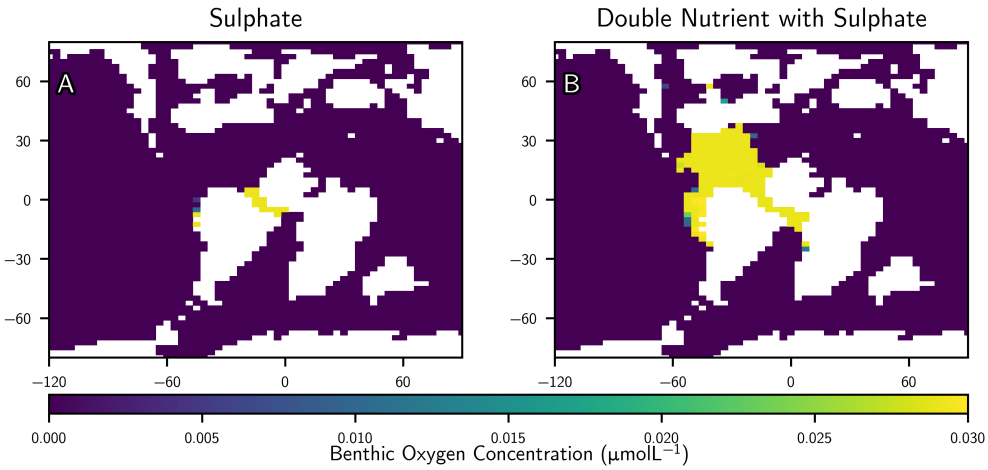

Figure A.4: Modelled H_2S at ocean bottom, in the single (left) and double (right) model runs with the new sulphate module.

(Figure A.3). Oxygen levels here are already near-zero, so the percentage change seen is very small, and the effect on the total inventory of oxygen in the global ocean is smaller still.

The small area in which the new sulphur module has had its biggest effect can be identified from those areas where hydrogen sulphide has been produced and is present in-situ (Figure A.4). In the run with 1x nutrient, this is only the proto-North Atlantic equatorial channel between America and Africa. In the double nutrient run, hydrogen sulphide is present across the whole of the proto-North Atlantic, reflecting the lower oxygen levels there. However, despite this wider extent, the impact on global ocean anoxia still remains small- hydrogen sulphide is only produced in areas where oxygen was already very low, meaning its oxygen-removing effects are limited by the lack of oxygen nearby to remove.

A.6 Discussion

The modelling of the ocean ecosystem has quite dramatic and important effects on the development of an OAE, and this has implications for our understanding of what conditions are required for an OAE to develop. The NPZD model included in HadOCC is significantly more complex than the ocean biochemistry included in cGENIE, and as a consequence the response of the ocean to a dramatic increase in nutrient is quite different.

In models without an ocean ecosystem, an increase in ocean nutrient causes a very direct increase in ocean primary production, biomass and consequently detritus, with this increase in detritus then resulting in a lowering of oxygen across the global ocean. In HadOCC, the more complex ecosystem means that nutrient and detritus are much less tightly coupled, and consequently a doubling of ocean nutrient, while reducing ocean oxygen by approximately 20 %, is not enough to cause anoxia globally.

The reduction in benthic oxygen seen when comparing our double nutrient run with that of the control is not as large as might be expected when compared to similar runs undertaken using cGENIE. cGENIE shows a somewhat larger drop in total mean oxygen, with the area of benthic low oxygen becoming much more widespread than that seen in HadCM3. This more widespread low oxygen is a better fit to the known extent of OAE2 when compared with known data points than the extent of low oxygen in HadCM3, but we would argue that this better agreement is for the wrong reason because of the over-simplification of the biological uptake. Doubling of ocean nutrient in HadCM3L did not have the same effect on

primary production in HadCM3 as in cGENIE. In cGENIE, a doubling of ocean nutrient is seen to cause a doubling in primary production, whereas the doubling of ocean nutrient in HadCM3 caused only an approximately one-third increase in phytoplankton.

The effects of adding the sulphur cycle to HadCM3 were significantly less important than expected in the context of the global ocean, in HadCM3 only causing a very small decrease in global ocean oxygen. The build-up of hydrogen sulphide in the proto-North Atlantic seen in the model does not result in large drops in global oxygen concentration; oxygen in this area is already low and therefore most of this hydrogen sulphide cannot oxidise to consume oxygen, therefore oxygen levels are not lowered. The restricted circulation in the proto-North Atlantic acts against this hydrogen sulphide building having a large effect on the rest of the worldwide ocean.

A.7 Conclusion

In this paper we have shown that modelling of ocean biology can have important effects on how models respond to forcing associated with OAE2. Additional weathering and the introduction of nutrient to the ocean is thought to be one of the principal drivers of OAE2. We have shown that the use of an NPZD ecosystem has the potential to reduce but not eliminate, the effect of adding nutrient to the ocean when compared with models without this ecosystem. This implies that an addition of considerably more than a doubling of nutrient would be required to cause an OAE in HadCM3, and implies a serious underestimate of the required nutrient increase required

to induce OAE2. On the other hand, our simulations suggest that the sulphur cycle is less important, which we attribute to the effect of H_2S only occurring in areas that already have low oxygen. Further simulations are required to determine a set of parameters that cause HadCM3 to develop a globally anoxic OAE2 ocean, and if the sulphur cycle is required to achieve this.

References

Adams, Derek D., Matthew T. Hurtgen, and Bradley B. Sageman (2010). 'Volcanic triggering of a biogeochemical cascade during Oceanic Anoxic Event 2'. In: *Nature Geoscience* 3.3, pp. 201–204. ISSN: 17520894. DOI: 10.1038/ngeo743.

Adloff, Markus (2021). 'Quantitative constraints on carbon fluxes and volcanic activity during Oceanic Anoxic Event 1a'. PhD thesis. URL: https://ethos.bl.uk/OrderDetails.do?uin=uk.bl.ethos.828416.

Adloff, Markus et al. (July 2021). 'Inclusion of a suite of weathering tracers in the cGENIE Earth system model-muffin release v.0.9.23'. In: *Geoscientific Model Development* 14.7, pp. 4187–4223. ISSN: 19919603. DOI: 10.5194/gmd-14-4187-2021.

Aksnes, Dug L. and Paul Wassmann (July 1993). 'Modeling the significance of zooplankton grazing for export production'. In: *Limnology and Oceanography* 38.5, pp. 978–985. ISSN: 00243590. DOI: 10.4319/lo.1993.38.5.0978. URL: http://doi.wiley.com/10.4319/lo.1993.38.5.0978.

Alcott, Lewis J., Benjamin J. W. Mills, and Simon W. Poulton (Dec. 2019). 'Stepwise Earth oxygenation is an inherent property of global biogeo-

chemical cycling'. In: *Science* 366.6471, pp. 1333–1337. ISSN: 0036-8075. DOI: 10.1126/science.aax6459.

Alcott, Lewis J. et al. (Mar. 2022). 'Earth's Great Oxidation Event facilitated by the rise of sedimentary phosphorus recycling'. In: *Nature Geoscience* 15.3, pp. 210–215. ISSN: 1752-0894. DOI: 10.1038/s41561-022-00906-5.

Anderson, TR and HW Ducklow (2001). 'Microbial loop carbon cycling in ocean environments studied using a simple steady-state model'. In: *Aquatic Microbial Ecology* 26.1, pp. 37–49. ISSN: 0948-3055. DOI: 10.3354/ame026037. URL: http://www.int-res.com/abstracts/ame/v26/n1/p37-49/.

Andjić, Goran, Peter O. Baumgartner, and Claudia Baumgartner-Mora (Sept. 2019). 'Collision of the Caribbean Large Igneous Province with the Americas: Earliest evidence from the forearc of Costa Rica'. In: *GSA Bulletin* 131.9-10, pp. 1555–1580. ISSN: 0016-7606. DOI: 10.1130/B35037.1. URL: https://pubs.geoscienceworld.org/gsa/gsabulletin/article/131/9-10/1555/569524/Collision-of-the-Caribbean-Large-Igneous-Province.

Ando, A. et al. (Oct. 2009). 'Onset Of Seawater 87Sr/86Sr Excursion Prior to Cenomanian-Turonian Oceanic Anoxic Event 2? New Late Cretaceous Strontium Isotope Curve from the Central Pacific Ocean'. In: *The Journal of Foraminiferal Research* 39.4, pp. 322–334. ISSN: 0096-1191. DOI: 10.2113/gsjfr.39.4.322. URL: https://pubs.geoscienceworld.org/jfr/article/39/4/322-334/77167.

Anneville, Orlane et al. (Nov. 2019). 'The paradox of re-oligotrophication: the role of bottom–up versus top–down controls on the phytoplankton community'. In: *Oikos* 128.11, pp. 1666–1677. ISSN: 0030-1299. DOI: 10.1111/oik.06399.

Armstrong, Howard A. et al. (Aug. 2016). 'Hadley circulation and precipitation changes controlling black shale deposition in the Late Jurassic Boreal Seaway'. In: *Paleoceanography* 31.8, pp. 1041–1053. ISSN: 08838305. DOI: 10.1002/2015PA002911. URL: http://doi.wiley.com/10.1002/2015PA002911.

Arning, E.T. et al. (July 2009). 'Genesis of phosphorite crusts off Peru'. In: *Marine Geology* 262.1-4, pp. 68–81. ISSN: 00253227. DOI: 10.1016/j.margeo.2009.03.006.

Arthur, M. A., S. O. Schlanger, and Hugh C. Jenkyns (1987). 'The Cenomanian-Turonian Oceanic Anoxic Event, II. Palaeoceanographic controls on organic-matter production and preservation'. In: *Geological Society Special Publication* 26.26, pp. 401–420. ISSN: 03058719. DOI: 10.1144/GSL.SP.1987.026.01.25.

Arthur, Michael A and B B Sageman (May 1994). 'Marine Black Shales: Depositional Mechanisms and Environments of Ancient Deposits'. In: *Annual Review of Earth and Planetary Sciences* 22.1, pp. 499–551. ISSN: 0084-6597. DOI: 10.1146/annurev.ea.22.050194.002435. URL: http://www.annualreviews.org/doi/10.1146/annurev.ea.22.050194.002435.

Arthur, Michael A., Walter E. Dean, and Lisa M. Pratt (Oct. 1988). 'Geochemical and climatic effects of increased marine organic carbon burial

at the Cenomanian/Turonian boundary'. In: *Nature* 335.6192, pp. 714–717. ISSN: 0028-0836. DOI: 10.1038/335714a0. URL: http://www.nature.com/articles/335714a0.

Arthur, Michael A. and Bradley B. Sageman (Aug. 2011). 'Sea-Level Control on Source-Rock Development: Perspectives from the Holocene Black Sea, the Mid-Cretaceous Western Interior Basin of North America, and the Late Devonian Appalachian Basin'. In: *Deposition of Organic-Carbon-Rich Sediments: Models*. Vol. 82. 82. SEPM (Society for Sedimentary Geology), pp. 35–59. ISBN: 1565761103. DOI: 10.2110/pec.05.82.0035. URL: https://pubs.geoscienceworld.org/books/book/1129/chapter/10557885/.

Azam, F et al. (1983). 'The Ecological Role of Water-Column Microbes in the Sea'. In: *Marine Ecology Progress Series* 10.3, pp. 257–263. DOI: 10.3354/meps010257. URL: http://www.int-res.com/articles/meps/10/m010p257.pdf.

Banse, Karl (1992). 'Grazing, Temporal Changes of Phytoplankton Concentrations, and the Microbial Loop in the Open Sea'. In: *Primary Productivity and Biogeochemical Cycles in the Sea*. Boston, MA: Springer US, pp. 409–440. DOI: 10.1007/978-1-4899-0762-2{_}22.

— (1995). *I. Biomass and production measurements Zooplankton: Pivotal role in the control of ocean production*. Tech. rep., pp. 265–277. URL: https://academic.oup.com/icesjms/article/52/3-4/265/841465.

Barron, Eric J., Michael A. Arthur, and Erle G. Kauffman (Mar. 1985). 'Cretaceous rhythmic bedding sequences: a plausible link between orbital variations and climate'. In: *Earth and Planetary Science Letters*

72.4, pp. 327–340. ISSN: 0012821X. DOI: 10.1016/0012-821X(85)90056-1.

Batenburg, Sietske J. et al. (2016). 'Orbital control on the timing of oceanic anoxia in the Late Cretaceous'. In: *Climate of the Past* 12.10, pp. 2009–2016. ISSN: 18149332. DOI: 10.5194/cp-12-1995-2016.

Beaufort, Luc et al. (Nov. 1997). 'Insolation Cycles as a Major Control of Equatorial Indian Ocean Primary Production'. In: *Science* 278.5342, pp. 1451–1454. ISSN: 0036-8075. DOI: 10.1126/science.278.5342.1451.

Beckmann, Britta et al. (2005). 'Orbital forcing of Cretaceous river discharge in tropical Africa and ocean response'. In: *Nature* 437.7056, pp. 241–244. ISSN: 00280836. DOI: 10.1038/nature03976.

Behrooz, L. et al. (2018). 'Astronomically Driven Variations in Depositional Environments in the South Atlantic During the Early Cretaceous'. In: *Paleoceanography and Paleoclimatology* 33.8, pp. 894–912. ISSN: 25724525. DOI: 10.1029/2018PA003338.

Beil, Sebastian et al. (Apr. 2020). 'Cretaceous oceanic anoxic events prolonged by phosphorus cycle feedbacks'. In: *Climate of the Past* 16.2, pp. 757–782. ISSN: 18149332. DOI: 10.5194/cp-16-757-2020.

Berger, A., M. F. Loutre, and J. Laskar (1992). 'Stability of the astronomical frequencies over the earth's history for paleoclimate studies'. In: *Science* 255.5044, pp. 560–566. ISSN: 00368075. DOI: 10.1126/science.255.5044.560.

Berger, A. and M.F. Loutre (Jan. 1991). 'Insolation values for the climate of the last 10 million years'. In: *Quaternary Science Reviews* 10.4, pp. 297–317. ISSN: 02773791. DOI: 10.1016/0277-3791(91)90033-Q.

Berger, A.L., M. F. Loutre, and J. L. Mélice (2006). 'Equatorial insolation: from precession harmonics to eccentricity frequencies'. In: *Climate of the Past Discussions* 2.4, pp. 519–533. DOI: 10.5194/cpd-2-519-2006.

Berger, Andre. (Dec. 1978). 'Long-Term Variations of Daily Insolation and Quaternary Climatic Changes'. In: *Journal of the Atmospheric Sciences* 35.12, pp. 2362–2367. ISSN: 0022-4928. DOI: 10.1175/1520-0469(1978)035<2362:LTVODI>2.0.CO;2. URL: http://journals.ametsoc.org/doi/10.1175/1520-0469(1978)035%3C2362:LTVODI%3E2.0.CO;2.

Berger, W, Victor Smetacek, and Gerold Wefer (1989). 'Ocean productivity and paleoproductivity - An overview'. In: *Productivity in the Ocean - Present and Past*, pp. 1–34.

Bjerrum, C. J., J. Bendtsen, and J. J.F. Legarth (2006). 'Modeling organic carbon burial during sea level rise with reference to the Cretaceous'. In: *Geochemistry, Geophysics, Geosystems* 7.5. ISSN: 15252027. DOI: 10.1029/2005GC001032.

Blackburn, Terrence J. et al. (May 2013). 'Zircon U-Pb Geochronology Links the End-Triassic Extinction with the Central Atlantic Magmatic Province'. In: *Science* 340.6135, pp. 941–945. ISSN: 0036-8075. DOI: 10.1126/science.1234204.

Boer, P. L. de and D. G. Smith (Apr. 2009). 'Orbital Forcing and Cyclic Sequences'. In: *Orbital Forcing and Cyclic Sequences*. Oxford, UK: Blackwell Publishing Ltd., pp. 1–14. DOI: 10.1002/9781444304039.ch1.

Bralower, Timothy J. and Hans R. Thierstein (1984). 'Low productivity and slow deep-water circulation in mid-Cretaceous oceans'. In: *Geology* 12.10, p. 614. ISSN: 0091-7613. DOI: 10.1130/0091-7613(1984)12<614:LPASDC>2.0.CO;2. URL: https://pubs.geoscienceworld.org/geology/article/12/10/614-618/190079.

Brookfield, M.E. and R.E. Hannigan (Sept. 2021). 'Carbon and oxygen isotope variations in shell beds from the Upper Ordovician (mid-Cincinnatian: Maysvillian to early Richmondian) of Ontario: Evaluation of the Warm Saline Deep Ocean hypothesis, paleoceanographic changes, and Milankovitch orbital cycles in the transition to the Hirnantian glaciation'. In: *Palaeogeography, Palaeoclimatology, Palaeoecology* 577, p. 110528. ISSN: 00310182. DOI: 10.1016/j.palaeo.2021.110528.

Bryan, Scott E. et al. (Oct. 2010). 'The largest volcanic eruptions on Earth'. In: *Earth-Science Reviews* 102.3-4, pp. 207–229. ISSN: 00128252. DOI: 10.1016/j.earscirev.2010.07.001.

Buchs, David M. et al. (Dec. 2019). 'Volcanic contribution to emergence of Central Panama in the Early Miocene'. In: *Scientific Reports* 9.1. ISSN: 20452322. DOI: 10.1038/s41598-018-37790-2.

Caddy, J.F. and A. Bakun (Jan. 1994). 'A tentative classification of coastal marine ecosystems based on dominant processes of nutrient supply'. In: *Ocean & Coastal Management* 23.3, pp. 201–211. ISSN: 09645691. DOI: 10.1016/0964-5691(94)90019-1. URL: http://linkinghub.elsevier.com/retrieve/pii/0964569194900191.

Caswell, B. A. and A. L. Coe (Nov. 2013). 'Primary productivity controls on opportunistic bivalves during Early Jurassic oceanic deoxygenation'. In: *Geology* 41.11, pp. 1163–1166. ISSN: 0091-7613. DOI: 10.1130/G34819.1.

Cavan, E. L. et al. (Mar. 2017). 'Remineralization of particulate organic carbon in an ocean oxygen minimum zone'. In: *Nature Communications* 8. ISSN: 20411723. DOI: 10.1038/ncomms14847.

Charbonnier, Guillaume et al. (2018). 'Obliquity pacing of the hydrological cycle during the Oceanic Anoxic Event 2'. In: *Earth and Planetary Science Letters* 499, pp. 266–277. ISSN: 0012821X. DOI: 10.1016/j.epsl.2018.07.029. URL: https://doi.org/10.1016/j.epsl.2018.07.029.

Chavez, Francisco P. et al. (1991). 'Growth rates, grazing, sinking, and iron limitation of equatorial Pacific phytoplankton'. In: *Limnology and Oceanography* 36.8, pp. 1816–1833. ISSN: 19395590. DOI: 10.4319/lo.1991.36.8.1816.

Chen, Hongjin et al. (Feb. 2022). 'Enhanced hydrological cycle during Oceanic Anoxic Event 2 at southern high latitudes: New insights from IODP Site U1516'. In: *Global and Planetary Change* 209, p. 103735. ISSN: 09218181. DOI: 10.1016/j.gloplacha.2022.103735. URL: https://linkinghub.elsevier.com/retrieve/pii/S0921818122000029.

Cheng, Hai et al. (Apr. 2021). 'Orbital-scale Asian summer monsoon variations: Paradox and exploration'. In: *Science China Earth Sciences* 64.4, pp. 529–544. ISSN: 1674-7313. DOI: 10.1007/s11430-020-9720-y.

Cheng, Keyi, Maya Elrick, and Stephen J. Romaniello (2020). 'Early mississippian ocean anoxia triggered organic carbon burial and late paleozoic

cooling: Evidence from uranium isotopes recorded in marine limestone'. In: *Geology* 48.4, pp. 363–367. ISSN: 19432682. DOI: 10.1130/G46950.1.

Claussen, M. et al. (2002). 'Earth system models of intermediate complexity: Closing the gap in the spectrum of climate system models'. In: *Climate Dynamics* 18.7, pp. 579–586. ISSN: 09307575. DOI: 10.1007/s00382-001-0200-1.

Coccioni, R. (Apr. 2004). 'Planktonic Foraminifera and Environmental Changes Across the Bonarelli Event (OAE2, Latest Cenomanian) in its Type Area: A High-Resolution Study From the Tethyan Reference Bottaccione Section (Gubbio, Central Italy)'. In: *The Journal of Foraminiferal Research* 34.2, pp. 109–129. ISSN: 0096-1191. DOI: 10.2113/0340109.

Coccioni, Rodolfo and Valeria Luciani (Aug. 2005). 'Planktonic foraminifers across the Bonarelli Event (OAE2, latest Cenomanian): The Italian record'. In: *Palaeogeography, Palaeoclimatology, Palaeoecology* 224.1-3, pp. 167–185. ISSN: 00310182. DOI: 10.1016/j.palaeo.2005.03.039.

Coccioni, Rodolfo, Valeria Luciani, and Andrea Marsili (May 2006). 'Cretaceous oceanic anoxic events and radially elongated chambered planktonic foraminifera: Paleoecological and paleoceanographic implications'. In: *Palaeogeography, Palaeoclimatology, Palaeoecology* 235.1-3, pp. 66–92. ISSN: 00310182. DOI: 10.1016/j.palaeo.2005.09.024.

Corbett, Matthew J. and David K. Watkins (Dec. 2013). 'Calcareous nannofossil paleoecology of the mid-Cretaceous Western Interior Seaway and evidence of oligotrophic surface waters during OAE2'. In: *Palaeogeography, Palaeoclimatology, Palaeoecology* 392, pp. 510–523. ISSN: 00310182. DOI: 10.1016/j.palaeo.2013.10.007.

Cosmidis, Julie et al. (Nov. 2013). 'Microscopy evidence of bacterial microfossils in phosphorite crusts of the Peruvian shelf: Implications for phosphogenesis mechanisms'. In: *Chemical Geology* 359, pp. 10–22. ISSN: 00092541. DOI: 10.1016/j.chemgeo.2013.09.009.

Cox, P.M, C Huntingford, and R.J Harding (Dec. 1998). 'A canopy conductance and photosynthesis model for use in a GCM land surface scheme'. In: *Journal of Hydrology* 212-213, pp. 79–94. ISSN: 00221694. DOI: 10.1016/S0022-1694(98)00203-0.

Cox, Peter M et al. (Nov. 2000). 'Acceleration of global warming due to carbon-cycle feedbacks in a coupled climate model'. In: *Nature* 408.6809, pp. 184–187. ISSN: 0028-0836. DOI: 10.1038/35041539. URL: http://www.nature.com/articles/35041539.

Dauvin, Jean Claude (2012). 'Are the eastern and western basins of the English Channel two separate ecosystems?' In: *Marine Pollution Bulletin* 64.3, pp. 463–471.

Devol, A. H. and H. E. Hartnett (2001). 'Role of the oxygen-deficient zone in transfer of organic carbon to the deep ocean'. In: *Limnology and Oceanography* 46.7, pp. 1684–1690. ISSN: 00243590. DOI: 10.4319/lo.2001.46.7.1684.

Dickson, Robert R. and Juan Brown (1994). 'The production of North Atlantic Deep Water: Sources, rates, and pathways'. In: *Journal of Geophysical Research* 99.C6, p. 12319. ISSN: 0148-0227. DOI: 10.1029/94JC00530. URL: http://doi.wiley.com/10.1029/94JC00530.

Donnadieu, Yannick et al. (2016). 'A better-ventilated ocean triggered by Late Cretaceous changes in continental configuration'. In: *Nature Communications* 7. ISSN: 20411723. DOI: 10.1038/ncomms10316.

Du Vivier, Alice D.C. et al. (2014). 'Marine 187Os/188Os isotope stratigraphy reveals the interaction of volcanism and ocean circulation during Oceanic Anoxic Event 2'. In: *Earth and Planetary Science Letters* 389, pp. 23–33. ISSN: 0012821X. DOI: 10.1016/j.epsl.2013.12.024. URL: http://dx.doi.org/10.1016/j.epsl.2013.12.024.

Ducklow, Hugh (2000). 'Bacterial Production and Biomass in the Oceans'. In: February, pp. 85–120.

Dummann, Wolf et al. (Feb. 2021). 'Driving mechanisms of organic carbon burial in the Early Cretaceous South Atlantic Cape Basin (DSDP Site 361)'. In: *Climate of the Past* 17.1, pp. 469–490. ISSN: 18149332. DOI: 10.5194/cp-17-469-2021.

Dürkefälden, Antje et al. (Mar. 2019). 'Age and geochemistry of the Beata Ridge: Primary formation during the main phase (
89 Ma) of the Caribbean Large Igneous Province'. In: *Lithos* 328-329, pp. 69–87. ISSN: 00244937. DOI: 10.1016/j.lithos.2018.12.021. URL: https://linkinghub.elsevier.com/retrieve/pii/S0024493718304833.

Edwards, Andrew M., Trevor Platt, and Shubha Sathyendranath (Jan. 2004). 'The high-nutrient, low-chlorophyll regime of the ocean: limits on biomass and nitrate before and after iron enrichment'. In: *Ecological Modelling* 171.1-2, pp. 103–125. ISSN: 03043800. DOI: 10.1016/j.ecolmodel.2003.06.001.

Edwards, Neil R. and Robert Marsh (Mar. 2005). 'Uncertainties due to transport-parameter sensitivity in an efficient 3-D ocean-climate model'. In: *Climate Dynamics* 24.4, pp. 415–433. ISSN: 09307575. DOI: 10.1007/s00382-004-0508-8.

Edwards, Neil R., Andrew J. Willmott, and Peter D. Killworth (May 1998). 'On the Role of Topography and Wind Stress on the Stability of the Thermohaline Circulation'. In: *Journal of Physical Oceanography* 28.5, pp. 756–778. ISSN: 0022-3670. DOI: 10.1175/1520-0485(1998)028<0756:OTROTA>2.0.CO;2. URL: http://journals.ametsoc.org/doi/10.1175/1520-0485(1998)028%3C0756:OTROTA%3E2.0.CO;2.

Elderbak, Khalifa and R. Mark Leckie (May 2016). 'Paleocirculation and foraminiferal assemblages of the Cenomanian-Turonian Bridge Creek Limestone bedding couplets: Productivity vs. dilution during OAE2'. In: *Cretaceous Research* 60, pp. 52–77. ISSN: 01956671. DOI: 10.1016/j.cretres.2015.11.009. URL: https://linkinghub.elsevier.com/retrieve/pii/S019566711530118X.

Eldrett, James S., Daniel Minisini, and Steven C. Bergman (July 2014). 'Decoupling of the carbon cycle during Ocean Anoxic Event 2'. In: *Geology* 42.7, pp. 567–570. ISSN: 1943-2682. DOI: 10.1130/G35520.1.

Eldrett, James S. et al. (2015). 'An astronomically calibrated stratigraphy of the Cenomanian, Turonian and earliest Coniacian from the Cretaceous Western Interior Seaway, USA: Implications for global chronostratigraphy'. In: *Cretaceous Research* 56, pp. 316–344. ISSN: 1095998X. DOI: 10.1016/j.cretres.2015.04.010. URL: http://dx.doi.org/10.1016/j.cretres.2015.04.010.

Elrick, Maya et al. (Jan. 2009). 'C-isotope stratigraphy and paleoenvironmental changes across OAE2 (mid-Cretaceous) from shallow-water platform carbonates of southern Mexico'. In: *Earth and Planetary Science Letters* 277.3-4, pp. 295–306. ISSN: 0012821X. DOI: 10.1016/j.epsl.2008.10.020.

Erba, Elisabetta (Aug. 2004). 'Calcareous nannofossils and Mesozoic oceanic anoxic events'. In: *Marine Micropaleontology* 52.1-4, pp. 85–106. ISSN: 03778398. DOI: 10.1016/j.marmicro.2004.04.007.

Erba, Elisabetta et al. (2019). 'The response of calcareous nannoplankton to oceanic anoxic events: The Italian pelagic record'. In: *Bollettino della Societa Paleontologica Italiana* 58.1, pp. 51–71. ISSN: 03757633. DOI: 10.4435/BSPI.2019.08.

Erbacher, Jochen (1998). *29. Mid-Cretaceous Radiolarians from the Eastern Equatorial Atlantic and their Paleoceanography*. Tech. rep.

Erbacher, Jochen et al. (Jan. 2001). 'Increased thermohaline stratification as a possible cause for an ocean anoxic event in the Cretaceous period'. In: *Nature* 409.6818, pp. 325–327. ISSN: 0028-0836. DOI: 10.1038/35053041. URL: http://www.nature.com/articles/35053041.

Everett, Jason D. et al. (Mar. 2017). *Modeling what we sample and sampling what we model: Challenges for zooplankton model assessment*. DOI: 10.3389/fmars.2017.00077.

Falzoni, Francesca and Maria Rose Petrizzo (2020). 'Patterns of planktonic foraminiferal extinctions and eclipses during Oceanic Anoxic Event 2 at Eastbourne (SE England) and other mid-low latitude locations'. In: *Cretaceous Research* 116, p. 104593. ISSN: 1095998X. DOI: 10.1016/j.

cretres.2020.104593. URL: https://doi.org/10.1016/j.cretres.2020.104593.

Fasham, M. J.R., H. W. Ducklow, and S. M. McKelvie (1990). 'A nitrogen-based model of plankton dynamics in the oceanic mixed layer'. In: *Journal of Marine Research* 48.3, pp. 591–639. ISSN: 00222402. DOI: 10.1357/002224090784984678.

Fennel, Wolfgang and Thomas Neumann (Aug. 2001). 'Coupling Biology and Oceanography in Models'. In: *AMBIO: A Journal of the Human Environment* 30.4, pp. 232–236. ISSN: 0044-7447. DOI: 10.1579/0044-7447-30.4.232. URL: http://www.bioone.org/doi/abs/10.1579/0044-7447-30.4.232.

Ferreira, David et al. (Nov. 2014). 'Climate at high-obliquity'. In: *Icarus* 243, pp. 236–248. ISSN: 00191035. DOI: 10.1016/j.icarus.2014.09.015.

Flögel, S. et al. (Sept. 2008). 'Evolution of tropical watersheds and continental hydrology during the Late Cretaceous greenhouse; impact on marine carbon burial and possible implications for the future'. In: *Earth and Planetary Science Letters* 274.1-2, pp. 1–13. ISSN: 0012821X. DOI: 10.1016/j.epsl.2008.06.011.

Flögel, S. et al. (2011). 'Simulating the biogeochemical effects of volcanic CO2 degassing on the oxygen-state of the deep ocean during the Cenomanian/Turonian Anoxic Event (OAE2)'. In: *Earth and Planetary Science Letters* 305.3-4, pp. 371–384. ISSN: 0012821X. DOI: 10.1016/j.epsl.2011.03.018. URL: http://dx.doi.org/10.1016/j.epsl.2011.03.018.

Flögel, Sascha (2001). 'On the influence of precessional Milankovitch cycles on the Late Cretaceous climate system: comparison of GCM-results, geochemical, and sedimentary proxies for the Western Interior Seaway of North America'. In: *Thesis*, 143pp. URL: http://deposit.d-nb.de/cgi-bin/dokserv?idn=971979928.

Forkner, R. M. et al. (2021). 'Anatomy of an extinction revealed by molecular fossils spanning OAE2'. In: *Scientific Reports* 11.1, pp. 1–9. ISSN: 20452322. DOI: 10.1038/s41598-021-92817-5. URL: https://doi.org/10.1038/s41598-021-92817-5.

Foster, Gavin L., Dana L. Royer, and Daniel J. Lunt (Apr. 2017). 'Future climate forcing potentially without precedent in the last 420 million years'. In: *Nature Communications* 8. ISSN: 20411723. DOI: 10.1038/ncomms14845.

Friedrich, Oliver (July 2010). 'Benthic foraminifera and their role to decipher paleoenvironment during mid-Cretaceous Oceanic Anoxic Events – the "anoxic benthic foraminifera" paradox'. In: *Revue de Micropaléontologie* 53.3, pp. 175–192. ISSN: 00351598. DOI: 10.1016/j.revmic.2009.06.001.

Friedrich, Oliver, Jens O. Herrle, and Christoph Hemleben (2005). 'Climatic changes in the late campanian - Early maastrichtian: Micropaleontological and stable isotopic evidence from an epicontinental sea'. In: *Journal of Foraminiferal Research* 35.3, pp. 228–247. ISSN: 00961191. DOI: 10.2113/35.3.228.

Friedrich, Oliver, Richard D. Norris, and Jochen Erbacher (2012). 'Evolution of middle to late Cretaceous oceans-A 55 m.y. Record of Earth's

temperature and carbon cycle'. In: *Geology* 40.2, pp. 107–110. ISSN: 00917613. DOI: 10.1130/G32701.1.

Frijia, G. et al. (June 2019). 'Cyanobacteria Proliferation in the Cenomanian-Turonian Boundary Interval of the Apennine Carbonate Platform: Immediate Response to the Environmental Perturbations Associated With OAE-2?' In: *Geochemistry, Geophysics, Geosystems* 20.6, pp. 2698–2716. ISSN: 15252027. DOI: 10.1029/2019GC008306.

Gangl, S.K. et al. (July 2019). 'High-resolution records of Oceanic Anoxic Event 2: Insights into the timing, duration and extent of environmental perturbations from the palaeo-South Pacific Ocean'. In: *Earth and Planetary Science Letters* 518, pp. 172–182. ISSN: 0012821X. DOI: 10.1016/j.epsl.2019.04.028.

Gebhardt, Holger et al. (Oct. 2010). 'Paleoceanographic changes at the northern Tethyan margin during the Cenomanian–Turonian Oceanic Anoxic Event (OAE-2)'. In: *Marine Micropaleontology* 77.1-2, pp. 25–45. ISSN: 03778398. DOI: 10.1016/j.marmicro.2010.07.002. URL: https://linkinghub.elsevier.com/retrieve/pii/S0377839810000630.

Gordon, C. et al. (Feb. 2000). 'The simulation of SST, sea ice extents and ocean heat transports in a version of the Hadley Centre coupled model without flux adjustments'. In: *Climate Dynamics* 16.2-3, pp. 147–168. ISSN: 0930-7575. DOI: 10.1007/s003820050010. URL: http://link.springer.com/10.1007/978-3-642-20367-1_25%20http://link.springer.com/10.1007/s003820050010.

Gusha, Molline N.C. et al. (Feb. 2019). 'Zooplankton grazing pressure is insufficient for primary producer control under elevated warming and

nutrient levels'. In: *Science of The Total Environment* 651, pp. 410–418. ISSN: 00489697. DOI: 10.1016/j.scitotenv.2018.09.132. URL: https://linkinghub.elsevier.com/retrieve/pii/S0048969718335769.

Halfter, Svenja et al. (Sept. 2020). *The Role of Zooplankton in Establishing Carbon Export Regimes in the Southern Ocean – A Comparison of Two Representative Case Studies in the Subantarctic Region*. DOI: 10.3389/fmars.2020.567917.

Handoh, Itsuki C. and Timothy M. Lenton (2003). 'Periodic mid-Cretaceous oceanic anoxic events linked by oscillations of the phosphorus and oxygen biogeochemical cycles'. In: *Global Biogeochemical Cycles* 17.4, pp. 1–11. ISSN: 08866236. DOI: 10.1029/2003gb002039.

Harrison, W. G. and G. F. Cota (Jan. 1991). 'Primary production in polar waters: relation to nutrient availability'. In: *Polar Research* 10.1, pp. 87–104. ISSN: 1751-8369. DOI: 10.3402/polar.v10i1.6730. URL: https://polarresearch.net/index.php/polar/article/view/2301.

Harwood, David M., Vladimir A. Nikolaev, and Diane M. Winter (Oct. 2007). 'Cretaceous Records of Diatom Evolution, Radiation, and Expansion'. In: *The Paleontological Society Papers* 13, pp. 33–59. ISSN: 1089-3326. DOI: 10.1017/S1089332600001455.

Hasegawa, T. (May 1997). 'Cenomanian-Turonian carbon isotope events recorded in terrestrial organic matter from northern Japan'. In: *Palaeogeography, Palaeoclimatology, Palaeoecology* 130.1-4, pp. 251–273. ISSN: 00310182. DOI: 10.1016/S0031-0182(96)00129-0. URL: https://linkinghub.elsevier.com/retrieve/pii/S0031018296001290.

Hasegawa, Takashi et al. (2004). 'Upper Cretaceous stable carbon-isotope stratigraphy of terrestrial organic matter from Sakhalin, Russian Far East: a proxy for the isotopic composition of paleoatmospheric CO2'. In: *Palaeogeography, Palaeoclimatology, Palaeoecology* 215.1-2, pp. 179–182. ISSN: 00310182. DOI: 10.1016/j.palaeo.2004.09.003.

Hay, W (Dec. 1988). 'Paleoceanography: A review for the GSA Centennial'. In: *Geological Society of America Bulletin* 100.12, pp. 1934–1956. ISSN: 00167606. DOI: 10.1130/0016-7606(1988)100<1934:PARFTG>2.3.CO;2.

Hay, William W. (2008). 'Evolving ideas about the Cretaceous climate and ocean circulation'. In: *Cretaceous Research* 29.5-6, pp. 725–753. ISSN: 01956671. DOI: 10.1016/j.cretres.2008.05.025. URL: http://dx.doi.org/10.1016/j.cretres.2008.05.025.

Hays, J. D., J. Imbrie, and N. J. Shackleton (Dec. 1976). 'Variations in the Earth's Orbit: Pacemaker of the Ice Ages'. In: *Science* 194.4270, pp. 1121–1132. ISSN: 0036-8075. DOI: 10.1126/science.194.4270.1121. URL: https://www.sciencemag.org/lookup/doi/10.1126/science.194.4270.1121.

Helmond, N. A. G. M. van et al. (Feb. 2014). 'A perturbed hydrological cycle during Oceanic Anoxic Event 2'. In: *Geology* 42.2, pp. 123–126. ISSN: 0091-7613. DOI: 10.1130/G34929.1.

Helmond, N. A.G.M. van et al. (Mar. 2015). 'Freshwater discharge controlled deposition of Cenomanian-Turonian black shales on the NW European epicontinental shelf (Wunstorf, northern Germany)'. In: *Climate*

of the Past 11.3, pp. 495–508. ISSN: 18149332. DOI: 10.5194/cp-11-495-2015.

Herbert, Timothy D. (Aug. 1997). 'A long marine history of carbon cycle modulation by orbital-climatic changes'. In: *Proceedings of the National Academy of Sciences* 94.16, pp. 8362–8369. ISSN: 0027-8424. DOI: 10.1073/pnas.94.16.8362. URL: https://pnas.org/doi/full/10.1073/pnas.94.16.8362.

Hetzel, Almut et al. (Aug. 2011). 'Geochemical environment of Cenomanian - Turonian black shale deposition at Wunstorf (northern Germany)'. In: *Cretaceous Research* 32.4, pp. 480–494. ISSN: 01956671. DOI: 10.1016/j.cretres.2011.03.004.

Higgins, Meytal B et al. (2012). 'Dominant eukaryotic export production during ocean anoxic events reflects the importance of recycled NH 4'. In: *PNAS* 109.7. DOI: 10.1073/pnas.1104313109/-/DCSupplemental.

Holling, C. S. (May 1965). 'The Functional Response of Predators to Prey Density and its Role in Mimicry and Population Regulation'. In: *Memoirs of the Entomological Society of Canada* 97.S45, pp. 5–60. ISSN: 0071-075X. DOI: 10.4039/entm9745fv. URL: https://www.cambridge.org/core/product/identifier/S0071075X00000862/type/journal_article.

Holte, James and Lynne Talley (Sept. 2009). 'A New Algorithm for Finding Mixed Layer Depths with Applications to Argo Data and Subantarctic Mode Water Formation'. In: *Journal of Atmospheric and Oceanic Technology* 26.9, pp. 1920–1939. ISSN: 1520-0426. DOI: 10.1175/2009JTECHO543.

1. URL: http://journals.ametsoc.org/doi/10.1175/2009JTECHO543.1.

Houghton, J. T. (John Theodore) et al. (1997). *An introduction to simple climate models used in the IPCC second assessment report*. Intergovernmental Panel on Climate Change, p. 47. ISBN: 9291691011.

Hülse, Dominik et al. (2016). 'The biological carbon pump in the ocean: Reviewing model representations and its feedbacks on climate perturbations'. In: *Geophysical Research Abstracts* 18, EPSC2016–1020.

Jarvis, Ian et al. (Sept. 2011). 'Black shale deposition, atmospheric CO 2 drawdown, and cooling during the Cenomanian-Turonian Oceanic Anoxic Event'. In: *Paleoceanography* 26.3, n/a–n/a. ISSN: 08838305. DOI: 10.1029/2010PA002081. URL: http://doi.wiley.com/10.1029/2010PA002081.

Jenkyns, Hugh C. (1980). 'Cretaceous anoxic events: from continents to oceans.' In: *Journal of the Geological Society* 137.2, pp. 171–188. ISSN: 00167649. DOI: 10.1144/gsjgs.137.2.0171.

— (Mar. 2010). 'Geochemistry of oceanic anoxic events'. In: *Geochemistry, Geophysics, Geosystems* 11.3, n/a–n/a. ISSN: 15252027. DOI: 10.1029/2009GC002788. URL: http://doi.wiley.com/10.1029/2009GC002788.

Jenkyns, Hugh C. and G. P. Weedon (2003). 'Evidence for rapid climate change in the Mesozoic-Palaeogene greenhouse world'. In: *Philosophical Transactions of the Royal Society A: Mathematical, Physical and Engineering Sciences* 361.1810, pp. 1885–1916. ISSN: 1364503X. DOI: 10.1098/rsta.2003.1240.

Jenkyns, Hugh C. et al. (Sept. 2007). 'Nitrate reduction, sulfate reduction, and sedimentary iron isotope evolution during the Cenomanian-Turonian oceanic anoxic event'. In: *Paleoceanography* 22.3. ISSN: 08838305. DOI: 10.1029/2006PA001355.

Joo, Young Ji, Bradley B. Sageman, and Matthew T. Hurtgen (2020). 'Data-model comparison reveals key environmental changes leading to Cenomanian-Turonian Oceanic Anoxic Event 2'. In: *Earth-Science Reviews* 203.October 2019, p. 103123. ISSN: 00128252. DOI: 10.1016/j.earscirev.2020.103123. URL: https://doi.org/10.1016/j.earscirev.2020.103123.

Junium, Christopher K. and Michael A. Arthur (Mar. 2007). 'Nitrogen cycling during the Cretaceous, Cenomanian- Turonian Oceanic Anoxic Event II'. In: *Geochemistry, Geophysics, Geosystems* 8.3. ISSN: 15252027. DOI: 10.1029/2006GC001328.

Kolonic, Sadat et al. (2005). 'Black shale deposition on the northwest African Shelf during the Cenomanian/Turonian oceanic anoxic event: Climate coupling and global organic carbon burial'. In: *Paleoceanography* 20.1, pp. 1–18. ISSN: 08838305. DOI: 10.1029/2003PA000950.

Kraal, Peter et al. (Sept. 2010). 'Phosphorus cycling from the margin to abyssal depths in the proto-Atlantic during oceanic anoxic event 2'. In: *Palaeogeography, Palaeoclimatology, Palaeoecology* 295.1-2, pp. 42–54. ISSN: 00310182. DOI: 10.1016/j.palaeo.2010.05.014. URL: https://linkinghub.elsevier.com/retrieve/pii/S0031018210003019.

Kuhlbrodt, T. et al. (June 2007). *On the driving processes of the Atlantic meridional overturning circulation*. DOI: 10.1029/2004RG000166.

Kuhnt, Wolfgang et al. (Feb. 2005). 'Orbital-scale record of the late Cenomanian-Turonian oceanic anoxic event (OAE-2) in the Tarfaya Basin (Morocco)'. In: *International Journal of Earth Sciences* 94.1, pp. 147–159. ISSN: 1437-3254. DOI: 10.1007/s00531-004-0440-5. URL: http://link.springer.com/10.1007/s00531-004-0440-5.

Kuhnt, Wolfgang et al. (2017). 'Unraveling the onset of Cretaceous Oceanic Anoxic Event 2 in an extended sediment archive from the Tarfaya-Laayoune Basin, Morocco'. In: *Paleoceanography* 32.8, pp. 923–946. ISSN: 19449186. DOI: 10.1002/2017PA003146.

Kump, Lee R. and Michael A. Arthur (Sept. 1999). 'Interpreting carbon-isotope excursions: carbonates and organic matter'. In: *Chemical Geology* 161.1-3, pp. 181–198. ISSN: 00092541. DOI: 10.1016/S0009-2541(99)00086-8. URL: https://linkinghub.elsevier.com/retrieve/pii/S0009254199000868.

Kuroda, Junichiro et al. (2007). 'Contemporaneous massive subaerial volcanism and late cretaceous Oceanic Anoxic Event 2'. In: *Earth and Planetary Science Letters* 256.1-2, pp. 211–223. ISSN: 0012821X. DOI: 10.1016/j.epsl.2007.01.027.

Kuypers, Marcel M. M. et al. (Dec. 2002). 'Enhanced productivity led to increased organic carbon burial in the euxinic North Atlantic basin during the late Cenomanian oceanic anoxic event'. In: *Paleoceanography* 17.4, pp. 3–1. ISSN: 08838305. DOI: 10.1029/2000PA000569. URL: http://doi.wiley.com/10.1029/2000PA000569.

Kwon, Eun Young, François Primeau, and Jorge L. Sarmiento (Aug. 2009). 'The impact of remineralization depth on the air-sea carbon balance'.

In: *Nature Geoscience* 2.9, pp. 630–635. ISSN: 1752-0894. DOI: 10.1038/ngeo612. URL: http://www.nature.com/doifinder/10.1038/ngeo612.

Ladant, Jean Baptiste et al. (Mar. 2018). 'Meridional Contrasts in Productivity Changes Driven by the Opening of Drake Passage'. In: *Paleoceanography and Paleoclimatology* 33.3, pp. 302–317. DOI: 10.1002/2017PA003211.

Ladant, Jean-baptiste et al. (2020). 'Paleogeographic controls on the evolution of Late Cretaceous ocean circulation'. In: pp. 973–1006.

Lam, Phyllis and Marcel M.M. Kuypers (2011). 'Microbial Nitrogen Cycling Processes in Oxygen Minimum Zones'. In: *Annual Review of Marine Science* 3.1, pp. 317–345. ISSN: 1941-1405. DOI: 10.1146/annurev-marine-120709-142814. URL: http://www.annualreviews.org/doi/abs/10.1146/annurev-marine-120709-142814.

Landry, Michael R. et al. (Feb. 2011). 'Phytoplankton growth, grazing and production balances in the HNLC equatorial Pacific'. In: *Deep Sea Research Part II: Topical Studies in Oceanography* 58.3-4, pp. 524–535. ISSN: 09670645. DOI: 10.1016/j.dsr2.2010.08.011. URL: https://linkinghub.elsevier.com/retrieve/pii/S0967064510002286.

Laskar, J., F. Joutel, and F. Boudin (1993). 'Orbital, precessional, and insolation quantities for the Earth from -20 Myr to +10 Myr'. In: *Astronomy and Astrophysics -Berlin-* 270.1, pp. 522–522. ISSN: 0004-6361.

Laskar, J. et al. (2004). 'A long-term numerical solution for the insolation quantities of the Earth'. In: *Astronomy and Astrophysics* 428.1, pp. 261–285. ISSN: 00046361. DOI: 10.1051/0004-6361:20041335.

Laskar, J. et al. (2011). 'La2010: A new orbital solution for the long-term motion of the Earth'. In: *Astronomy and Astrophysics* 532. ISSN: 00046361. DOI: 10.1051/0004-6361/201116836.

Laugié, Marie et al. (July 2021). 'Exploring the Impact of Cenomanian Paleogeography and Marine Gateways on Oceanic Oxygen'. In: *Paleoceanography and Paleoclimatology* 36.7. ISSN: 25724525. DOI: 10.1029/2020PA004202.

Le Quéré, Corinne et al. (July 2016). 'Role of zooplankton dynamics for Southern Ocean phytoplankton biomass and global biogeochemical cycles'. In: *Biogeosciences* 13.14, pp. 4111–4133. ISSN: 17264189. DOI: 10.5194/bg-13-4111-2016.

Leckie, R. Mark, Timothy J. Bralower, and Richard Cashman (2002). 'Oceanic anoxic events and plankton evolution: Biotic response to tectonic forcing during the mid-Cretaceous'. In: *Paleoceanography* 17.3, pp. 13–1. ISSN: 08838305. DOI: 10.1029/2001pa000623.

Leckie, R.Mark (Sept. 1989). 'A paleoceanographic model for the early evolutionary history of planktonic foraminifera'. In: *Palaeogeography, Palaeoclimatology, Palaeoecology* 73.1-2, pp. 107–138. ISSN: 00310182. DOI: 10.1016/0031-0182(89)90048-5.

Lenton, T. M. et al. (Nov. 2007). 'Effects of atmospheric dynamics and ocean resolution on bi-stability of the thermohaline circulation examined using the Grid ENabled Integrated Earth system modelling (GENIE) framework'. In: *Climate Dynamics* 29.6, pp. 591–613. ISSN: 09307575. DOI: 10.1007/s00382-007-0254-9.

Lenton, Timothy M. (Aug. 2020). 'On the use of models in understanding the rise of complex life'. In: *Interface Focus* 10.4. ISSN: 20428901. DOI: 10.1098/rsfs.2020.0018.

Lenton, Timothy M. and Andrew J. Watson (Mar. 2000). 'Redfield revisited: 2. What regulates the oxygen content of the atmosphere?' In: *Global Biogeochemical Cycles* 14.1, pp. 249–268. DOI: 10.1029/1999gb900076.

Li, Yong Xiang et al. (2017). 'Astronomical constraints on global carbon-cycle perturbation during Oceanic Anoxic Event 2 (OAE2)'. In: *Earth and Planetary Science Letters* 462, pp. 35–46. ISSN: 0012821X. DOI: 10.1016/j.epsl.2017.01.007. URL: http://dx.doi.org/10.1016/j.epsl.2017.01.007.

Lindemann, Christian and Michael A. St. John (2014). 'A seasonal diary of phytoplankton in the North Atlantic'. In: *Frontiers in Marine Science* 1.SEP. ISSN: 22967745. DOI: 10.3389/fmars.2014.00037.

Linnert, Christian et al. (Sept. 2014). 'Evidence for global cooling in the Late Cretaceous'. In: *Nature Communications* 5.1, p. 4194. ISSN: 2041-1723. DOI: 10.1038/ncomms5194. URL: http://www.nature.com/articles/ncomms5194.

Loewen, Matthew W. et al. (Oct. 2013). 'Prolonged plume volcanism in the Caribbean Large Igneous Province: New insights from Curaçao and Haiti'. In: *Geochemistry, Geophysics, Geosystems* 14.10, pp. 4241–4259. ISSN: 15252027. DOI: 10.1002/ggge.20273.

Lovecchio, Elisa and Timothy M. Lenton (Apr. 2020). 'BPOP-v1 model: Exploring the impact of changes in the biological pump on the shelf sea and ocean nutrient and redox state'. In: *Geoscientific Model Devel-*

opment 13.4, pp. 1865–1883. ISSN: 19919603. DOI: 10.5194/gmd-13-1865-2020.

Lowe, J.J., M.J.C. Walker, and S.C. Porter (2013). 'INTRODUCTION | Understanding Quaternary Climatic Change'. In: *Encyclopedia of Quaternary Science*. Elsevier, pp. 26–35. DOI: 10.1016/B978-0-444-53643-3.00004-2. URL: https://linkinghub.elsevier.com/retrieve/pii/B9780444536433000042.

Ma, Chao, Stephen R. Meyers, and Bradley B. Sageman (2017). 'Theory of chaotic orbital variations confirmed by Cretaceous geological evidence'. In: *Nature* 542.7642, pp. 468–470. ISSN: 14764687. DOI: 10.1038/nature21402. URL: http://dx.doi.org/10.1038/nature21402.

MacLeod, Kenneth G., Ellen E. Martin, and Susanna W. Blair (2008). 'Nd isotopic excursion across Cretaceous ocean anoxic event 2 (Cenomanian-Turonian) in the tropical North Atlantic'. In: *Geology* 36.10, p. 811. ISSN: 0091-7613. DOI: 10.1130/G24999A.1.

Markwick, Paul J. and Paul J. Valdes (Oct. 2004). 'Palaeo-digital elevation models for use as boundary conditions in coupled ocean-atmosphere GCM experiments: a Maastrichtian (late Cretaceous) example'. In: *Palaeogeography, Palaeoclimatology, Palaeoecology* 213.1-2, pp. 37–63. ISSN: 00310182. DOI: 10.1016/j.palaeo.2004.06.015. URL: http://linkinghub.elsevier.com/retrieve/pii/S003101820400330X.

Marsh, R., A. E. Hickman, and J. Sharples (2015). 'S2P3-R (v1.0): a framework for efficient regional modelling of physical and biological structures and processes in shelf seas'. In: *Geoscientific Model Development Discussions* 8.1, pp. 673–713. ISSN: 1991-962X. DOI: 10.5194/gmdd-8-

673-2015. URL: http://www.geosci-model-dev-discuss.net/8/673/2015/.

Marsh, R. et al. (Nov. 2011). 'Incorporation of the C-GOLDSTEIN efficient climate model into the GENIE framework: "eb_go_gs" configurations of GENIE'. In: *Geoscientific Model Development* 4.4, pp. 957–992. DOI: 10.5194/gmd-4-957-2011.

Marshak, Stephen (2012). *Earth: Portrait of a Planet*. Ed. by Jack Repcheck and Eric Svendsen. 4th. W. W. Norton & Company. ISBN: 978-0-939-93518-9.

Marshall, John and Kevin Speer (Mar. 2012). 'Closure of the meridional overturning circulation through Southern Ocean upwelling'. In: *Nature Geoscience* 5.3, pp. 171–180. ISSN: 1752-0894. DOI: 10.1038/ngeo1391.

Martin, E. E. et al. (2012). 'Water mass circulation on Demerara Rise during the Late Cretaceous based on Nd isotopes'. In: *Earth and Planetary Science Letters* 327-328, pp. 111–120. ISSN: 0012821X. DOI: 10.1016/j.epsl.2012.01.037. URL: http://dx.doi.org/10.1016/j.epsl.2012.01.037.

Martin, John H. et al. (May 1989). 'Vertex: phytoplankton/iron studies in the Gulf of Alaska'. In: *Deep Sea Research Part A. Oceanographic Research Papers* 36.5, pp. 649–680. DOI: 10.1016/0198-0149(89)90144-1. URL: http://linkinghub.elsevier.com/retrieve/pii/0198014989901441.

Maslin, Mark (May 2020). 'Tying celestial mechanics to Earth's ice ages'. In: *Physics Today* 73.5, pp. 48–53. ISSN: 0031-9228. DOI: 10.1063/PT.

3.4474. URL: http://physicstoday.scitation.org/doi/10.1063/PT.3.4474.

Merlis, Timothy M. et al. (2013). 'The tropical precipitation response to orbital precession'. In: *Journal of Climate* 26.6, pp. 2010–2021. ISSN: 08948755. DOI: 10.1175/JCLI-D-12-00186.1.

Meyer, Katja M. and Lee R. Kump (May 2008). 'Oceanic Euxinia in Earth History: Causes and Consequences'. In: *Annual Review of Earth and Planetary Sciences* 36.1, pp. 251–288. ISSN: 0084-6597. DOI: 10.1146/annurev.earth.36.031207.124256. URL: http://www.annualreviews.org/doi/10.1146/annurev.earth.36.031207.124256.

Meyers, Stephen R., Bradley B. Sageman, and Michael A. Arthur (2012). 'Obliquity forcing of organic matter accumulation during Oceanic Anoxic Event 2'. In: *Paleoceanography* 27.3, pp. 1–19. ISSN: 08838305. DOI: 10.1029/2012PA002286.

Meyers, Stephen R., Bradley B. Sageman, and Linda A. Hinnov (2001). 'Integrated quantitative stratigraphy of the cenomanian-turonian bridge creek limestone member using evolutive harmonic analysis and stratigraphic modeling'. In: *Journal of Sedimentary Research* 71.4, pp. 628–644. ISSN: 15271404. DOI: 10.1306/012401710628.

Mitchell, Ross N. et al. (2008). 'Oceanic anoxic cycles? Orbital prelude to the Bonarelli Level (OAE 2)'. In: *Earth and Planetary Science Letters* 267.1-2, pp. 1–16. ISSN: 0012821X. DOI: 10.1016/j.epsl.2007.11.026.

Mollier-Vogel, Elfi et al. (Sept. 2013). 'Rainfall response to orbital and millennial forcing in northern Peru over the last 18 ka'. In: *Quater-*

nary Science Reviews 76, pp. 29–38. ISSN: 02773791. DOI: 10.1016/j.quascirev.2013.06.021.

Monteiro, F. M., S. Dutkiewicz, and M. J. Follows (2011). 'Biogeographical controls on the marine nitrogen fixers'. In: *Global Biogeochemical Cycles* 25.2. ISSN: 08866236. DOI: 10.1029/2010GB003902.

Monteiro, F. M. et al. (Dec. 2012). 'Nutrients as the dominant control on the spread of anoxia and euxinia across the Cenomanian-Turonian oceanic anoxic event (OAE2): Model-data comparison'. In: *Paleoceanography* 27.4, pp. 1–17. ISSN: 08838305. DOI: 10.1029/2012PA002351. URL: http://doi.wiley.com/10.1029/2012PA002351.

Moore, C. M. et al. (Mar. 2013). 'Processes and patterns of oceanic nutrient limitation'. In: *Nature Geoscience* 6.9, pp. 701–710. ISSN: 1752-0894. DOI: 10.1038/ngeo1765. URL: 10.1038/ngeo1765%20http://www.nature.com/doifinder/10.1038/ngeo1765.

Morozov, Andrew Yu. (July 2010). 'Emergence of Holling type III zooplankton functional response: Bringing together field evidence and mathematical modelling'. In: *Journal of Theoretical Biology* 265.1, pp. 45–54. ISSN: 00225193. DOI: 10.1016/j.jtbi.2010.04.016.

Mort, Haydon P. et al. (2007). 'Phosphorus and the roles of productivity and nutrient recycling during oceanic anoxic event 2'. In: *Geology* 35.6, p. 483. ISSN: 0091-7613. DOI: 10.1130/G23475A.1. URL: https://pubs.geoscienceworld.org/geology/article/35/6/483-486/129857.

Moullade, M et al. (1998). *35. Mesozoic Biostratigraphic, Paleoenvironmental, and Paleobiogeographic Synthesis, Equatorial Atlantic*. Tech. rep.

Munk, Walter (2005). '9 Internal Waves and Small-Scale Processes'. In: *Evolution of Physical Oceanography*.

Musavu-Moussavou, Benjamin and Taniel Danelian (July 2006). 'The Radiolarian biotic response to Oceanic Anoxic Event 2 in the southern part of the Northern proto-Atlantic (Demerara Rise, ODP Leg 207)'. In: *Revue de Micropaléontologie* 49.3, pp. 141–163. ISSN: 00351598. DOI: 10.1016/j.revmic.2006.04.004. URL: https://linkinghub.elsevier.com/retrieve/pii/S0035159806000225.

Naafs, B. David A. et al. (Dec. 2019). 'Fundamentally different global marine nitrogen cycling in response to severe ocean deoxygenation'. In: *Proceedings of the National Academy of Sciences* 116.50, pp. 24979–24984. ISSN: 0027-8424. DOI: 10.1073/pnas.1905553116. URL: http://www.pnas.org/lookup/doi/10.1073/pnas.1905553116.

Nederbragt, Alexandra J. et al. (July 2004). 'Modelling oceanic carbon and phosphorus fluxes: implications for the cause of the late Cenomanian Oceanic Anoxic Event (OAE2)'. In: *Journal of the Geological Society* 161.4, pp. 721–728. ISSN: 0016-7649. DOI: 10.1144/0016-764903-075. URL: http://jgs.lyellcollection.org/lookup/doi/10.1144/0016-764903-075.

Nouri, Fatemeh et al. (Mar. 2016). 'Age and petrogenesis of Na-rich felsic rocks in western Iran: Evidence for closure of the southern branch of the Neo-Tethys in the Late Cretaceous'. In: *Tectonophysics* 671, pp. 151–172. ISSN: 00401951. DOI: 10.1016/j.tecto.2015.12.014. URL: https://linkinghub.elsevier.com/retrieve/pii/S0040195115006770.

Olsen, Paul E. and Dennis V. Kent (July 1999). 'Long-period Milankovitch cycles from the Late Triassic and Early Jurassic of eastern North America and their implications for the calibration of the Early Mesozoic time-scale and the long-term behaviour of the planets'. In: *Philosophical Transactions of the Royal Society of London. Series A: Mathematical, Physical and Engineering Sciences* 357.1757. Ed. by N. J. Shackleton, I. N. McCave, and G. P. Weedon, pp. 1761–1786. ISSN: 1364-503X. DOI: 10.1098/rsta.1999.0400. URL: https://royalsocietypublishing.org/doi/10.1098/rsta.1999.0400.

Ostrander, Chadlin M., Jeremy D. Owens, and Sune G. Nielsen (2017). 'Constraining the rate of oceanic deoxygenation leading up to a Cretaceous Oceanic Anoxic Event (OAE-2:
94 Ma)'. In: *Science Advances* 3.8, pp. 1–6. ISSN: 23752548. DOI: 10.1126/sciadv.1701020.

Otto-Bliesner, Bette L., Esther C. Brady, and Christine Shields (2002). 'Late Cretaceous ocean: Coupled simulations with the National Center for Atmospheric Research Climate System Model'. In: *Journal of Geophysical Research Atmospheres* 107.1-2. ISSN: 01480227. DOI: 10.1029/2001jd000821.

Owens, Jeremy D., Timothy W. Lyons, and Christopher M. Lowery (Oct. 2018). 'Quantifying the missing sink for global organic carbon burial during a Cretaceous oceanic anoxic event'. In: *Earth and Planetary Science Letters* 499, pp. 83–94. ISSN: 0012821X. DOI: 10.1016/j.epsl.2018.07.021.

Owens, Jeremy D. et al. (Sept. 2012). 'Iron isotope and trace metal records of iron cycling in the proto-North Atlantic during the Cenomanian-Turonian oceanic anoxic event (OAE-2)'. In: *Paleoceanography* 27.3. ISSN: 08838305. DOI: 10.1029/2012PA002328.

Palmer, Jr and Ij Totterdell (2001). 'Production and export in a global ecosystem model'. In: *Deep-Sea Research I* 48, pp. 1169–1198. ISSN: 09670637. DOI: 10.1016/S0967-0637(00)00080-7.

Pancost, Richard D. et al. (May 2004). 'Further evidence for the development of photic-zone euxinic conditions during Mesozoic oceanic anoxic events'. In: *Journal of the Geological Society* 161.3, pp. 353–364. ISSN: 0016-7649. DOI: 10.1144/0016764903-059. URL: http://jgs.lyellcollection.org/cgi/doi/10.1144/0016764903-059%20http://jgs.lyellcollection.org/lookup/doi/10.1144/0016764903-059.

Park, Jeffrey and Robert J. Oglesby (1991). 'Milankovitch rhythms in the Cretaceous: A GCM modelling study'. In: *"Palaeogeography, Palaeoclimatology, Palaeoecology"* 90.4, pp. 329–355. ISSN: 00310182. DOI: 10.1016/S0031-0182(12)80034-4. URL: http://dx.doi.org/10.1016/S0031-0182(12)80034-4.

Payne, J and L Kump (Apr. 2007). 'Evidence for recurrent Early Triassic massive volcanism from quantitative interpretation of carbon isotope fluctuations'. In: *Earth and Planetary Science Letters* 256.1-2, pp. 264–277. ISSN: 0012821X. DOI: 10.1016/j.epsl.2007.01.034. URL: https://linkinghub.elsevier.com/retrieve/pii/S0012821X07000611.

Pedersen, T. F. and S. E. Calvert (1990). 'Anoxia vs. Productivity: What Controls the Formation of Organic-Carbon-Rich Sediments and Sedi-

mentary Rocks?' In: *AAPG Bulletin* 74. ISSN: 0149-1423. DOI: 10.1306/0C9B232B-1710-11D7-8645000102C1865D. URL: http://search.datapages.com/data/doi/10.1306/0C9B232B-1710-11D7-8645000102C1865D.

Percival, L. M.E. et al. (Oct. 2015). 'Globally enhanced mercury deposition during the end-Pliensbachian extinction and Toarcian OAE: A link to the Karoo-Ferrar Large Igneous Province'. In: *Earth and Planetary Science Letters* 428, pp. 267–280. ISSN: 0012821X. DOI: 10.1016/j.epsl.2015.06.064.

Peterson, John A. (2012). 'Better mathematical constraints on ages of Carboniferous stage boundaries using radiometric tuff dates and cyclostratigraphy'. In: *Geochemistry, Geophysics, Geosystems* 12.5, pp. 1–7. ISSN: 15252027. DOI: 10.1029/2010GC003467.

Petrizzo, Maria Rose et al. (Nov. 2021). 'Exploring the paleoceanographic changes registered by planktonic foraminifera across the Cenomanian-Turonian boundary interval and Oceanic Anoxic Event 2 at southern high latitudes in the Mentelle Basin (SE Indian Ocean)'. In: *Global and Planetary Change* 206. ISSN: 09218181. DOI: 10.1016/j.gloplacha.2021.103595.

Pitchford, J (Mar. 1999). 'Iron limitation, grazing pressure and oceanic high nutrient-low chlorophyll (HNLC) regions'. In: *Journal of Plankton Research* 21.3, pp. 525–547. ISSN: 14643774. DOI: 10.1093/plankt/21.3.525. URL: https://academic.oup.com/plankt/article-lookup/doi/10.1093/plankt/21.3.525.

Pletsch, T et al. (June 2001). 'Cretaceous separation of Africa and South America: the view from the West African margin (ODP Leg 159)'. In:

Journal of South American Earth Sciences 14.2, pp. 147–174. ISSN: 08959811. DOI: 10.1016/S0895-9811(01)00020-7.

Pope, V. D. et al. (Feb. 2000). 'The impact of new physical parametrizations in the Hadley Centre climate model: HadAM3'. In: *Climate Dynamics* 16.2-3, pp. 123–146. ISSN: 0930-7575. DOI: 10.1007/s003820050009. URL: http://link.springer.com/10.1007/s003820050009.

Poulsen, Chris J. et al. (1998). 'The impact of paleogeographic evolution on the surface oceanic circulation and the marine environment within the mid-Cretaceous Tethys'. In: *Paleoceanography* 13.5, pp. 546–559. ISSN: 08838305. DOI: 10.1029/98PA01789.

Poulsen, Christopher J. et al. (Dec. 2001). 'Response of the Mid-Cretaceous global oceanic circulation to tectonic and CO 2 forcings'. In: *Paleoceanography* 16.6. Ed. by Intergovernmental Panel on Climate Change, pp. 576–592. ISSN: 08838305. DOI: 10.1029/2000PA000579. URL: https://www.cambridge.org/core/product/identifier/CBO9781107415324A009/type/book_part%20http://doi.wiley.com/10.1029/2000PA000579.

Poulton, Simon W. et al. (2015). 'A continental-weathering control on orbitally driven redox-nutrient cycling during Cretaceous oceanic anoxic event 2'. In: *Geology* 43.11, pp. 963–966. ISSN: 19432682. DOI: 10.1130/G36837.1.

Price, G.D., B.W. Sellwood, and P.J. Valdes (Dec. 1995). 'Sedimentological evaluation of general circulation model simulations for the "greenhouse" Earth: Cretaceous and Jurassic case studies'. In: *Sedimentary Geology* 100.1-4, pp. 159–180. ISSN: 00370738. DOI: 10.1016/0037-0738(95)00106-9.

Price, N M, B A Ahner, and F M M Morel (1994). 'The equatorial Pacific Ocean: grazer controlled phytoplankton populations in an iron-limited ecosystem'. In: *Limnology and Oceanography* 39.3, pp. 520–534.

Puceat, E, C Lecuyer, and L Reisberg (Aug. 2005). 'Neodymium isotope evolution of NW Tethyan upper ocean waters throughout the Cretaceous'. In: *Earth and Planetary Science Letters* 236.3-4, pp. 705–720. ISSN: 0012821X. DOI: 10.1016/j.epsl.2005.03.015.

Raju, Komaragiri Srinivasa and Dasika Nagesh Kumar (Sept. 2020). *Review of approaches for selection and ensembling of GCMS*. DOI: 10.2166/wcc.2020.128.

Raven, J. A. and P G Falkowski (June 1999). 'Oceanic sinks for atmospheric CO 2'. In: *Plant, Cell and Environment* 22.6, pp. 741–755. ISSN: 0140-7791. DOI: 10.1046/j.1365-3040.1999.00419.x. URL: http://doi.wiley.com/10.1046/j.1365-3040.1999.00419.x.

Raymo, Maureen E. and Peter Huybers (2008). 'Unlocking the mysteries of the ice ages'. In: *Nature* 451.7176, pp. 284–285. ISSN: 14764687. DOI: 10.1038/nature06589.

Richardson, Philip L. (Mar. 2008). 'On the history of meridional overturning circulation schematic diagrams'. In: *Progress in Oceanography* 76.4, pp. 466–486. ISSN: 00796611. DOI: 10.1016/j.pocean.2008.01.005. URL: https://linkinghub.elsevier.com/retrieve/pii/S0079661108000086.

Ridgwell, A et al. (Jan. 2007). 'Marine geochemical data assimilation in an efficient Earth System Model of global biogeochemical cycling'. In: *Biogeosciences* 4.1, pp. 87–104. ISSN: 1726-4189. DOI: 10.5194/bg-4-

87-2007. URL: http://www.biogeosciences.net/4/87/2007/bg-4-87-2007.html%20http://www.biogeosciences.net/4/87/2007/.

Ridgwell, Andy and J. C. Hargreaves (June 2007). 'Regulation of atmospheric CO 2 by deep-sea sediments in an Earth system model'. In: *Global Biogeochemical Cycles* 21.2, n/a–n/a. ISSN: 08866236. DOI: 10.1029/2006GB002764. URL: http://doi.wiley.com/10.1029/2006GB002764.

Robinson, Stuart A. et al. (Oct. 2010). 'Formation of "Southern Component Water" in the Late Cretaceous: Evidence from Nd-isotopes'. In: *Geology* 38.10, pp. 871–874. ISSN: 1943-2682. DOI: 10.1130/G31165.1.

Robinson, Stuart A. et al. (2017). 'Mesozoic climates and oceans - a tribute to Hugh Jenkyns and Helmut Weissert'. In: *Sedimentology* 64.1, pp. 1–15. ISSN: 13653091. DOI: 10.1111/sed.12349.

Robinson, Stuart A. et al. (Feb. 2019). 'Southern Hemisphere sea-surface temperatures during the Cenomanian-Turonian: Implications for the termination of Oceanic Anoxic Event 2'. In: *Geology* 47.2, pp. 131–134. ISSN: 0091-7613. DOI: 10.1130/G45842.1. URL: https://pubs.geoscienceworld.org/gsa/geology/article/47/2/131/568052/Southern-Hemisphere-seasurface-temperatures-during.

Rose, Julie M. and David A. Caron (2007). *Does low temperature constrain the growth rates of heterotrophic protists? Evidence and implications for algal blooms in cold waters.* DOI: 10.4319/lo.2007.52.2.0886.

Ruddiman, William F. (Apr. 2006). 'What is the timing of orbital-scale monsoon changes?' In: *Quaternary Science Reviews* 25.7-8, pp. 657–658. ISSN: 02773791. DOI: 10.1016/j.quascirev.2006.02.004.

Ruvalcaba Baroni, I. et al. (2014). 'Biogeochemistry of the North Atlantic during oceanic anoxic event 2: Role of changes in ocean circulation and phosphorus input'. In: *Biogeosciences* 11.4, pp. 977–993. ISSN: 17264170. DOI: 10.5194/bg-11-977-2014.

Ruvalcaba Baroni, Itzel et al. (Sept. 2018). 'Ocean Circulation in the Toarcian (Early Jurassic): A Key Control on Deoxygenation and Carbon Burial on the European Shelf'. In: *Paleoceanography and Paleoclimatology* 33.9, pp. 994–1012. ISSN: 25724525. DOI: 10.1029/2018PA003394.

Sageman, Bradley B., Stephen R. Meyers, and Michael A. Arthur (2006). 'Orbital time scale and new C-isotope record for Cenomanian-Turonian boundary stratotype'. In: *Geology* 34.2, p. 125. ISSN: 0091-7613. DOI: 10.1130/G22074.1. URL: https://pubs.geoscienceworld.org/geology/article/34/2/125-128/129449.

Sarr, A. C. et al. (Oct. 2022). 'Ventilation Changes Drive Orbital-Scale Deoxygenation Trends in the Late Cretaceous Ocean'. In: *Geophysical Research Letters* 49.19. ISSN: 19448007. DOI: 10.1029/2022GL099830.

Scaife, J. D. et al. (Dec. 2017). 'Sedimentary Mercury Enrichments as a Marker for Submarine Large Igneous Province Volcanism? Evidence From the Mid-Cenomanian Event and Oceanic Anoxic Event 2 (Late Cretaceous)'. In: *Geochemistry, Geophysics, Geosystems* 18.12, pp. 4253–4275. ISSN: 15252027. DOI: 10.1002/2017GC007153. URL: http://doi.wiley.com/10.1002/2017GC007153.

Schlanger, S.O. and Hugh C. Jenkyns (1976). 'Cretaceous oceanic anoxic events: causes and consequences'. In: *Geologie en Mijnbouw/Netherlands Journal of Geosciences* 55.3-4, pp. 179–184. ISSN: 02646021.

Scholle, Peter A. and Michael A. Arthur (1980). 'Carbon Isotope Fluctuations in Cretaceous Pelagic Limestones: Potential Stratigraphic and Petroleum Exploration Tool'. In: *AAPG Bulletin* 64. ISSN: 0149-1423. DOI: 10.1306/2F91892D-16CE-11D7-8645000102C1865D. URL: http://search.datapages.com/data/doi/10.1306/2F91892D-16CE-11D7-8645000102C1865D.

Scopelliti, Giovanna et al. (June 2004). 'High-resolution geochemical and biotic records of the Tethyan 'Bonarelli Level' (OAE2, latest Cenomanian) from the Calabianca–Guidaloca composite section, northwestern Sicily, Italy'. In: *Palaeogeography, Palaeoclimatology, Palaeoecology* 208.3-4, pp. 293–317. ISSN: 00310182. DOI: 10.1016/j.palaeo.2004.03.012.

Scotese, C. R. (2014). 'Atlas of Late Cretaceous Maps, PALEOMAP Atlas for ArcGIS, volume 2, The Cretaceous, Maps 16 - 22, Mollweide Projection'. In: *PALEOMAP Project, Evanston, IL*. 2.October. DOI: 10.13140/2.1.4691.3284.

Sellar, Alistair A. et al. (2019). 'UKESM1: Description and Evaluation of the U.K. Earth System Model'. In: *Journal of Advances in Modeling Earth Systems* 11.12, pp. 4513–4558. ISSN: 19422466. DOI: 10.1029/2019MS001739.

Sellwood, Bruce W. and Paul J. Valdes (Aug. 2006). 'Mesozoic climates: General circulation models and the rock record'. In: *Sedimentary Geology* 190.1-4, pp. 269–287. ISSN: 00370738. DOI: 10.1016/j.sedgeo.2006.05.013.

Sepúlveda, Julio et al. (May 2009). 'Molecular isotopic evidence of environmental and ecological changes across the Cenomanian–Turonian bound-

ary in the Levant Platform of central Jordan'. In: *Organic Geochemistry* 40.5, pp. 553–568. ISSN: 01466380. DOI: 10.1016/j.orggeochem.2009.02.009.

Sherr, Evelyn B and Barry F Sherr (2002). *Significance of predation by protists in aquatic microbial food webs*. Tech. rep., pp. 293–308.

Singarayer, Joy S. and Paul J. Valdes (Jan. 2010). 'High-latitude climate sensitivity to ice-sheet forcing over the last 120kyr'. In: *Quaternary Science Reviews* 29.1-2, pp. 43–55. ISSN: 02773791. DOI: 10.1016/j.quascirev.2009.10.011.

Singh, Bhart, Seema Singh, and Uday Bhan (Feb. 2022). 'Oceanic anoxic events in the Earth's geological history and signature of such event in the Paleocene-Eocene Himalayan foreland basin sediment records of NW Himalaya, India'. In: *Arabian Journal of Geosciences* 15.3. ISSN: 1866-7511. DOI: 10.1007/s12517-021-09180-y.

Sinninghe Damsté, J. S. (1998). 'Preservation of Sedimentary Organic Matter Through Natural Sulphurisation: An Overview'. In: *Mineralogical Magazine* 62A.3, pp. 1419–1420. ISSN: 0026-461X. DOI: 10.1180/minmag.1998.62A.3.77. URL: http://www.minersoc.org/pages/Archive-MM/Volume_62A/62A-3-1419.pdf.

Small, Lawrence F. and David W. Menzies (Feb. 1981). 'Patterns of primary productivity and biomass in a coastal upwelling region'. In: *Deep Sea Research Part A. Oceanographic Research Papers* 28.2, pp. 123–149. ISSN: 01980149. DOI: 10.1016/0198-0149(81)90086-8.

Snow, Laura J., Robert A. Duncan, and Timothy J. Bralower (Sept. 2005). 'Trace element abundances in the Rock Canyon Anticline, Pueblo, Col-

orado, marine sedimentary section and their relationship to Caribbean plateau construction and ocean anoxic event 2'. In: *Paleoceanography* 20.3, pp. 1–14. ISSN: 08838305. DOI: 10.1029/2004PA001093.

Soudry, D. et al. (Sept. 2006). 'Evolution of Tethyan phosphogenesis along the northern edges of the Arabian-African shield during the Cretaceous-Eocene as deduced from temporal variations of Ca and Nd isotopes and rates of P accumulation'. In: *Earth-Science Reviews* 78.1-2, pp. 27–57. ISSN: 00128252. DOI: 10.1016/j.earscirev.2006.03.005.

Spencer, Hilary, Rowan Sutton, and Julia M. Slingo (May 2007). 'El Niño in a coupled climate model: Sensitivity to changes in mean state induced by heat flux and wind stress corrections'. In: *Journal of Climate* 20.10, pp. 2273–2298. ISSN: 08948755. DOI: 10.1175/JCLI4111.1.

Stampfli, G.M and G.D Borel (Feb. 2002). 'A plate tectonic model for the Paleozoic and Mesozoic constrained by dynamic plate boundaries and restored synthetic oceanic isochrons'. In: *Earth and Planetary Science Letters* 196.1-2, pp. 17–33. ISSN: 0012821X. DOI: 10.1016/S0012-821X(01)00588-X. URL: https://linkinghub.elsevier.com/retrieve/pii/S0012821X0100588X.

Stampfli, Gterard M (2000). *Tethyan oceans*. Tech. rep. URL: https://www.lyellcollection.org/doi/pdf/10.1144/gsl.sp.2000.173.01.01.

Stott, Peter A. and J. A. Kettleborough (Apr. 2002). 'Origins and estimates of uncertainty in predictions of twenty-first century temperature rise'. In: *Nature* 416.6882, pp. 723–726. ISSN: 0028-0836. DOI: 10.1038/416723a.

Stukel, Michael R., Michael R. Landry, and Karen E. Selph (Feb. 2011). 'Nanoplankton mixotrophy in the eastern equatorial Pacific'. In: *Deep*

Sea Research Part II: Topical Studies in Oceanography 58.3-4, pp. 378–386. ISSN: 09670645. DOI: 10.1016/j.dsr2.2010.08.016. URL: https://linkinghub.elsevier.com/retrieve/pii/S0967064510002456.

Sullivan, Daniel L. et al. (Sept. 2020). 'High resolution osmium data record three distinct pulses of magmatic activity during cretaceous Oceanic Anoxic Event 2 (OAE-2)'. In: *Geochimica et Cosmochimica Acta* 285, pp. 257–273. ISSN: 00167037. DOI: 10.1016/j.gca.2020.04.002.

Tatebe, Hiroaki et al. (Dec. 2018). 'Impact of deep ocean mixing on the climatic mean state in the Southern Ocean'. In: *Scientific Reports* 8.1. ISSN: 20452322. DOI: 10.1038/s41598-018-32768-6.

Thamdrup, Bo, Henrik Fossing, and Bo Barker Jørgensen (Dec. 1994). 'Manganese, iron and sulfur cycling in a coastal marine sediment, Aarhus bay, Denmark'. In: *Geochimica et Cosmochimica Acta* 58.23, pp. 5115–5129. ISSN: 00167037. DOI: 10.1016/0016-7037(94)90298-4. URL: https://linkinghub.elsevier.com/retrieve/pii/0016703794902984.

Thibault, Nicolas et al. (Feb. 2016). 'Late Cretaceous (late Campanian-Maastrichtian) sea-surface temperature record of the Boreal Chalk Sea'. In: *Climate of the Past* 12.2, pp. 429–438. ISSN: 1814-9332. DOI: 10.5194/cp-12-429-2016. URL: https://cp.copernicus.org/articles/12/429/2016/.

Tivig, Miriam, David P. Keller, and Andreas Oschlies (Oct. 2021). 'Riverine nitrogen supply to the global ocean and its limited impact on global marine primary production: A feedback study using an Earth system model'. In: *Biogeosciences* 18.19, pp. 5327–5350. ISSN: 17264189. DOI: 10.5194/bg-18-5327-2021.

Topper, R. P.M. et al. (2011). 'A regional ocean circulation model for the mid-Cretaceous North Atlantic Basin: Implications for black shale formation'. In: *Climate of the Past* 7.1, pp. 277–297. ISSN: 18149324. DOI: 10.5194/cp-7-277-2011.

Totman Parrish, Judith and Rebecca L. Curtis (Nov. 1982). 'Atmospheric circulation, upwelling, and organic-rich rocks in the Mesozoic and Cenozoic eras'. In: *Palaeogeography, Palaeoclimatology, Palaeoecology* 40.1-3, pp. 31–66. ISSN: 00310182. DOI: 10.1016/0031-0182(82)90084-0.

Trabucho Alexandre, João et al. (Dec. 2010). 'The mid-Cretaceous North Atlantic nutrient trap: Black shales and OAEs'. In: *Paleoceanography* 25.4, n/a–n/a. ISSN: 08838305. DOI: 10.1029/2010PA001925. URL: http://doi.wiley.com/10.1029/2010PA001925.

Tsandev, I. and C. P. Slomp (2009). 'Modeling phosphorus cycling and carbon burial during Cretaceous Oceanic Anoxic Events'. In: *Earth and Planetary Science Letters* 286.1-2, pp. 71–79. ISSN: 0012821X. DOI: 10.1016/j.epsl.2009.06.016. URL: http://dx.doi.org/10.1016/j.epsl.2009.06.016.

Tsikos, H. et al. (July 2004). 'Carbon-isotope stratigraphy recorded by the Cenomanian-Turonian Oceanic Anoxic Event: correlation and implications based on three key localities'. In: *Journal of the Geological Society* 161.4, pp. 711–719. ISSN: 0016-7649. DOI: 10.1144/0016-764903-077. URL: http://jgs.lyellcollection.org/lookup/doi/10.1144/0016-7649Er161-4%20http://jgs.lyellcollection.org/lookup/doi/10.1144/0016-764903-077.

Tsuda, Atsushi et al. (Dec. 2007). 'Evidence for the grazing hypothesis: Grazing reduces phytoplankton responses of the HNLC ecosystem to iron enrichment in the western subarctic pacific (SEEDS II)'. In: *Journal of Oceanography* 63.6, pp. 983–994. ISSN: 0916-8370. DOI: 10.1007/s10872-007-0082-x. URL: http://link.springer.com/10.1007/s10872-007-0082-x.

Turgeon, Steven C. and Robert A. Creaser (July 2008). 'Cretaceous oceanic anoxic event 2 triggered by a massive magmatic episode'. In: *Nature* 454.7202, pp. 323–326. ISSN: 0028-0836. DOI: 10.1038/nature07076.

Turner, Jefferson T. (Jan. 2015). 'Zooplankton fecal pellets, marine snow, phytodetritus and the ocean's biological pump'. In: *Progress in Oceanography* 130, pp. 205–248. ISSN: 00796611. DOI: 10.1016/j.pocean.2014.08.005.

Tyrrell, Toby (Aug. 1999). 'The relative influences of nitrogen and phosphorus on oceanic primary production'. In: *Nature* 400.6744, pp. 525–531. ISSN: 0028-0836. DOI: 10.1038/22941. URL: https://www.nature.com/articles/22941.

Uenzelmann-Neben, Gabriele et al. (Oct. 2017). 'Transition from the Cretaceous ocean to Cenozoic circulation in the western South Atlantic — A twofold reconstruction'. In: *Tectonophysics* 716, pp. 225–240. ISSN: 00401951. DOI: 10.1016/j.tecto.2016.05.036.

Vacher, H.L. and Mark P. Rowe (2004). 'Geology and Hydrogeology of Bermuda'. In: pp. 35–90. DOI: 10.1016/S0070-4571(04)80022-0.

Valdes, P. J., B. W. Sellwood, and G. D. Price (Jan. 1995). 'Modelling Late Jurassic Milankovitch climate variations'. In: *Geological Society,*

London, Special Publications 85.1, pp. 115–132. ISSN: 0305-8719. DOI: 10.1144/GSL.SP.1995.085.01.07.

Valdes, Paul J, Christopher R Scotese, and Daniel J Lunt (July 2021). 'Deep ocean temperatures through time'. In: *Climate of the Past* 17.4, pp. 1483–1506. ISSN: 1814-9332. DOI: 10.5194/cp-17-1483-2021. URL: https://cp.copernicus.org/articles/17/1483/2021/.

Valdes, Paul J., David J. Beerling, and Colin E. Johnson (Jan. 2005). 'The ice age methane budget'. In: *Geophysical Research Letters* 32.2, p. L02704. ISSN: 0094-8276. DOI: 10.1029/2004GL021004. URL: http://doi.wiley.com/10.1029/2004GL021004.

Valdes, Paul J. et al. (2017). 'The BRIDGE HadCM3 family of climate models: HadCM3@Bristol v1.0'. In: *Geoscientific Model Development Discussions*, pp. 1–42. ISSN: 1991-962X. DOI: 10.5194/gmd-2017-16. URL: https://www.geosci-model-dev-discuss.net/gmd-2017-16/.

Van Cappellen, Philippe and Ellery D. Ingall (Oct. 1994). 'Benthic phosphorus regeneration, net primary production, and ocean anoxia: A model of the coupled marine biogeochemical cycles of carbon and phosphorus'. In: *Paleoceanography* 9.5, pp. 677–692. ISSN: 08838305. DOI: 10.1029/94PA01455.

Vanhoutte-Brunier, Alice et al. (Feb. 2008). 'Modelling the Karenia mikimotoi bloom that occurred in the western English Channel during summer 2003'. In: *Ecological Modelling* 210.4, pp. 351–376. DOI: 10.1016/j.ecolmodel.2007.08.025. URL: https://linkinghub.elsevier.com/retrieve/pii/S0304380007004280.

Voigt, Silke et al. (Jan. 2007). 'Late Cenomanian to Middle Turonian high-resolution carbon isotope stratigraphy: New data from the Munsterland Cretaceous Basin, Germany'. In: *Earth and Planetary Science Letters* 253.1-2, pp. 196–210. ISSN: 0012821X. DOI: 10.1016/j.epsl.2006.10.026.

Wagner, T., P. Hofmann, and S. Flögel (May 2013). 'Marine black shale deposition and Hadley Cell dynamics: A conceptual framework for the Cretaceous Atlantic Ocean'. In: *Marine and Petroleum Geology* 43, pp. 222–238. ISSN: 02648172. DOI: 10.1016/j.marpetgeo.2013.02.005. URL: https://linkinghub.elsevier.com/retrieve/pii/S0264817213000330.

Wagner, Thomas and Thomas Pletsch (Jan. 1999). 'Tectono-sedimentary controls on Cretaceous black shale deposition along the opening Equatorial Atlantic Gateway (ODP Leg 159)'. In: *Geological Society, London, Special Publications* 153.1, pp. 241–265. ISSN: 0305-8719. DOI: 10.1144/GSL.SP.1999.153.01.15.

Wagner, Thomas et al. (2004). 'Euxinia and primary production in Late Cretaceous eastern equatorial Atlantic surface waters fostered orbitally driven formation of marine black shales'. In: *Paleoceanography* 19.3, pp. 1–13. ISSN: 08838305. DOI: 10.1029/2003PA000898.

Wallmann, K. (2003). 'Feedbacks between oceanic redox states and marine productivity: A model perspective focused on benthic phosphorus cycling'. In: *Global Biogeochemical Cycles* 17.3. ISSN: 08866236. DOI: 10.1029/2002gb001968.

Wallmann, Klaus (2010). 'Phosphorus imbalance in the global ocean?' In: *Global Biogeochemical Cycles* 24.4. ISSN: 08866236. DOI: 10.1029/2009GB003643.

Waltham, David (Aug. 2015). 'Milankovitch Period Uncertainties and Their Impact On Cyclostratigraphy'. In: *Journal of Sedimentary Research* 85.8, pp. 990–998. ISSN: 1527-1404. DOI: 10.2110/jsr.2015.66. URL: https://pubs.geoscienceworld.org/jsedres/article/85/8/990-998/145507.

Waterhouse, Amy F. et al. (2014). 'Global patterns of diapycnal mixing from measurements of the turbulent dissipation rate'. In: *Journal of Physical Oceanography* 44.7, pp. 1854–1872. ISSN: 15200485. DOI: 10.1175/JPO-D-13-0104.1.

Weedon, Graham P. et al. (1999). 'Astronomical calibration of the Jurassic time-scale from cyclostratigraphy in British mudrock formations'. In: *Philosophical Transactions of the Royal Society A: Mathematical, Physical and Engineering Sciences* 357.1757, pp. 1787–1813. ISSN: 1364503X. DOI: 10.1098/rsta.1999.0401.

Williams, George E. (Mar. 1993). 'History of the earth's obliquity'. In: *Earth-Science Reviews* 34.1, pp. 1–45. ISSN: 00128252. DOI: 10.1016/0012-8252(93)90004-Q.

Williams, J. H. T. et al. (Jan. 2013). 'Optimising the FAMOUS climate model: inclusion of global carbon cycling'. In: *Geoscientific Model Development* 6.1, pp. 141–160. DOI: 10.5194/gmd-6-141-2013.

Williams, Jonny H. T. et al. (July 2014). 'Numerical simulations of oceanic oxygen cycling in the FAMOUS Earth-System model: FAMOUS-ES,

version 1.0'. In: *Geoscientific Model Development* 7.4, pp. 1419–1431. ISSN: 1991-9603. DOI: 10.5194/gmd-7-1419-2014. URL: http://www.geosci-model-dev.net/7/1419/2014/%20https://gmd.copernicus.org/articles/7/1419/2014/.

Williams, K. D. et al. (2015). 'The Met Office Global Coupled model 2.0 (GC2) configuration'. In: *Geoscientific Model Development* 8.5, pp. 1509–1524. ISSN: 19919603. DOI: 10.5194/gmd-8-1509-2015.

Wilson, Paul A. and Richard D. Norris (2001). 'Warm tropical ocean surface and global anoxia during the mid-Cretaceous period'. In: *Nature* 412.6845, pp. 425–429. ISSN: 00280836. DOI: 10.1038/35086553.

Wyrtki, Klaus (Sept. 1981). 'An Estimate of Equatorial Upwelling in the Pacific'. In: *Journal of Physical Oceanography* 11.9, pp. 1205–1214. ISSN: 0022-3670. DOI: 10.1175/1520-0485(1981)011<1205:AEOEUI>2.0.CO;2. URL: http://journals.ametsoc.org/doi/10.1175/1520-0485(1981)011%3C1205:AEOEUI%3E2.0.CO;2.

Ye, Jing et al. (2017). 'Paleogeographic and structural evolution of northwestern Africa and its Atlantic margins since the early Mesozoic'. In: *Geosphere* 13.4, pp. 1254–1284. ISSN: 1553040X. DOI: 10.1130/GES01426.1.

Zeebe, Richard E. and Lucas J. Lourens (Aug. 2019). 'Solar System chaos and the Paleocene-Eocene boundary age constrained by geology and astronomy'. In: *Science* 365.6456, pp. 926–929. ISSN: 0036-8075. DOI: 10.1126/science.aax0612. URL: https://www.sciencemag.org/lookup/doi/10.1126/science.aax0612.

Zhang, Yurui et al. (July 2020). 'Early Eocene vigorous ocean overturning and its contribution to a warm Southern Ocean'. In: *Climate of the Past* 16.4, pp. 1263–1283. ISSN: 1814-9332. DOI: 10.5194/cp-16-1263-2020. URL: https://cp.copernicus.org/articles/16/1263/2020/.

Zheng, Xin-Yuan et al. (Feb. 2016). 'A climatic control on reorganization of ocean circulation during the mid-Cenomanian event and Cenomanian-Turonian oceanic anoxic event (OAE 2): Nd isotope evidence'. In: *Geology* 44.2, pp. 151–154. ISSN: 0091-7613. DOI: 10.1130/G37354.1. URL: https://pubs.geoscienceworld.org/geology/article/44/2/151-154/132055.

Zhou, Xiaoli et al. (May 2017). 'Organically bound iodine as a bottom-water redox proxy: Preliminary validation and application'. In: *Chemical Geology* 457, pp. 95–106. ISSN: 00092541. DOI: 10.1016/j.chemgeo.2017.03.016.